BIOCHEMICAL ANALYSIS OF TOPOSOME, A PROTEIN MEDIATING MEMBRANE-MEMBRANE INTERACTIONS IN THE SEA URCHIN EGG & EMBRYO

MICHAEL HAYLEY


CENTRE FOR NFLD. STUDIES
MEMORIAL UNIVERSITY
OF NEWFOUNDLAND

Biochemical analysis of toposome, a protein mediating membrane-membrane interactions in the sea urchin egg & embryo.

Michael Hayley

A Thesis Submitted to the School of Graduate Studies in Partial Fulfillment of the Requirements for the Degree of Doctor of Philosophy

Department of Biochemistry
Memorial University of Newfoundland

October 2007

St. John's NL Canada

Abstract

The yolk granule is the most abundant membrane-bound organelle present in sea urchin eggs and embryos. The major protein component of this organelle, major yolk protein/toposome, accounts for approximately 50 % of the total yolk protein and has also been shown to be localized to the embryonic cell surface. Biochemical and cell biological analysis in several laboratories have defined a role for toposome in mediating membrane-membrane interactions.

In this study we have examined calcium-toposome interaction. Increasing concentrations of calcium resulted in an increase in alpha helical content from 3.0 to 22.0 %, which occurred with an apparent dissociation constant (calcium) of 25 μM. In parallel experiments, toposome binding to liposomes required similar concentrations of calcium; an apparent dissociation constant (calcium) of 25 μM was recorded. Endogenous tryptophan fluorescence measurements, both in the presence and absence of liposomes, demonstrated that toposome tertiary structure was sensitive to increasing concentrations of calcium with an apparent dissociation constant (calcium) of 240 μM. Toposome-driven, liposome aggregation demonstrated a similar calcium-concentration dependence. Interestingly, the secondary structural change was required to facilitate toposome binding to bilayers while the tertiary structural change correlated with toposome-driven, membrane-membrane interaction.

We also showed that the thermal denaturation profile of toposome is dependent upon calcium. Following a calcium-induced change in secondary structure, toposome was increasingly resistant to thermal denaturation. However, the calcium-induced change in tertiary structure rendered toposome more susceptible to thermal denaturation when

compared to toposome following the secondary structural change. We also performed chymotryptic digestions in the presence of varying concentrations of calcium. The calcium-induced, secondary structural change had no effect on the chymotryptic cleavage pattern. Similarly, following the tertiary structural change, the chymotryptic digestion profile again remained unchanged. Interestingly, the chymotryptic digestion pattern of toposome bound to phosphatidylserine liposomes did vary as a function of calcium concentration.

In an effort to define the nature of the calcium binding sites on toposome, we investigated the interaction of this protein with various metal ions. Calcium, Mg^{2+}, Ba^{2+}, Cd^{2+}, Mn^{2+} and Fe^{3+} all bound to toposome. In addition, Cd^{2+} and Mn^{2+} displaced Ca^{2+}, prebound to toposome.

Also in this study we have expanded the analysis of toposome-membrane interaction by probing for toposome-induced changes to the lipid bilayer. Solid-state ^{2}H-NMR allowed us to define the nature of the association of toposome with the bilayer. We found that this protein interacts peripherally with the membrane and that this interaction is facilitated by the calcium-driven secondary structural change in toposome. In addition, we also examined the toposome-bilayer interaction using atomic force microscopy. In the absence of added calcium little or no binding of toposome occurred. In contrast, the calcium-induced secondary structural change caused significant binding of toposome to the bilayer. Following the calcium-induced tertiary structural change no further binding of protein to the bilayer was observed.

We utilized immunogold labeling to define the subcellular localization of toposome in the sea urchin egg and embryo. In the unfertilized egg, toposome was found

on the entire cell surface as well as stored in two different compartments, the yolk and cortical granules. Mitochondria and lipid vacuoles were not labeled. Label continued to be detected in the yolk granules and on the cell surface throughout development.

Collectively, these results provide a structural basis for a previously described role for toposome in mediating biologically relevant, membrane–membrane interactions. Calcium was found to induce two calcium concentration-dependent structural transitions in toposome: the first structural change was required to facilitate toposome binding to the membrane, while the second structural change enabled this protein to drive membrane-membrane adhesive interactions.

Acknowledgements

Foremost, I would like to thank Dr. John Robinson for being a great supervisor and friend. His guidance and support throughout the project and the thesis write up was amazing.

I sincerely thank my supervisory committee members, Drs. Phil Davis (My Co-supervisor as well) and Michael Morrow, for their helpful suggestions and comments throughout the thesis write-up.

Also, special thanks to Dr. Michael Morrow for his expertise in solid-state NMR and both Dr. Erika Merschrod and Ming Sun for all their expertise in atomic force microscopy.

Table of Contents

Abstract	ii
Acknowledgments	v
Table of Contents	vi
List of Figures	xii
List of Tables	xvi
Co-authorship statement	xvii
List of abbreviations	xviii
Chapter 1: Introduction	1
1.1: The sea urchin	2
1.2: The sea urchin – an ideal model for developmental studies	5
1.3: The yolk granule	8

1.4: The function of the yolk granule 11

1.5: Yolk Proteins 14

1.6: Toposome 15

1.6.1: Toposome - a brief introduction 15

1.6.2: Transport and packaging of toposome in the sea urchin during gametogenesis 16

1.6.3: Localization of toposome in the sea urchin egg and embryo 17

1.6.4: Proteolytic processing of toposome 18

1.6.5: Proteolysis of toposome is regulated by the acidification of yolk granules 23

1.6.6: Proteolytic cleavage site of MYP 24

1.7: Proposed functions of toposome 25

1.7.1: Role of toposome in mediating cell-cell adhesion in the developing embryo 25

1.7.2: Role of toposome in plasma membrane repair 27

1.7.3: Role of toposome as an iron transporter 29

1.8: Focus of the thesis 35

Chapter 2: Biochemical analysis of a calcium-dependent membrane-membrane interaction mediated by the sea urchin yolk granule protein, toposome 38

2.1: Introduction 39

2.2: Materials and Methods 42

2.2.1: Preparation of yolk granule protein extracts and fractionation by ion exchange chromatography 42

2.2.2: Circular dichroism spectroscopy measurements 43

2.2.3: Endogenous tryptophan fluorescence measurements 43

2.2.4: Toposome binding assay 44

2.2.5: Equilibrium dialysis 44

2.2.6: Liposome aggregation studies 45

2.3: Results 45

2.4: Discussion 57

Chapter 3: Interaction of toposome from sea-urchin yolk granules with dimyristoyl phosphatidylserine model membranes: a ^{2}H-NMR study 68

3.1: Introduction 69

3.2: Materials and Methods 72

3.2.1: Purification of toposome 72

3.2.2: Preparation of multilamellar vesicles 73

3.2.3: Solid-state deuterium-NMR 73

3.3: Results and Discussion 75

Chapter 4: Biochemical analysis of the interaction of calcium with toposome, a major protein component of the sea urchin egg and embryo 106

4.1: Introduction 107

4.2: Materials and Methods 109

4.2.1: Preparation of yolk granule protein extracts and fractionation by ion exchange chromatography 109

4.2.2: Lipid stamping 110

4.2.3: Circular dichroism spectroscopy measurements 110

4.2.4: Toposome digestion with chymotrypsin 111

4.2.5: Endogenous tryptophan fluorescence measurements 111

4.2.6: Displacement assay 112

4.3: Results and Discussion 112

Chapter 5: Localization of toposome in the sea urchin egg and embryo 129

5.1: Introduction 130

5.2: Materials and Methods 132

5.2.1: Growth of embryos 132

5.2.2: Fixation and embedding of eggs and embryos for electron microscopy 132

5.3: Results 134

5.4: Discussion 146

Chapter 6: Discussion 150

5.1: Overview 151

5.2: References 158

List of Figures

Figure 1.1: The adult sea urchin 3

Figure 1.2: The phylogenetic position of the sea urchin relative to other model systems and humans 6

Figure 1.3: The amino acid translation of MYP cDNA from *Strongylocentrotus purpuratus* 19

Figure 1.4: A scale diagram of MYP showing the predicted transferrin-like, iron binding domains 31

Figure 1.5: Proposed model of MYP as an iron transporter 33

Figure 2.1: Sodium dodecyl sulfate gel polyacrylamide gel electrophoretic analysis of yolk granule proteins eluted from a Q-Sepharose Fast Flow column 46

Figure 2.2: Quantification of calcium binding to toposome 49

Figure 2.3: Measurement of the alpha helical content of toposome as a function of calcium concentration and the determination of the calcium concentration dependence on toposome binding to liposomes 52

Figure 2.4: Correlation between the change in the emitted fluorescence of toposome as a function of calcium concentration and the effect of calcium on toposome-driven liposome aggregation 55

Figure 2.5: Comparative analysis of the calcium-concentration dependence of toposome tertiary structure in the presence and absence of multilamellar liposomes 58

Figure 2.6: Putative role of toposome in the patch hypothesis of membrane repair 66

Figure 3.1: ^{2}H-NMR spectra at selected temperatures for DMPS-d_{54}, DMPS-d_{54} plus calcium (100 μM Ca^{2+}) and DMPS-d_{54} plus Ca^{2+} (100 μM) and toposome 77

Figure 3.2: Depaked spectra at 40°C for DMPS-d_{54} and DMPS-d_{54} in the presence of Ca^{2+} (100 μM) and toposome 80

Figure 3.3: ^{2}H-NMR spectra at selected temperatures for DMPS-d_{54} plus toposome and calcium 82

Figure 3.4: Temperature dependence of first spectral moments (M_1) for the spectra in Figures 1 and 3 85

Figure 3.5: Temperature dependence of average quadrupole echo decay time (T_{2e}) extracted from Figures 1 and 3 89

Figure 3.6: Quadrupole Carr-Purcell_Meiboom-Gill (q-CPMG) echo train decays for DMPS-d_{54} and DMPS-d_{54} plus toposome in 100 μM Ca^{2+} 95

Figure 3.7: Results of simultaneously fitting q-CPMG decays for DMPS-d_{54} and DMPS-d_{54} plus toposome (lipid:protein = 80,000:1) in 100 μM Ca^{2+} 101

Figure 4.1: Atomic force microscopic analysis of toposome binding to phosphatidyl serine bilayers in the presence of various concentrations of calcium 114

Figure 4.2: Determination of the thermal unfolding profile of toposome under various conditions 117

Figure 4.3: SDS-PAGE analysis of the chymotryptic digestion products of toposome in the presence or absence of calcium and /or liposomes 119

Figure 4.4: Tryptophan fluorescence emission spectra of toposome in the presence of increasing concentrations of various metal ions 123

Figure 4.5: Displacement of toposome-bound calcium by selective metal ions 125

Figure 5.1: Western blot analysis of sea urchin eggs using the anti-toposome antiserum 135

Figure 5.2: Immunogold labeling of sea urchin eggs 137

Figure 5.3: Immunogold labeling of various stage embryos (1 and 9 HPF) 139

Figure 5.4: Immunogold labeling of various stage embryos (24, 45 and 69 HPF) 142

Figure 6.1: Working Model for the known cell-cell adhesive activity of toposome in the sea urchin embryo 154

List of Tables

Table 1.1: MYP amino acid composition 18

Table 5.1: Quantitation of immunogold labeling 144

Co-authorship Statement

Chapter 2 was published in Development growth and differentiation. The experimentation depicted in Figure 2.2 was carried out by Dr. John Robinson. In Figure 2.3, the determination of the calcium concentration dependence on toposome binding to liposomes was initially carried out by Aruni Perera. However, I did repeat and verify her data.

Chapter 3 was published in the Biophysical Journal. I was assisted with solid-state NMR by both Jason Emberly and Dr. Michael Morrow. Figure 3.7, which is the results of simultaneously fitting q-CPMG decays, was carried out and analyzed solely by Dr. Michael Morrow.

Chapter 4 was published in the Journal of Cellular Biochemistry. I was assisted with atomic force microscopy by both Ming Sun and Dr. Erika Merschrod.

Chapter 5 has yet to be published. However, the experimentation depicted in Figure 5.1 was carried out by Dr. John Robinson.

List of Abbreviations

BL	basal lamina
BPB	bromophenol blue
BSA	bovine serum albumin
CAMs	cell adhesion molecules
CBB	coomassie brilliant blue R-250
CD	circular dichroism
CG	cortical granule
CS	cell surface
DTT	dithiothreitol
ECM	extracellular matrix
EDTA	ethylenediaminetetraacetic acid
EGTA	ethylenebis (oxyethylenenitrilo) tetraacetic acid
HL	hyaline layer
HPF	hours post fertilization
LV	lipid vacuole
MFSW	Millipore filtered sea water
OD	optical density
PM	plasma membrane
SDS	sodium dodecyl sulfate
SDS-PAGE	sodium dodecyl sulfate polyacrylamide gel electrophoresis
TCA	trichloroacetic acid
UV	ultraviolet

Chapter 1: Introduction

1.1 The sea urchin

Sea urchins are small spiny sea creatures of the phylum Echinodermata, which also includes starfish, sea cucumbers, brittle stars, and crinoids. Like other echinoderms, the sea urchin exhibits a fivefold symmetry, called pentamerism. The pentamerous symmetry is not obvious at a casual glance but is easily seen in the dried shell of the urchin. On the oral surface of the sea urchin is a centrally located mouth made up of five united calcium carbonate teeth or jaws. The spines, which in some species are long and sharp, serve to protect the urchin from predators. Sea urchins feed mainly on algae, but can also feed on a wide range of invertebrates such as mussels, sponges and brittle stars.

Sea urchins are remarkably long-lived with life spans of *Strongylocentroitid* species extending to over a century and are highly fecund, producing millions of gametes each year (Sea urchin genome sequecning consortium, 2006). Adult urchins are typically from 3 to 10 cm in diameter and common colors include black and dull shades of green, olive, brown, purple, and red (Fig. 1.1).

Although a research model for developmetal biologists for a century and a half, few were aware of a very important characteristic of sea urchins, a character that directly enhances its significance for genomic analysis: echinoderms (and their sister phylum, the

Figure 1.1. The adult sea urchin. (A) The purple sea urchin (*Strongylocentrotus purpuratus*) (B) The green sea urchin (*Lytechinus variegates*) (C) The red sea urchin (*Strongylocentrotus franciscanus*) (D) The black crowned sea urchin (*Centrostephanus coronatus*). Source, http://www.liveaquaria.com.

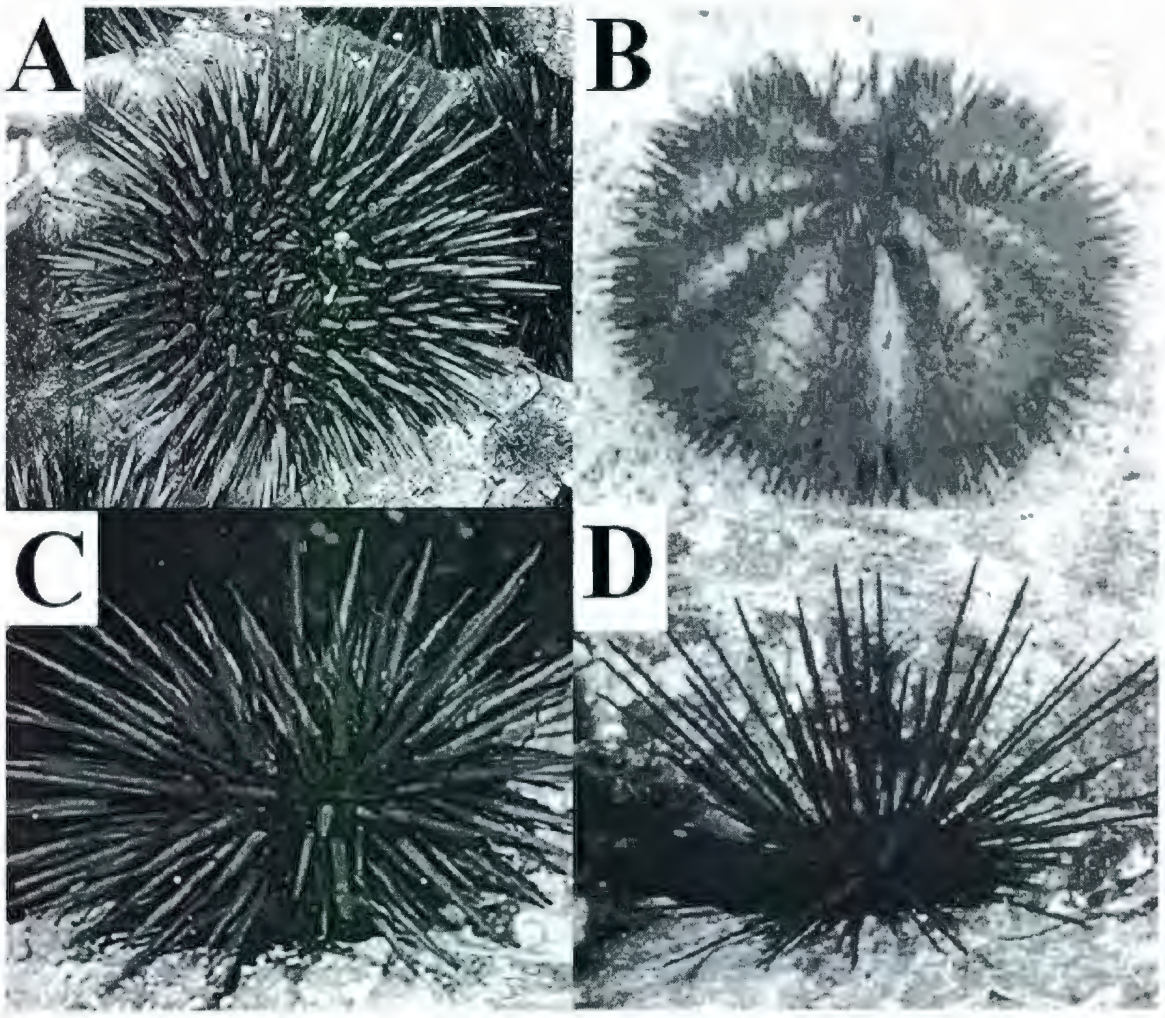
A
B
C
D

hemichordates) are the closest known relatives of the chordates (Fig. 1.2, Sea urchin genome sequencing consortium, 2006).

1.2 The sea urchin – an ideal model for developmental studies

The sea urchin came into prominence in embryology in the mid- to late 19th century and since then has provided great insight into developmental processes such as the chromosomal basis of development, maternal determinants, fertilization and maternal messenger RNA (Pederson, 2006). More recently, the sea urchin embryo has enabled researchers to conduct the most detailed gene expression analyses of any embryonic event (mesoendoderm specification) and this represents the most comprehensive dissection of gene regulatory networks in any metazoan creature (Pederson, 2006). The sea urchin became an attractive animal system for developmental studies for a number of simple reasons – the ease of obtaining large numbers of gametes from an abundant and gravid animal, the ability of those gametes to be fertilized *in vitro* and the ability of these embryos to be grown as synchronous cultures for biochemical studies. In addition, the eggs and early embryos of many commonly used species are beautifully transparent and have a relatively small number of cells in comparison to more complex organisms (the pluteus stage embryos of *Strongylocentrotus purpuratus* consist of approximately 1,500 cells, Angerer and Davidson, 1984). Cell lineages have been mapped and a number of molecular markers for specific gene products are available to follow the differentiation of cells during development. For example, the cytoskeletal actin genes, CyIII (Cox *et al.*, 1986) and Spec (Lynn *et al.*, 1983) (*Strongylocentrotus purpuratus* ectoderm specific), are expressed by aboral ectoderm cells. As well, the utility of the embryo has been

Figure 1.2. The phylogenetic position of the sea urchin relative to other model systems and humans (Sea urchin genome sequecning consortium, 2006).

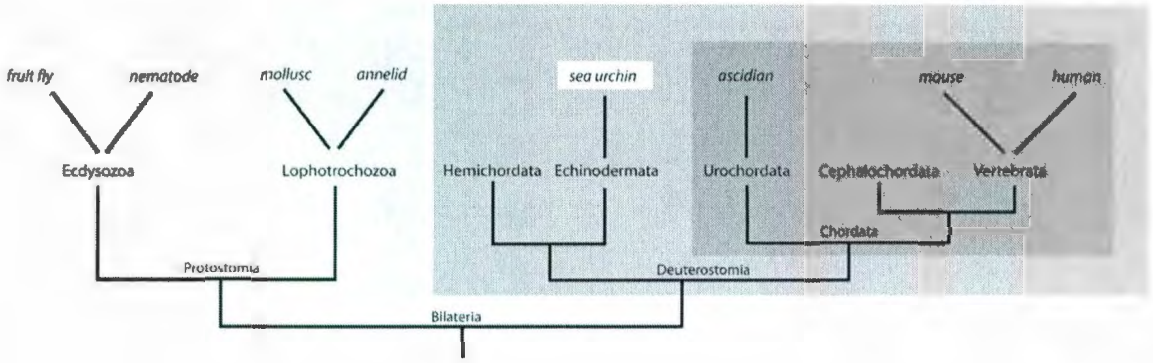
fruit fly
nematode
mollusc
annelid
sea urchin
ascidian
mouse
human
Ecdysozoa
Lophotrochozoa
Hemichordata
Echinodermata
Urochordata
Cephalochordata
Vertebrata
Chordata
Protostomia
Deuterostomia
Bilateria

enhanced by the ability to produce and culture transgenic embryos (Flytzanis *et al.*, 1985; Cameron and Davidson, 1991).

The sea urchin is also a widely used animal model in studying the function of the yolk granule, an abundant organelle in the sea urchin egg and embryo, during embryonic and larval development. Due to the abundance of the yolk granule in the sea urchin egg and embryo, it is possible to obtain large amounts of material for biochemical studies during development.

1.3 The yolk granule

Many animals store yolk in their eggs to be used as an energy source until the embryo can develop the tissue specializations necessary feed. The regulation of yolk storage during oogenesis and its subsequent utilization is crucial for development, and has been a major focus of study involving the yolk-laden eggs of chicken, frogs and flies. In some species, the yolk granules are stored in a separate compartment known as the yolk sac. A single layer of serosal cells line the yolk sac, which allows the yolk material to be separated from the rest of the cytoplasm. However, in echinoderms, the yolk sac is absent and the yolk granules are found spread throughout the cytoplasm of the eggs and embryonic cells.

The yolk granule is the most abundant membrane-bounded organelle present in the eggs, embryos and early larvae of the sea urchin. Yolk granules are evenly distributed throughout the cytoplasm, occupying approximately one-third of the

cytoplasmic volume. The yolk granule, which is spherical or oval in shape, is a relatively large organelle having a diameter of 1-2 μm with a membranous covering that is approximately 9 nm thick (Armant *et al.*, 1986). The yolk granule contains subparticles that resemble membrane-bound vesicles that range in diameter from 10-50 nm and are found in this organelle throughout development (Ii *et al.*, 1978; Armant *et al.*, 1986; Yokota *et al.*, 1993). These subparticles are thought to be lipoproteins, similar to VLDL, constituting about 40% of the total yolk material (Ii *et al.*, 1978).

The morphology of the yolk granule changes throughout embryonic development. As observed by electron microscopy, sea urchin yolk granules can be classified into four types according to their morphology; (i) dense, (ii) intermediate, (iii) sparse and (iv) lysosomal (Yokota *et al.*, 1993). As embryonic development proceeds, the prevalent dense yolk granules in sea urchins are gradually replaced by less dense structures. In the unfertilized egg, the majority of the population of yolk granules are dense, whereas by the gastrula stage, these dense granules are rarely observed. These morphological changes may be a direct result of the biochemical changes occurring in these granules. For example, high molecular weight glycoproteins present in the yolk granules of sea urchins are proteolytically processed into smaller molecular weight species as embryonic development proceeds (Scott and Lennarz, 1988; Yokota and Kato, 1988; Gratwhol *et al.*, 1991; Mallya *et al.*, 1992; Scott *et al.*, 1990; Reimer and Crawford, 1995). In addition, the lipid composition of the yolk granules also undergoes dynamic changes during embryonic development (Pelley, Davis and Robinson, unpublished data). These compositional changes of the yolk lipids are observed as early as 10 minutes post-

fertilization. Also, it has recently been shown that the yolk granule is actively involved in protein export, another process that could be partially responsible for the morphological changes of the sea urchin yolk granule during embryonic development (Gratwohl *et al.*, 1991; Mayne and Robinson 1998, 2002).

During the early stages of embryonic development, the yolk granules of sea urchins become slightly acidified. The same also occurs in certain species of insects such as the stick insect *Carausius morosus* (Fausto *et al.*, 2001). However, the time taken for acidification of the yolk granule varies from species to species. For instance, in the sea urchin *Strongylocentrotus purpuratus*, the acidification is complete by 6 hours post-fertilization, while in the sea urchin *Lytechinus pictus*, acidification of the granules takes an additional 42 hours (Mallya *et al.*, 1992). In the case of *Strongylocentrotus purpuratus*, the pH drops 0.7 units, from a pH of 6.8 to a pH of 6.1. There are two possible mechanisms for the acidification of the sea urchin yolk granules; (i) the activation of a Na^+/H^+ ATPase already present in the yolk granule membrane or (ii) the fusion of lysosomes or other endosomal vesicles with the yolk granules (Scheul *et al.*, 1975; Yokota *et al.*, 1993). A number of experiments carried out in both the sea urchin *Strongylocentrotus purpuratus* and the stick insect *Carausius morosus* support the notion that the yolk granule acidification is a direct result of the Na^+/H^+ ATPase proton pump (Mallya *et al.*, 1992; Fausto *et al.*, 2001).

1.4 The function of the yolk granule

The eggs of many organisms including amphibians, birds, insects, annelids, fish and echinoderms contain yolk. In amphibians, insects, annelids and echinoderms the yolk is stored in organelles variously named yolk granules, - platelets or –bodies. This terminology is used interchangeably and appears to describe the same membrane-bounded organelle. The classical embryological view of yolk was that it normally served as a transient, storage form of nutrients to be used by the developing embryo and larvae. However, this view of yolk is not universally accepted and a growing body of evidence suggests that, organisms whose cytoplasm contains yolk organized into membrane-bounded structures, possess an organelle which is considerably more dynamic than that expected of a benign, nutrient storage compartment. For instance, in early embryos of the insect, *Blattella germanica*, a cysteine protease was found labeled in only a sub-population of yolk granules. As development proceeded, the protease was found to be distributed to all yolk granules. Interestingly, label spread throughout the yolk granule population coincident with the "budding-off" of small vesicles from labeled yolk granules and their fusion to unlabeled granules (Giorgi *et al.*, 1997). Collectively, these results suggest that yolk granule membranes can engage in both budding and fusion reactions. Liao and Wang (1994) identified yolk granules of the bull frog (*Rana catesbeiana*) oocyte as the storage compartment for ribonuclease. The majority (94%) of activity was localized in yolk granules with the remaining 6% found in the cytoplasm (Wang *et al.*, 1995). These findings have been presented as evidence that yolk granules serve as a compartment that regulates the cytoplasmic access of some intracellular enzymes. In *Xenopus laevis*, Outenreath *et al.* (1988) identified a cell surface lectin that

was stored in the yolk granules prior to export. Yamada *et al* (2005) have shown that ecdysteroid-phosphates are released from the yolk granules to the cytosol, where they are predicted to participate in the regulation of morphological events during embryonic development. These results collectively establish the yolk granule as a dynamic storage compartment.

In the sea urchin, the classical view of the yolk granule was that it provided nutrition for the developing embryo and larvae (Williams, 1967). Schuel *et al.* (1975) also suggested that the yolk granules of sea urchins were the site of catabolism due to the presence of several acid hydrolases, which could generate amino acids, fatty acids and carbohydrates from stored macromolecules. However, it was not clear whether these acid hydrolases were from a yolk granule or lysosomal origin. Currently, there is little direct evidence supporting this view of yolk granule function in the sea urchin. In particular, the finding that the composition of the yolk granule is constant throughout embryonic development and that starvation does not lead to the loss of granule components (protein, lipid, carbohydrate and nucleic acid) suggests a non-nutritional role for this organelle (Armant *et al.*, 1986; Scott *et al.*, 1990). In *Strongylocentrotus purpuratus*, the yolk granules and their associated glycoproteins are usually not found past the seventh day of the feeding larval stage; starvation does not accelerate this process.

Recent data suggest that the sea urchin yolk granule is a dynamic organelle, involved in a variety of cellular processes, which contradicts a static, benign role for this

granule. Several studies have shown that yolk granules can act as a storage compartment for proteins destined for export to the cell surface. Mayne and Robinson (1998, 2002) have shown that both the 41 kDa collagenase/gelatinase and HLC-32, protein components of the hyaline layer, were found to be localized in the yolk granules of unfertilized eggs. However, as development proceeded, these proteins were detected on the embryonic cell surface. Similarly, it was shown that toposome, a protein localized in yolk granules, was transported to the plasma membrane (Gratwohl *et al.* 1991). These results collectively establish the sea urchin yolk granule as a dynamic storage compartment.

In addition, the yolk granule also appears to be required for membrane repair in the sea urchin egg and embryo. Plasma-membrane disruption is a normal and common cell event in many organisms, including the sea urchin (McNeil, 1993). Resealing is the membrane-repair process that allows either a cell or an organism to survive disruption and maintain viability. Plasma membrane lesions are resealed by a patching mechanism (McNeil, 1993). During disruption of the plasma membrane, an influx of sea water results in a high local concentration of calcium (10 mM) in the vicinity of the lesion which triggers fusion between individual yolk granules. Once tethered together, the yolk granules then fuse with the plasma membrane in a rapid, organized manner that patches the damaged area (McNeil, 1993; McNeil *et al.*, 2000). This reaction restores the structural integrity of the membrane. Isolated yolk granules exhibit three important

resealing compatible properties: (i) high calcium threshold, (ii) rapid kinetics and (iii) an impressive capacity to form large membrane barriers (McNeil et al. 2000).

1.5 Yolk proteins

The synthesis of yolk proteins in various tissues and their accumulation in oocytes is referred to as vitellogenesis. This process has been extensively studied in both invertebrate and vertebrate animals. In invertebrates, vitellogenin-derived proteins are produced in the intestine of both echinoderms and hermaphroditic nematodes (Kimble and Sharrock, 1983) and in the fat body of female insects (Wojchowski *et al.*, 1986). In vertebrates, these proteins are synthesized in the liver of avians (Bergink *et al.*, 1974; Tata, 1976) and amphibians (Wahli *et al.*, 1981).

In sea urchins, yolk granule proteins are synthesized by the intestine and secreted into the coelomic fluid (Harrington and Easton, 1982). From the coelom, yolk proteins are absorbed by nutritive phagocytes (accessory cells) of both the ovaries and testis. In females, yolk proteins are transported during the vitellogenic phase of oogenesis from the nutritive phagocytes to the growing oocytes where they are packaged into the yolk granules that are stored in matured eggs. In males, yolk proteins are suggested to serve as a nutrient store for spermatogenesis (Unuma *et al.*, 1998). Interestingly, these proteins do not completely fit the profile of other known vitellogenins as they are deposited in both the testes and ovaries of the sea urchin. In other animal species (nematode, insects, and vertebrates), vitellogenins are specific to females.

Sea urchin yolk proteins range in size from 35- to 300 kDa and comprise 10-15% of the total egg protein, of which the majority is glycosylated (Ichio *et a*l., 1978; Ozaki, 1980; Harrington and Easton, 1982; Kari and Rottmann, 1985). Yolk granule glycoproteins are predominantly N-linked and a comparison of their physical and chemical properties between different sea urchin species revealed striking similarities in amino acid and monosaccharide composition and pI values (Scott and Lennarz, 1988).

1.6 Toposome

1.6.1 Toposome - a brief introduction

Toposome is derived from the major yolk protein (MYP, 200 kDa) by proteolytic processing in the oocyte. The MYP is found in the coelomic fluid of both sexes and it is estimated that it comprises approximately 50% of the total protein in the coelomic fluid as well (Harrington and Easton, 1982; Cervello *et al.*, 1994). However, processing of MYP into toposome is oocyte specific.

Toposome was originally identified from homogenates of eggs and embryos from three species of sea urchins (Malkin *et al.*, 1965). The major protein component of the yolk granule is toposome, representing approximately 8% of the total egg protein and 50 % of the total yolk protein in the sea urchin (Kari & Rottmann 1980). Toposome has historically been classified as a vitellogenin based on its abundance and packaging into yolk granules (Shyu *et al.*, 1986, 1987). However, its precursor, MYP, is not a female-

specific protein and is synthesized and stored in cells of the testis (Shyu *et al.*, 1986; Unuma *et al.*, 1998). Toposome, isolated from the sea urchin *Tripneustus gratilla* or *Paracentrotus lividus* appears to be composed of six identical polypeptides of 160-170 kDa in size, depending on the species (Noll *et* al., 1985). Brooks and Wessel (2002) cloned the full-length cDNA of MYP from *Strongylocentrotus purpuratus*. The sequence contains 4,071 base pairs of open reading frame coding for 1357 amino acids (Fig. 1.3). The overall amino acid composition as predicted from cDNA matches the profile of amino acids previously reported (Table 1.1) (Kari and Rottman, 1985; Scott and Lennarz, 1989; Brooks and Wessel, 2003). In addition, the theoretical pI (7.04) from the cDNA is in the range of that previously measured for the native protein (7.0 – 7.8) (Table 1.1, Scott and Lennarz, 1989; Brooks and Wessel, 2003).

1.6.2 Transport and packaging of MYP in the sea urchin during gametogenesis

The major yolk protein is predominantly synthesized in the intestine of the adult sea urchin and is secreted into the coelomic fluid (Shyu *et al.*, 1986). Before gametogenesis, MYP is stored in nutritive phagocytes. During oogenesis, MYP is transported from the nutritive phagocytes to the growing oocyte where it is stored in yolk granules (Fuji *et al.*, 1969; Harrington and Ozaki, 1986; Ozaki *et al.*, 1986; Unuma *et al.*, 1998).

Gametogenesis is tightly linked to the growth and differentiation of the nutritive phagocytes. In both sexes of the sea urchin, the follicular lumen of the gonads is filled with MYP-laden nutritive phagocytes prior to gametogenesis. As gametogenesis

proceeds, the nutritive phagocytes regress as the gametes develop. In females, the accumulation of toposome, a direct result of MYP processing, in the yolk granules of ripening ova is coincident with the depletion of MYP in the regressing nutritive phagocytes (Ozaki *et al.*, 1986; Harrington and Ozaki, 1986). During this process, the MYP storage granules in the nutritive phagocytes break down and MYP is transported to the periphery of the oocytes where it is endocytosed by a dynamin-dependent mechanism and proteolytically processed (Takashima and Takashima, 1966; Tsukahara and Sugiyama, 1969; Tsukahara, 1971; Geary, 1978; Brooks and Wessel, 2003; Brooks and Wessel, 2004). In males, the regressing nutritive phagocytes are depleted of MYP as spermatocytes develop. Interestingly, the protein does not appear in the developing sperm cells (Unuma *et al.*, 1998).

1.6.3 Localization of toposome in the sea urchin egg and embryo

The ultrastructural localization of toposome has been examined in a number of laboratories by immunogold labeling (Gratwohl *et al.*, 1991; Scott and Lennarz, 1991). However, conflicting results have been obtained. Scott and Lennarz (1989) show that toposome is stored exclusively in the yolk granules and that the amount of labeling remains consistent throughout development. Conversely, Gratwohl *et al.* (1991) reveal that in the egg, toposome is present on the surface of the plasma membrane, as well as stored in yolk granules and in the electron dense lamellar compartment of the cortical granules. The localization of toposome in the sea urchin egg and embryo will be presented in Chapter 5.

1.6.4 Proteolytic processing of toposome

As embryonic development proceeds, toposome is proteolytically processed post-fertilization into smaller molecular mass species, as the result of a cathepsin B-like protease, sensitive to thiol-protease inhibitors and also the serine protease inhibitor, benzamidine (Kari and Rotman, 1985; Armant *et al.*, 1986; Yokota and Kato, 1988; Scott and Lennarz, 1989; Lee *et* al., 1989; Mallya *et al.*, 1992; Yokota *et al.*, 2003). This proteolytic processing into smaller molecular mass species is developmentally controlled, and as a result, the protein profile is specific to each stage of development. These changes in the protein profile can be easily monitored using reducing SDS-PAGE analysis of toposome from different developmental stages. Despite the proteolytic cleavage of toposome, the total mass of the non-reduced protein remains constant throughout embryonic development. The proteolytic products of toposome remain covalently bound to each other as a result of numerous intrachain disulfide bonds. Interestingly, the functional significance of toposome processing remains to be determined.

Figure 1.3. The amino acid translation of MYP cDNA from *Strongylocentrotus purpuratus*

MRAAILFCLVASSMAVPSGSLGSRPGTCPPQPSDQVMIEATRCSYVYGLTWDWN
CNSQGQENYKCCQYENDIRICVPPIPADVDEEVGVEQPSQSVDQVRQAIQKTQDF
IRKVGLYPAPDQRRRTTPTPDTVRWCVSSRCQMTKCQRMVSEFTYSPNMVPRK
QWKCTQATSQEQCMFWIEQGWADIMTTREGQVYSANTTFNLKPIAYETTINDQQ
PEIQILKHYQNVTFALKSSRLVNPNTFSELRDKTTCHAGIDMPDFDMPASFADPV
CNLIKEGVIPVTGNYIESFSDFVQESCVPGVLNMTYNKNGTYPLSLVTLCEDQQY
KYSGIKGALSCLESGKGQVTFVDQKVIKKIMSDPNVRDNFQVVCRDESRPLDEEI
FTDVTCHVGHTARPTIFINKNNTQQKETDIKTLVVKMMELYGNTDRDVNFNIFDS
SVYDCGKCQMTGKPLNKNLIFLEESNTMKIVDDSKVYAGEVYAAYNVCSKLVP
KPRAKICVTNVTEYEACRRFKGIAENIPEVKKVAWGCVLANSSIECMQAVHNNT
ADLFKANPMETFIAGKEFLLDPLMSVHRNDSVTMNHTYTRTLAVIKRSSLAKFP
GLLSVPEGQPKYIKDLWKLKICSAGLKNFSAFHSPIGYLLANGTIPRIGSVFESVN
RYFQATCVPEIEPETWRLDSDLLLGREMNWGFSSLNMYNFTGQEWLLWNTPAT
WNFLTYNRKVSTGLDIKKLIELKKQNLTSHIFNQNLSSPRNVELLDDLVGVEGISD
LVKGVQDTIGPEGKQKMNMLRDRLSNSFPNFEAVRTLSDKVDIVNKMKDARQQ
RLQNKDHPFGNVIQETFQGHLMVDVFSKLLELRSDKISTLEEIISHVKTIPYLTDFK
DVEITTVLKHPAIMSYVEIYFPRLSQTFVEPFDNVELREREFNRYTNPLWLSPKVH
TYLDLVKNHQTEITKTCNSNLPLNFKGYEGALRCLKSGVADLASSTSRPSVTRTL
RDTDLSTGWVHLQRPPPSLPQRQVVEIDVNMDIAKVCNFGEVMNPVLVTAYNTS
GSWRWNITKALMIAHQSVALPALFGEGTVMGKDYDMLLPIAPLNQSYQPFLGSK
PLRSMEAIVKASSYDWFKDQTGICYGETYTNIVKQRNETCQAIVKDVTCVGTPR
MKKISVGRFGAKQFKMIKMCSRPSKFVRKMADFQCDNGFGYLKPVITAVACEC
MLCEEMIEYNTSFTEDNMWSDVSNKYVLTGEQDIYRQIPIWGNNSYFYDHTLNK
NFELGNHSIIVEHVQTVVVERPSPGILSQVNSEVDPEVQVQMDSASLTKTCETVW
NGQSWLPERFQGYKTSGSCVVPETGANAKSRVDRFRQIMQRKQQLVDHHH

Table 1.1. MYP amino acid composition. The amino acid composition of *Strongylocentrotus purpuratus* toposome predicted from cDNA ([+]Brooks and Wessel, 2002) recapitulates what was biochemically determined (*Scott and Lennarz, 1989). ND, not determined.

Residue	Cognate cDNA sequence [+]	Experimental [*]
Ala	4.4	5.2
Arg	4.6	6.2
Asx	11.4	13.0
Cys	3.0	0.5
Glx	10.9	14.1
Gly	5.0	3.5
His	1.7	1.5
Ile	5.5	5.5
Leu	7.3	8.0
Lys	6.3	7.0
Met	3.1	0.5
Phe	4.1	5.5
Pro	5.3	7.0
Ser	7.1	4.2
Thr	6.9	6.0
Trp	1.6	ND[a]
Tyr	3.3	3.5
Val	8.3	8.0
pI	7.04	7.0 – 7.8

Studies conducted with different species of sea urchins revealed that the protein profile of toposome processing during development is species specific. In *Strongylocentrotus purpuratus*, toposome has an apparent molecular mass of 160 kDa (Scott *et al.*, 1990; Scott and Lennarz, 1988). As embryonic development proceeds, toposome is proteolytically processed into smaller molecular weight species of 115-, 108-, 90-, 83- and 68 KDa. In *Hemicentrotus pulcherrimus*, toposome has an apparent molecular mass of 178 kDa and is proteolytically processed into smaller molecular weight species of 114-, 94-, 72-, and 61 kDa (Yokota and Kato, 1987; Yokota *et al.*, 1993). Toposome, isolated from the sea urchin *Anthocidaris crassispina*, has an apparent molecular mass of 180 kDa and is processed into smaller molecular weight products of 112-, 92-, 70-, and 56 kDa (Yokota and Kato, 1987). Studies carried out in insect models have also shown that yolk proteins undergo limited proteolysis to generate a number of smaller molecular weight species (Fausto *et al.*, 2001b; Cecchettini *et al.*, 2001).

1.6.5 Proteolysis of toposome is regulated by the acidification of yolk granules

As mentioned earlier, toposome undergoes limited, step-wise proteolytic processing during early development as the result of a cathepsin B-like protease (Kari and Rotman, 1985; Armant *et al.*, 1986; Yokota and Kato, 1988; Scott and Lennarz, 1989; Lee *et* al., 1989; Mallya *et al.*, 1992; Yokota *et al.*, 2003). The cleavage sites have been identified as described by Noll *et* al. (2007). The activation of toposome proteolysis by the acidification of the yolk granule was suggested by Yokota and Kato (1988) and experimentally confirmed by Mallya *et al.* (1992). In the case of both *Strongylocentrotus purpuratus* and *Lytechinus pictus* embryos, the pH activity profile of the protease

revealed that the enzyme was inactive at pH 6.8. Upon acidification of the yolk granules, which resulted in a pH drop of 0.75 pH units (final pH ~6.1-6.2), maximal activity of the protease was observed. This profile was similar to that obtained by Okada and Yokota (1990), using the partially purified yolk proteinase from another species of sea urchin.

Within the class Echinoidea, the acidification of the yolk granules and the activation of the cathepsin B-like protease vary between species. For example, in *Strongylocentrotus purpuratus*, the processing of toposome commences 6 hours post-fertilization, while in *Lytechinus pictus*, toposome processing is initiated 48 hours post-fertilization (Mallya *et al.*, 1992). However, in all sea urchin species, the cathepsin B-like protease involved in toposome processing is present in all stages of development, and it seems quite clear, that the pH regulation of the yolk granule is a key factor in controlling toposome proteolysis.

1.6.6 **Proteolytic cleavage site of MYP**

The cDNA and the deduced amino acid sequence of MYP from a number of sea urchin species have been determined and are highly homologous to one another (Unuma *et* al., 2001; Brooks and Wessel, 2002; Yokota *et al.*, 2003). Interestingly, the amino acid sequence showed that there are no cysteine residues between amino acids 661 and 944 in *Strongylocentrotus purpuratus* (Brooks and Wessel, 2002), between 653 and 938 in *Hemicentrotus pulcherrimus* (Yokota *et al.*, 2003) and between 656 and 941 in *Pseudocentrotus depressus* (Unuma *et al.*, 2001). The site of cleavage was determined by regulated proteolysis, using the cathepsin B-like thiol protease, in conjunction with

amino acid sequencing of the N-terminal region of the protein (Yokota *et al.*, 2003). The sites proteolyzed during embryogenesis were found to be located in regions devoid of cysteine. Yokota *et al.* (2003) suggest that this protein has a characteristic molecular shape with specific protease-susceptible domain(s) located on the molecule surface that permits proteolysis.

1.7 Proposed functions of toposome

1.7.1 Role of toposome in mediating cell-cell adhesion in the developing embryo

In the kingdom Animalia, differentiation of cell structures during embryonic development, tissue formation, and coordinated dynamic interactions of cells in various processes requires direct contact between cell surfaces and between cells and the extracellular matrix. The proteins through which these contacts are made are the cell adhesion molecules (CAMs). These molecules can be divided into two general classes: those that require the presence of calcium to mediate cell-cell adhesion, and those that do not (Takeichi, 1977; Edelman and Crossin, 1991; Chothia and Jones, 1997). It has also been established that calcium protects calcium-dependent CAMs from enzymatic proteolysis (Takeichi, 1977). Cell adhesion molecules such as CAMs, selectins and cadherins are all transmembranous proteins that engage in signaling processes. In contrast, toposome is clearly a peripherally associated protein (Refer to Chapter 3).

In the sea urchin embryo, removal of calcium and magesium causes the embryo to dissociate into single cells. Remarkably, upon readdition of these ions, cell-cell

interactions are restored and the dissocatied cells reaggregate spontaneously to reform a developing embryo (Herbst, 1900; Giudice, 1962). However, reaggregation is blocked in a strictly genus-specific manner by antibodies (or their Fab fragments) against purified membranes or against butanol extracts from purified membranes (Noll *et al.*, 1979; Noll *et al.*, 1981).

Toposome isolated from the sea urchin, *Paracentrotus lividus*, has been suggested to be involved in cell-cell adhesion in the developing embryo. The function of toposome in the process of cell adhesion was defined by its ability to: (i) stimulate the rate and the extent of reaggregation of dissociated blastula cells, (ii) restore aggregation and embryonic development to cells rendered reaggregation-incompetent by butanol extraction and (iii) neutralize antibodies that inhibit cell adhesion (Noll *et al.*, 1985; Matranga *et al.*, 1986). In fact, cells lacking toposome are not able to aggregate, even in the presence of calcium and magnesium. This suggests that both toposome and calcium must cooperate in a manner promoting cell-cell interactions.

It has been suggested that toposome exported to the cell surface of newly formed cells from yolk granules is responsible for position-specific cellular adhesion. This suggests that the proteolytic processing of toposome may serve to produce variants in the protein located on the cell surface in order to direct morphogenic cell movements and generate epigenetic diversity, as shown by earlier results with different toposome-specific monoclonal antibodies, which stained topologically different parts of sea urchin blastulae (Noll *et al.*, 1985; Matranga *et al.*, 1986; Matranga *et al.*, 1987). Strikingly, a

similar glycoprotein complex was discovered on the surface of imaginal disc cells of *Drosophila melongaster* by screening for monoclonal antibodies with positional specificity and has been shown to be involved in cell-cell adhesion (Wilcox *et al.*, 1984). It seems logical that prospective cell surface components, such as toposome, are stored in the egg since the development from egg to pluteus consists largely of the rapid conversion of the cytoplasmic contents into newly formed membranes.

1.7.2 Role of toposome in plasma membrane repair

Plasma membrane disruption is a normal event in many cells and occurs often in nature and in the laboratory, when for example a cell is impaled by a microneedle. Resealing is the membrane-repair process that allows cells to survive disruption, preventing the loss of irreplaceable cell types or eliminating the cost of replacing large and/or frequently injured cell types (such as skeletal muscle cells). Therefore, resealing is a necessary rapid emergency response.

Early studies on the embryonic fate of egg fragments clearly demonstrated that metazoan cells could survive rupture of their surface membranes (Wilson, 1924). Sea urchins, such as *Strongylocentrotus purpuratus,* are primarily found in the low intertidal zone and thrive amid strong wave action and areas with churning aerated water. In this environment there are many risk factors that could potentially lead to plasma membrane disruption, especially since both sexes release their gametes into the ocean where fertilization occurs. Both the eggs and fertilized embryos are at high risk of damage, and

if so, there is a need for a quick repair response. The sea urchin egg/oocyte has the capacity for surviving disruptions. A study conducted by Heilbrunn (1930a,b) described a surface precipitation reaction that occurred when a portion of the sea urchin egg surface was torn and showed that egg survival, that is, retention of intracellular compartments, depended on a calcium-initiated event. In recent experiments, the yolk granules have been shown to be the critical element in membrane resealing. During disruption of the sea urchin plasma membrane, an influx of sea water results in a high local concentration of calcium (10 mM), resulting in the tethering (aggregation) of yolk granules. Subsequently, the aggregated yolk granules fuse with the plasma membrane in a rapid, organized manner that patches the damaged area (McNeil et al., 1997, 2000). A high calcium threshold, rapid kinetics and an impressive capacity to form large membrane barriers are all important resealing compatible properties (Terasaki *et* al., 1997; McNeil *et al.* 2000).

Upon an influx of sea water, the yolk granules in the sea urchin egg become reversibly tethered to one another to form large aggregates of more than 100 granules in vitro (McNeil and Kirchhausen, 2005). Further studies have shown the existence of a high molecular weight complex associated with the yolk granules and that monoclonal antibodies directed against this protein complex could inhibit the tethering activity (McNeil and Kirchhausen, 2005). Recently, Perera *et al.* (2004) have shown that toposome is responsible for this tethering activity: (i) toposome can be dissociated from isolated yolk granules with EGTA resulting in the loss of calcium-dependent, yolk granule aggregation. Readdition of purified toposome to the EGTA-treated yolk granules

reconstituted calcium-dependent aggregation; (ii) preincubation of purified toposome with antitoposome antibody resulted in the inability of added protein to reconstitute calcium-dependent aggregation in EGTA-treated yolk granules; (iii) when isolated yolk granules were treated with trypsin, they no longer aggregated in the presence of calcium. Incubation of the trypsin-treated granules with purified toposome again restored calcium-dependent aggregation; and (iv) when purified yolk granules were preincubated with antitoposome antibody followed by assay for calcium-dependent aggregation, no aggregation occurred (Perera *et al.*, 2004).

1.7.3 Role of toposome as an iron transporter

Iron is essential for a number of protein functions and physiological processes, yet there is a need for the strict control of iron transport and storage for cell viability as free iron can generate oxidative radicals that damage lipids, proteins, and DNA (Boldt, 1999; Nappi and Vass, 2000; Brooks and Wessel, 2002). In vertebrates, transferrins are glycoproteins involved in the transportation of iron. Vertebrate transferrins are monomeric glycoproteins (~80 kDa) that consist of two domains with similar amino acid sequences, each containing a single iron binding site (Baker and Lindley, 1992). These iron binding sites are stabilized by intrachain disulfides (Baker and Lindley, 1992). Functional transferrins reversibly bind iron as Fe^{3+} with an extremely high affinity and are capable of transporting concentrations of iron at or below the nano-molar range (Baker *et al.*, 2003).

As mentioned earlier, Brooks and Wessel (2002) cloned the full-length cDNA of MYP from *Strongylocentrotus purpuratus*. When this sequence was compared with other proteins in the NCBI database, Brooks and Wessel (2002) found no similarity to reported vitellogenins. Instead, it was found to contain two transferrin-like motifs (Fig. 1.4). The MYP showed sequence identity between 24-28% to both vertebrate and invertebrate transferrins. This consensus includes serum transferrin, lactoferrin (from milk, white blood cells, and other secretory fluids), ovotransferrin (from egg white), and melanotransferrin from vertebrates and insects. Experimentally, Brooks and Wessel (2002) demonstrated that MYP was able to bind iron as determined by an overlay assay, followed by phosphoimaging. Brooks and Wessel (2002) also demonstrated, via an immunoprecipitation study, that MYP present in the coelomic fluid could also bind iron.

Brooks and Wessel (2002) have proposed a model (Fig. 1.5) for MYP (toposome) function based on their qualitative iron binding study. "MYP is present in the gut of adult sea urchins and is an abundant protein in the coelomocytes (Cervello *et al.*, 1994) where it functions to transport iron ions to various tissues in adults including the nutritive phagocytes of the ovary and testis. During gametogenesis MYP (toposome) is mobilized from these cells and in females it is selectively incorporated into the yolk granules of developing oocytes where it delivers iron to cytoplasmic metalloproteins likely through a ferritin intermediate. Toposome is processed into distinct smaller fragments in yolk granules concomitant with their acidification that occurs during embryogenesis (Mallya *et al.*, 1992). This processing could be a timed mechanism for iron release as it has been shown that many transferrins release iron at low pH".

Figure 1.4. A scale diagram of MYP showing the predicted transferrin-like, iron binding domains (Brooks and Wessel, 2002).

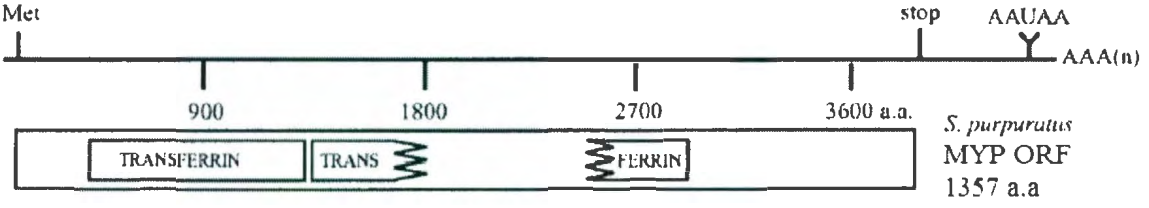
Met
stop
AAUAA
AAA(n)
900
1800
2700
3600 a.a.
TRANSFERRIN
TRANS
FERRIN
S. purpuratus
MYP ORF
1357 a.a

Figure 1.5. Proposed model of MYP as an iron transporter. Brooks and Wessel (2002) suggest that MYP is an iron transporter in the coelomic fluid. Delivery of iron to the ovary and testis may support gametogenesis and the packaging of toposome into yolk granules may serve as a mechanism of iron delivery during embryogenesis.

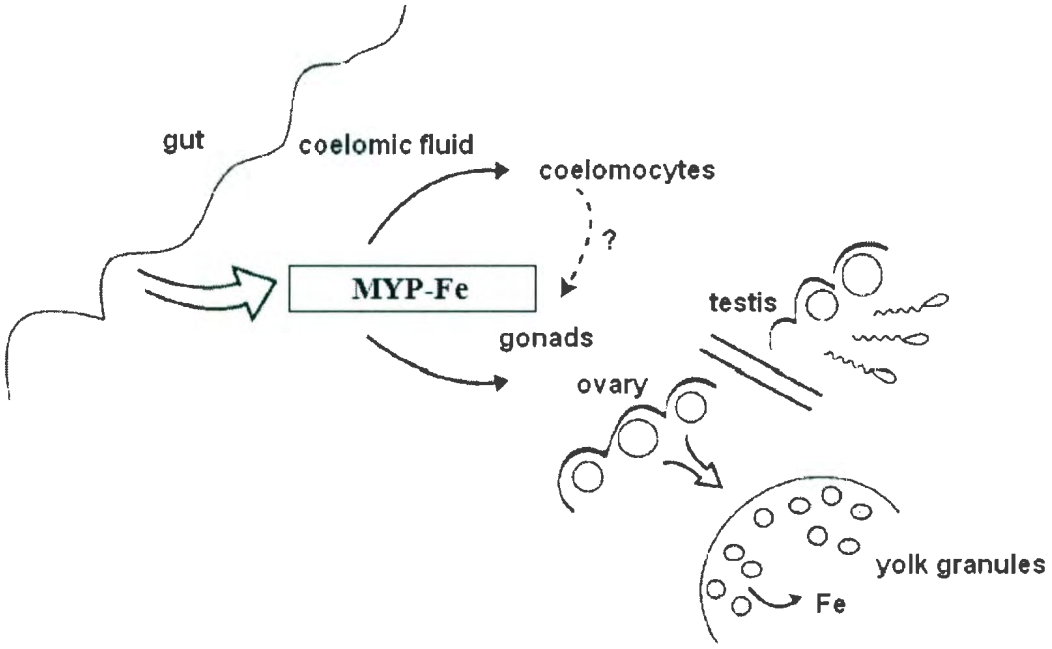
gut
coelomic fluid
coelomocytes
?
MYP-Fe
gonads
testis
ovary
yolk granules
Fe

1.8 Focus of the Thesis

To date, there has been much descriptive work done on toposome, but, there has been little or no detailed analysis of the purified protein. It has been shown that toposome, associated with the cell surface, promotes cell-cell adhesion in the developing embryo (Noll *et al.*, 1985; Matranga *et al.*, 1986) and that toposome localized to the yolk granule surface appears to be important in the yolk granule-dependent repair of damaged plasma membranes (Perera *et al.*, 2004). Previous work conducted in our laboratory has shown that toposome binding to liposomes is calcium-dependent and that toposome bound to liposomes can drive liposome aggregation (Perera *et al.*, 2004).

Generally, we are interested in studying the calcium-toposome interaction at calcium concentrations that are physiologically relevant in the marine environment. More specifically, we are interested in defining in detail: (i) the calcium-toposome interaction; (ii) how calcium facilitates toposome binding to the membrane; (iii) expanding our current understanding of the biochemical nature of toposome interaction with the membrane bilayer; (iv) probing the specificity of the calcium-binding sites on toposome and (v) carrying out a detailed immunolocalization study to identify the subcellular localization of toposome in the egg and embryo.

Initially I employed circular dichroism and fluorescence spectroscopy to detect calcium-dependent changes in the secondary and tertiary structure, respectively, of toposome and to determine if these structural changes had an effect on the ability of toposome to both bind to a membrane bilayer and/or mediate membrane-membrane

interactions. Based on the data collected, it was shown that toposome underwent two calcium concentration-dependent structural transitions: a secondary structural change occurred at low concentrations of calcium and this was followed by a tertiary structural change at much higher concentrations of this cation. Interestingly, the first structural change was required to facilitate toposome binding to bilayers while the second structural change correlated with toposome-driven, membrane-membrane interaction (Chapter 2). I then decided to focus my research on the toposome-membrane interaction. Using solid-state ^{2}H-NMR, I examined the toposome-membrane interaction in the presence of calcium concentrations known to induce either the secondary and/or tertiary structural changes in toposome. Solid-state ^{2}H-NMR allowed us to define the nature of the association of toposome with the bilayer. We found that this protein interacts peripherally with the membrane and that this interaction is facilitated by the calcium-driven secondary structural change in toposome (Chapter 3). Given the importance of these calcium-driven, structural transitions in toposome, I decided to probe the specificity of the calcium-binding sites. Our results clearly indicate that under physiologically relevant conditions, the calcium-binding sites on toposome are calcium specific and that the function(s) of toposome is regulated by calcium (Chapter 4). The subcellular localization of toposome was also determined. In summary, toposome was found on the entire cell surface as well as stored in two different compartments, the yolk and cortical granules (Chapter 5).

Collectively, our results provide a mechanistic basis for the role of toposome in mediating biologically relevant membrane–membrane interactions and suggest that under physiological conditions, the function(s) of toposome is regulated by calcium.

Chapter 2:

Biochemical analysis of a calcium-dependent membrane–membrane interaction mediated by the sea urchin yolk granule protein, toposome

[1] This chapter has been previously published; Hayley, M., Perera, A. and Robinson, J.J. 2006. Develop. Growth Differ. **48**: 401-409.

2.1 Introduction

The functional role of the yolk granule in sea urchin embryonic development has yet to be clearly defined. Yolk granules appear to be evenly distributed throughout the cytoplasm, occupying approximately one-third of the cytoplasmic volume. Present in the eggs, embryos and early larvae of the sea urchin, this abundant membrane-bounded organelle was believed to function as a reservoir of nutrients during embryogenesis (Williams, 1967). However, more recent studies reveal that the composition of the yolk granule remains constant throughout embryonic development, even during nutrient deprivation, suggesting a non-nutritional role for this subcellular organelle (Armant *et al.*, 1986; Scott *et al.*, 1990).

Recent reports have changed the traditional view of the yolk granule. The yolk granule can now be viewed as a dynamic organelle, involved in a variety of cellular processes. Yolk granules have recently been reported as a storage compartment for proteins destined for export to the cell surface. A 41 kDa collagenase/gelatinase and HLC-32, a protein component of the extra-embryonic matrix, were found to be localized in the yolk granules of unfertilized eggs. However, as development proceeds, these proteins are detected on the embryonic cell surface (Mayne and Robinson, 1998, 2002). Similarly, it was shown that toposome, a protein localized in yolk granules, was detected in the plasma membrane where it may be involved in a cell adhesion function (Noll *et al.*, 1985; Matranga *et al.*, 1986; Cervello and Matranga, 1989; Gratwohl *et al.*, 1991). The yolk granule appears also to be required for membrane repair. Plasma membrane lesions are resealed by a patching mechanism (McNeil, 1993). When plasma membrane

disruption occurs, an influx of seawater results in a high local concentration of calcium which triggers yolk granules to fuse with the plasma membrane in a rapid, chaotic manner that patches the damaged area (McNeil *et al.*, 2000). The molecular machinery required for these events remains undefined. The dynamic nature of the yolk granule is also revealed by morphological changes which accompany embryonic development (Yokota *et al.*, 1993). Electron microscopy revealed that yolk granules become increasingly less dense as embryonic development proceeds (Yokota *et al.*, 1993). This change in morphology may be a direct result of biochemical reactions, such as the proteolytic processing of glycoproteins that occur in the yolk granule during embryogenesis (Scott and Lennarz, 1989).

Yolk proteins, ranging from 35 to 300 kDa comprise 10–15% of the total egg protein, of which the majority are glycosylated (Ichio *et al.*, 1978; Ozaki, 1980; Harrington and Easton, 1982; Kari and Rottmann, 1985). The major protein component of the yolk granule is toposome, representing approximately 50% of the total yolk protein (Kari and Rottmann, 1980). With an apparent molecular mass of 240 kDa, toposome is proteolytically processed into lower molecular mass polypeptides. This processing is achieved by means of a cathepsin-like protease present in the yolk granules as embryonic development proceeds and is a direct result of the mild acidification of the yolk granule following fertilization (Scott *et al.*, 1990; Noll *et al.*, 1985; Medina *et al.*, 1988; Mallya *et al.*, 1992; Scaturro *et al.*, 1998; Fausto *et al.*, 2001; Unuma *et al.*, 2003; Perera *et al.*, 2004). The major components of toposome from the sea urchin *Strongylocentrotus purpuratus* are polypeptides of 160-, 120- and 90 kDa (Perera *et al.*, 2004). The 120- and

90 kDa species are proteolytic products of the 160 kDa polypeptide, more commonly known as the major yolk protein (Scott and Lennarz, 1989). Recent findings from Perera *et al.* (2004) suggest that toposome is peripherally associated with the yolk granule membrane. A well-defined functional role for toposome and its polypeptide products has yet to be determined. Studies conducted with the sea urchin *Paracentrotus lividus* suggests that toposome is involved in mediating cell–cell adhesion and is important in expressing positional information (Noll *et al.*, 1985; Matranga *et al.*, 1986; Cervello and Matranga, 1989). A recent finding also suggests that toposome can induce membrane–membrane interactions in a calcium-dependent manner (Perera *et al.*, 2004). Other reports of possible toposome functions suggest that the protein may be involved in the distribution of iron to components within gametes and that it may also serve as a reservoir of material for the synthesis of new materials in the gonads (Brooks and Wessel, 2002; Unuma *et al.*, 2003).

In the study reported here, we have investigated the relationship between calcium binding, toposome structure and membrane–membrane interactions. Our results suggest a two-step model linking calcium-driven structural transitions in toposome to a functional role for this protein in mediating membrane–membrane interactions.

2.2 Materials and Methods

2.2.1 Preparation of yolk granule protein extracts and fractionation by ion exchange chromatography

Strongylocentrotus purpuratus were purchased from SeaCology (Vancouver, Canada). Eggs were harvested and washed consecutively in Millipore-filtered seawater (MFSW). Preparation of the yolk granule protein extracts followed the procedure described previously with some modifications (Perera *et* al., 2004). Washed eggs were suspended in 0.5 M KCl (pH 7.0) and homogenized in a hand-held Dounce homogenizer at 0°C. The homogenate was then fractionated by centrifugation at 400 *g* for 4 min at 4°C. The supernatant then underwent fractionation by centrifugation at 2400 *g* for 10 min at 4°C. The final pellet was resuspended in 0.5 M KCl (pH 7.0) in the presence of 1 mM EDTA, fractionated by centrifugation at 50 000 *g* for 1 h at 4°C and the supernatant retained. Aliquots of the supernatant were dialyzed against starting buffer (10 mM Tris-HCl, pH 8.0) and were loaded onto a Q-Sepharose Fast Flow column (Amersham Pharmacia, Uppsala, Sweden) that had been previously equilibrated with starting buffer. The column was washed with three column volumes of buffer to remove any unbound proteins and followed by the elution of bound proteins with a NaCl step gradient (0.1–1.0 M), prepared in starting buffer. The eluted proteins were analyzed by sodium dodecyl sulfate polyacrylamide gel electrophoresis (SDS–PAGE) as described by Laemmli (1970), and the gel stained with silver (Amersham Pharmacia, Uppsala, Sweden).

2.2.2 Circular dichroism spectroscopy measurements

Circular dichroism spectra in the far-ultraviolet region (190–230 nm) were recorded using a Jasco-810 spectrapolarimeter. Aliquots of toposome (0.1 mg/mL) were dissolved and dialyzed against 20 mM Tris-HCl, pH 8.0, and the absorbance at 222 nm of the protein/reagents mixture was checked to ensure that it did not exceed 1.0. The temperature (15°C) was controlled by a CTC-345 circulating water bath and the scanning speed of the instrument was set at 100 nm/min with normal sensitivity. A water-jacketed cell (light path = 5 mm) was used and spectra were collected between 190 and 300 nm. Baselines were established using the appropriate buffers and 12 spectra were collected for each sample and averaged. Toposome was incubated with varying amounts of calcium for 30 min at 15°C prior to the collection of spectra. Secondary structural features were calculated from the collected spectra using the computer program K2d (Andrade *et al.*, 1993). This program can be accessed at www.embl-heidelberg.de/~andrade/k2d.

2.2.3 Endogenous tryptophan fluorescence measurements

Tryptophan fluorescence was measured at room temperature in a Shimadzu Model RF-540 spectrofluorimeter. The excitation wavelength was 287 nm and emission spectra were measured between 300 and 400 nm. In all cases, aliquots of toposome (50 μg) were dissolved in 20 mM Tris-HCl, pH 8.0, unless otherwise stated.

2.2.4 Toposome binding assay

Toposome was incubated with multilamellar brain lipid liposomes (10% (w/w) PI, 50% (w/w) phosphatidyl serine and several other lipids; Sigma-Aldrich Canada, Oakville, Ontario, Canada) in the presence of different concentrations of calcium for 30 min. After the 30 min incubation, the liposome pellets and supernatants were harvested by centrifugation. Both the liposome pellet and corresponding supernatant were fractionated in an 8% (w/v) SDS–PAGE gel, which was stained with Coomassie Brilliant Blue R-250 and the 160 kDa band in the pellets and supernatants was quantified by densitometry, using a gel documentation system (ChemiImager software program; Alpha Innotech Corporation). The percentage of bound protein was calculated and plotted against calcium concentration.

2.2.5 Equilibrium dialysis

One milliliter aliquots (20 μg to 50 μg) of toposome in 50 mM Tris-HCl, pH 8.0, were dialyzed for 72 h at 4°C against 100 mL of a solution containing 50 mM Tris-HCL, pH 8.0, 20 μCi 45 $CaCl_2$ (Amersham; 0.0148 Bq) and various concentrations of $CaCl_2$ (50 μm to 1.5 mM). After 72 h of dialysis the contents of the each bag were added to a liquid scintillation vial. The inside of each bag was washed with 1 mL of 50 mM Tris-HCl, pH 8.0, which was also added to each vial. The appropriate volume of dialysate in 50 mM Tris-HCl, pH 8.0, was added to liquid scintillation vials. Counting was performed in a Beckman Model LS 9000 liquid scintillation counter. The counting efficiency was determined to be 88%. In several experiments the dialysis bag was counted following washing with 50 mM Tris-HCl, pH 8.0, and no significant counts

above background were detected. All glassware used in the experiment was soaked overnight in 5 mM EDTA and washed extensively in deionized water. All plastic ware was siliconized.

2.2.6 Liposome aggregation studies

Brain lipid extract (10% (w/w) PI, 50% (w/w) phosphatidyl serine and several other lipids; Sigma-Aldrich Canada) was used to prepare multilamellar liposomes. The lipid was solubilized in chloroform: methanol (2:1) by vortexing for 4 min, evaporated to dryness under nitrogen gas and dried under vacuum for 1 h. The dried lipid film was resuspended in liposome binding buffer (50 mM Imidazole, 150 mM NaCl, 0.1 mM EDTA, pH 7.4) to a final concentration of 20 mg/mL and was hydrated at a temperature of 5°C above its phase transition temperature for 2 h. Liposome aggregation assays were performed with a fixed amount (5 μg) of toposome and varying amounts of calcium. The initial rates of aggregation (OD_{350} /min) were determined and plotted against calcium concentration.

2.3 Results

Toposome was purified from the yolk granule extract of the sea urchin egg by Q-Sepharose Fast Flow chromatography. When the fractions were analyzed by reducing SDS–PAGE, the 0.3 M and 0.4 M salt fractions were found to contain the purified toposome, consisting of three major polypeptides, with apparent molecular masses of 160-, 120- and 90 kDa (Fig. 2.1, lanes 3 and 4). Previous work has shown that the 160

Figure 2.1. Sodium dodecyl sulfate gel polyacrylamide gel electrophoretic analysis of yolk granule proteins eluted from a Q-Sepharose Fast Flow column. Soluble extracts of purified yolk granules were prepared as described in Materials and Methods. Lane 1: unbound fraction; Lane 2: 0.2 M NaCl fraction; Lane 3: 0.3 M NaCl fraction; Lane 4: 0.4 M NaCl fraction; Lane 5: 0.5 M NaCl fraction; Lane 6: 1 M NaCl fraction.

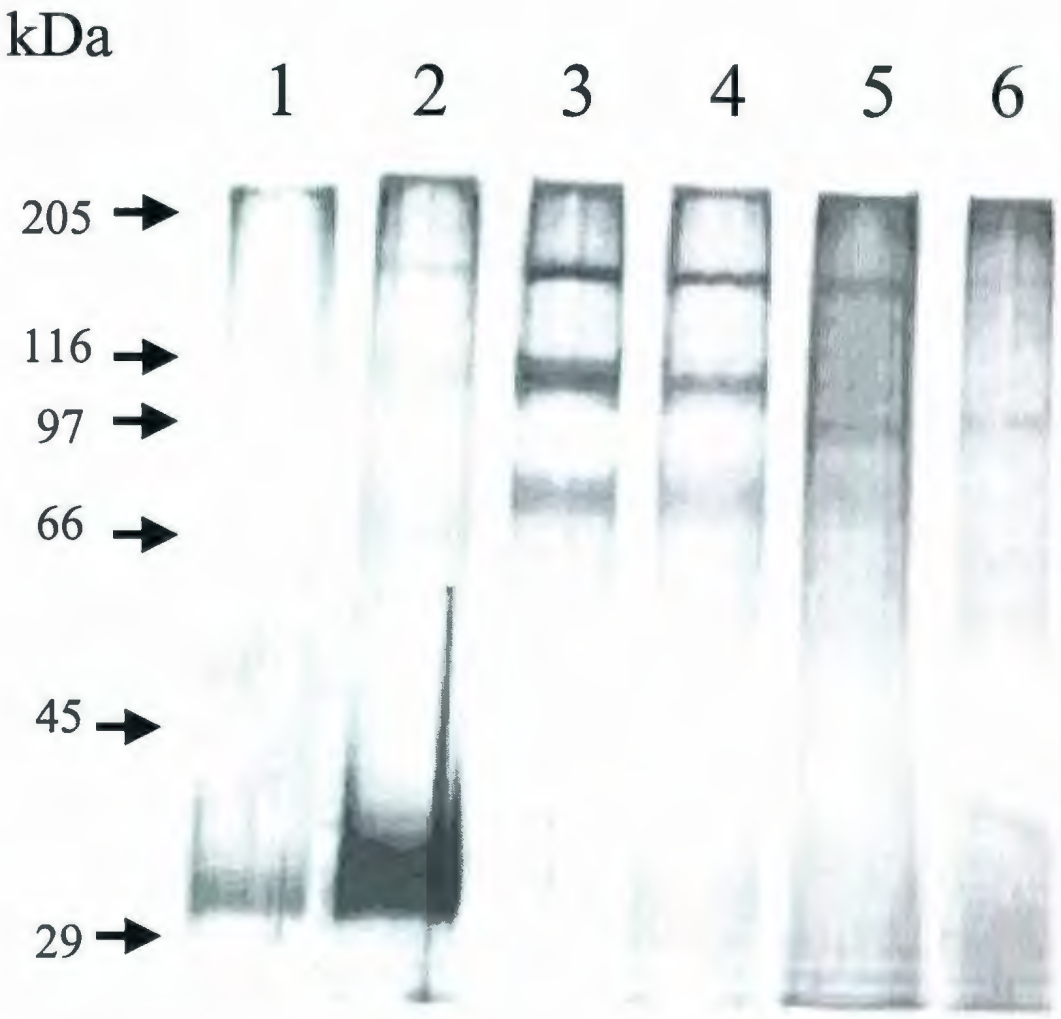
kDa
1
2
3
4
5
6
205
116
97
66
45
29

kDa protein is the major yolk granule protein (MYP) whereas the 120- and 90 kDa peptides are proteolytic products of the MYP (Perera *et al.*, 2004).

To quantify calcium binding to toposome, equilibrium dialysis measurements were performed over a range of calcium concentrations (Fig. 2.2). Monophasic binding of up to 600 moles of calcium per mole of toposome, a hexamer of six identical subunits, was detected with an intrinsic dissociation constant (calcium) of 240 μM. These weak binding sites are expected to have shared specificity for other metal ions and most likely consist of carbonyl oxygen atoms in peptide bonds as well as the oxygen atoms in the alcohol and acidic amino acids. In the presence of 10 mM calcium, the concentration of this cation in seawater, these binding sites would be expected to be fully occupied.

Circular dichroism spectroscopy was utilized to determine if calcium-induced changes in secondary structure occurred and, if so, to define the calcium concentration dependence of this effect. A significant shift in the magnitude of ellipticity occurred at 222 nm as the calcium concentration was increased from 0 to 1 mM (data not shown). The calcium-induced conformational change was characterized by an increase in alpha-helical content and a corresponding decrease in beta-sheet structure. In the absence of calcium, alpha-helical and beta-sheet contents of 3.0% and 50.0%, respectively, were recorded. Addition of calcium to 1 mM induced a secondary structural change that resulted in a conformation containing 22.0% alpha-helix and 39.0% beta-sheet. Calcium concentrations above 50 μM did not induce any further change in alpha-helical content

Figure 2.2. Quantification of calcium binding to toposome. Equilibrium dialysis was performed using a range of free calcium concentrations from 50 μM to 1.5 mM. Free calcium concentrations were determined using the EQCAL computer program from Biosoft (Cambridge, England). The data presented represents the results from three independent experiments.

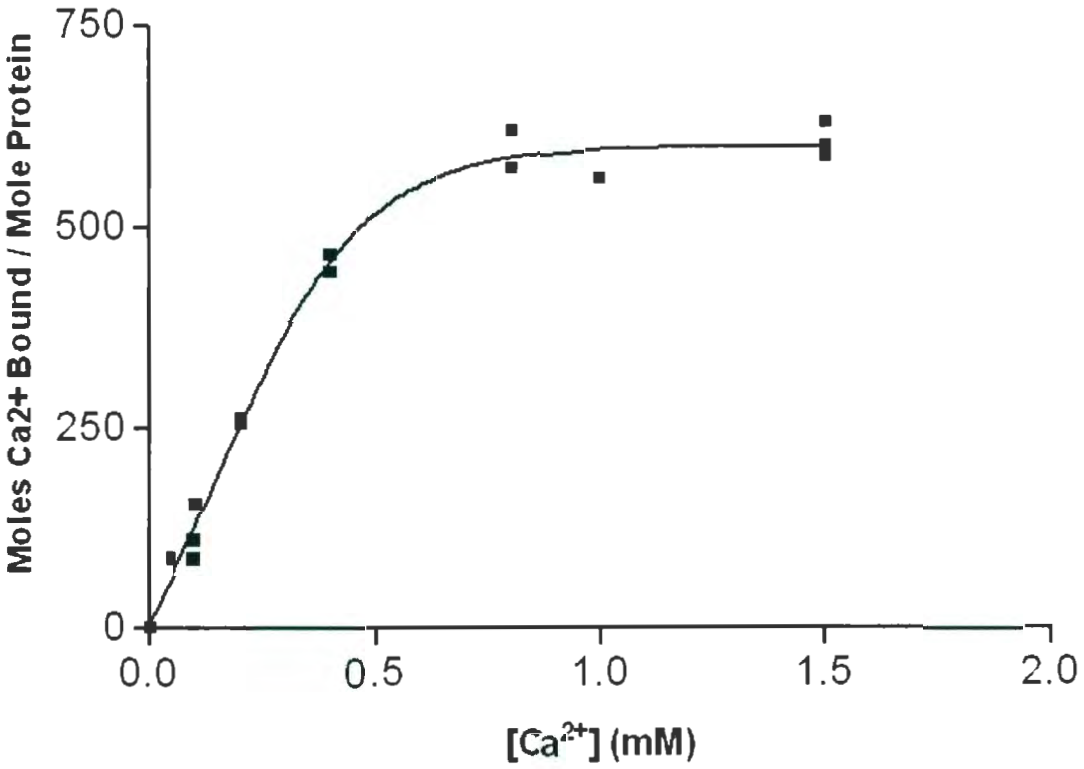
750
500
250
0
0.0
0.5
1.0
1.5
2.0
Moles Ca2+ Bound / Mole Protein
[Ca2+] (mM)

(Fig. 2.3). The calcium-induced change in alpha helix occurred with an apparent dissociation constant (calcium) of 25 μM.

We next quantified the calcium concentration dependence of toposome binding to liposomes. Following incubation of toposome with liposomes in the presence of various concentrations of calcium, we separated the liposome bound and unbound protein fractions. The unbound and bound fractions were analyzed by SDS–PAGE and the gel was stained with Coomassie Brilliant Blue. The 160 kDa band was quantified by densitometry and the percentage bound was determined and plotted against calcium concentration (Fig. 2.3). Protein binding increased in the presence of increasing concentrations of calcium with an apparent dissociation constant (calcium) of approximately 25 μM (Fig. 2.3). These results demonstrate a strong correlation between the calcium concentration dependence of toposome secondary structure and liposome binding.

To further explore the effect of calcium on toposome structure, endogenous tryptophan fluorescence measurements were undertaken. Emission spectra were measured by excitation at 287 nm and monitoring the emitted light between 300 and 400 nm. The maximum emission wavelength (λ_{MAX}) for toposome was 333 nm. The steady state fluorescence emission spectrum of toposome was compared in the presence and absence of calcium. In the presence of increasing concentrations of calcium, the emission spectrum was altered. Although the λ_{MAX} for toposome remained unchanged at 333 nm, there was a reduction in the fluorescence intensity with increasing

Figure 2.3. Measurement of the alpha helical content of toposome as a function of calcium concentration (•) and the determination of the calcium concentration dependence on toposome binding to liposomes (□). Prior to the determination of alpha helical content, toposome was incubated with varying amounts of calcium for 30 min at 15°C. Alpha helical content was calculated as described in Materials and Methods. In the binding experiments, toposome was incubated with multilamellar brain lipid liposomes in the presence of different concentrations of calcium for 30 min followed by separation of the liposomal and soluble fractions. Both the liposomal pellets and supernants were quantified as described in Materials and Methods.

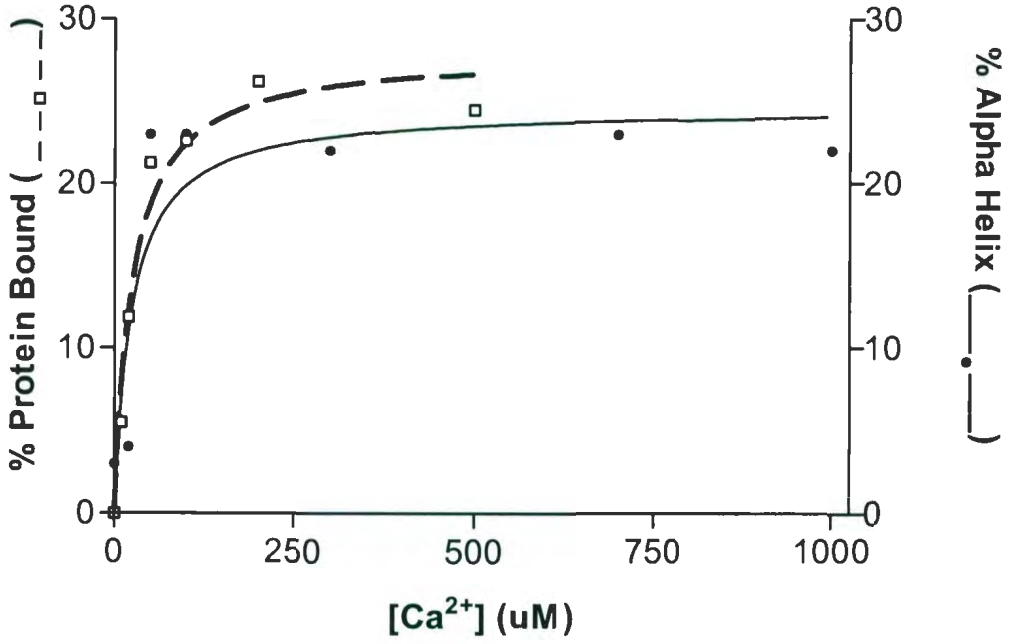
% Protein Bound (_ □ _)
% Alpha Helix (•)
30
20
10
0
0
250
500
750
1000
[Ca2+] (uM)

concentrations of calcium (Fig. 2.4). This quenching of fluorescence suggests that calcium binding has altered the environment of a tryptophan residue(s) most likely through a conformational change. This change was not however, accompanied by a shift in the wavelength of maximal emission suggesting that the polarity of the tryptophan residue(s) was not significantly changed. An apparent dissociation constant (calcium) of 240 μM was recorded.

To determine the effect of calcium on liposome aggregation, two sets of aggregation assays were performed. The first involved different concentrations of calcium in the absence of protein to determine the effect of calcium alone on aggregation. These experiments revealed that protein independent, calcium-driven liposome aggregation required a cation concentration of at least 1.5 mM (data not shown). In a second set of experiments, various concentrations of calcium were used in the presence of a fixed amount of toposome (5 μg) to determine the effect of calcium concentration on protein-dependent liposome aggregation. Toposome was capable of driving liposome aggregation in the presence of calcium concentrations well below 1.5 mM (Fig. 2.4). In the presence of toposome, liposome aggregation occurred in a manner consistent with the calcium concentration dependence of protein tertiary structure.

Endogenous tryptophan fluorescence measurements were also carried out on toposome that was pre-bound to liposomes. Toposome was incubated with multilamellar liposomes, prepared from phosphatidyl serine, in the presence of 100 μM calcium, harvested by centrifugation, and the pellet resuspended in buffer containing 100 μM

Figure 2.4. Correlation between the change in the emitted fluorescence of toposome as a function of calcium concentration (○) and the effect of calcium on toposome-driven liposome aggregation (■). In all fluorescence experiments, aliquots of toposome (0.080 mg/mL) were incubated for 30 minutes at room temperature in the presence of various concentrations of calcium followed by spectrophotometric analysis. In the liposome aggregation study, aliquots of toposome (5 μg) in the presence of different concentrations of calcium were added to multilamellar liposomes. The initial rates of liposome aggregation (ΔOD_{350}/min) in the presence of protein and calcium were calculated and plotted against the calcium concentration.

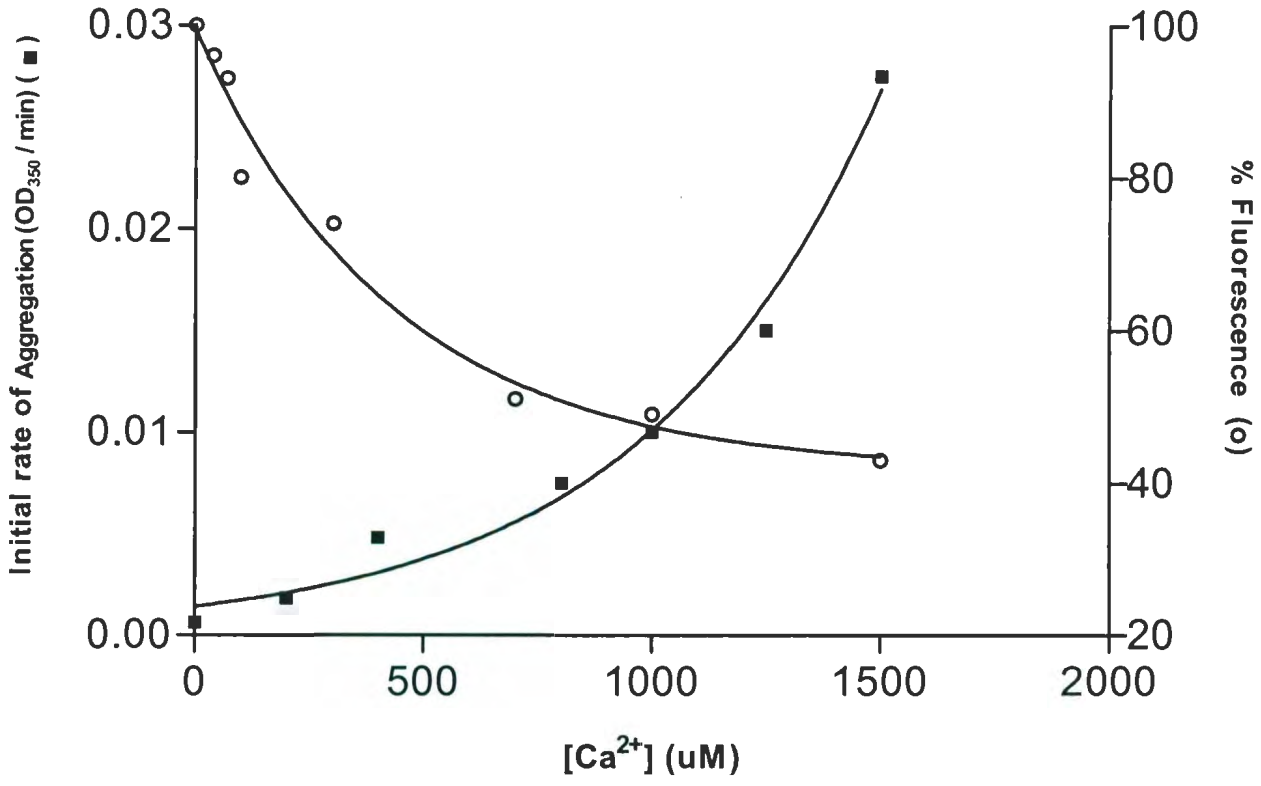
0.03
0.02
0.01
0.00
0
500
1000
1500
2000
100
80
60
40
20
Initial rate of Aggregation (OD350 / min) (■)
% Fluorescence (o)
[Ca2+] (uM)

calcium to ensure that all toposome present was bound to liposomes. Similar to the tryptophan fluorescence emission spectra of toposome alone, liposome bound toposome had a λ_{MAX} of 333 nm (data not shown). The fluorescence emission spectrum changed with increasing concentrations of calcium in a manner paralleling that seen for the purified protein (Fig. 2.5). The apparent dissociation constant (calcium) was determined to be 240 μM. Upon completion of the fluorescence study, the sample was harvested by centrifugation and analyzed by reducing SDS–PAGE. The toposome remained associated with the liposomes throughout the fluorescence study (data not shown).

2.4 Discussion

Membrane fusion is an important physiological event and is a ubiquitous process that occurs in all types of cells. Membrane–membrane interaction can occur extracellularly in such events as fertilization, organ development, and viral infection. In addition, it can occur intracellularly in such processes as exocytosis and membrane trafficking (Tamm *et al.*, 2003). In both cases, two membranes join in a manner that allows the contents of each membrane to mix freely and react together. To achieve membrane fusion in biological systems, energy must be supplied by highly specialized fusion proteins to overcome the hydration repulsion between the approaching membranes in order to disrupt the normal bilayer of the fusing membranes (Tamm *et al.*, 2003). In the developing sea urchin embryo, membrane–membrane interaction is an event which is required for membrane repair and protein export. The yolk granule, once thought to be simply a storage organelle providing the developing embryo with lipid and protein nutrients (Ichio *et al.*, 1978; Yokota and Kato, 1988; Yokota *et al.*, 1993), may serve as a

Figure 2.5. Comparative analysis of the calcium-concentration dependence of toposome tertiary structure in the presence and absence of multilamellar liposomes. Endogenous tryptophan fluorescence measurements were made in the presence (○) or absence (■) of liposomes. Toposome was bound to liposomes in the presence of 100 μM calcium and endogenous tryptophan fluorescence was measured. Further measurements were then made following the addition of calcium to the final concentrations indicated.

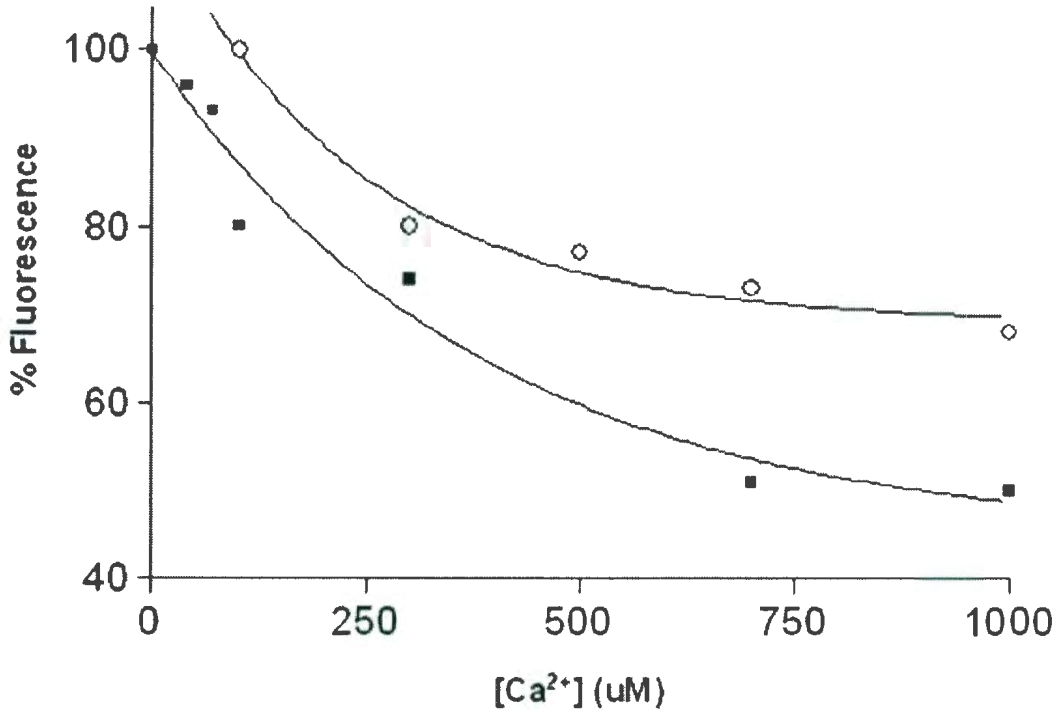
100
80
60
40
% Fluorescence
0
250
500
750
1000
[Ca2+] (uM)

reservoir of membrane for utilization in membrane–membrane interactions. McNeil *et al.* (2000) have shown that an influx of calcium, as a result of damage to the plasma membrane of the sea urchin egg or embryo, initiates membrane fusion between the yolk granule and the plasma membrane. This fusion reaction repairs the damaged plasma membrane, maintaining cell viability.

Research carried out by Mayne and Robinson (1998, 2002) clearly demonstrated that the yolk granule is involved in protein export. HCL-32 and a 41 kDa collagenase are both exported from the yolk granule to the extracellular matrices, the hyaline layer and basal lamina. The secretory pathway of protein export from the rough endoplasmic reticulum through the Golgi complex may be insufficient for rapid protein export to the extracellular matrices of the developing sea urchin embryo. Additional reports, mainly from the insect literature, suggest that proteins are exported though small cargo vesicles that 'bud off' from the yolk granule (Giorgi *et al.*, 1997; Snigirevskaya *et al.*, 1997). These vesicles are then available to fuse with the plasma membrane. In the unfertilized sea urchin egg, Gratwohl *et al.* (1991) have demonstrated that toposome is localized to the yolk granule, cortical granule and plasma membrane. As embryonic development proceeds, the proteolytically processed yolk granule toposome is exported to the plasma membrane while the cortical granule localized toposome is released into the apical extracellular matrix. This latter pool of toposome is believed to rivet the extracellular matrix to the cell surface. Both Noll *et al.*, (1985) and Matranga *et al.*, (1986) have also shown that toposome is exported from the yolk granule to the cell surface where it may fulfill a cell adhesion function. These proposed roles for toposome require that the protein be both

bivalent and interactive with the cell membrane. Additional recent findings suggest that toposome may also serve as a reservoir of material for new synthesis in the gonads and participate in the distribution of iron to components within gametes (Brooks and Wessel, 2002; Unuma *et al.*, 2003).

In the current study, we focused on the interaction between toposome and calcium, in an attempt to define the calcium-dependence of toposome structure and to determine if the calcium-activated protein could mediate membrane–membrane interaction. Equilibrium dialysis measurements revealed that toposome binds a large amount of calcium with weak affinity (intrinsic kDa of 240 μm; Fig. 2.2). This calcium binding is likely mediated through acidic and amide amino acids, and the carbonyl oxygen atoms in peptide bonds. The existence of a large number of low affinity, calcium-binding sites is reflective of the high concentration (10 mM) of this cation present in seawater. Under physiological conditions, we expect these sites to be occupied by calcium and actively involved in modulating the biological activity of toposome. In fact, sequence analysis of the major yolk granule protein/toposome failed to identify any of the known high affinity, calcium binding motifs but did reveal a 27.1 M percentage content of acidic and amide residues, all potential low affinity calcium binding sites (Brooks & Wessel 2002).

At relatively low concentrations of calcium, a major change occurred in the alpha helical content of toposome (Fig. 2.3). An apparent K_d of 25 μM was noted. Toposome binding to multilamellar liposomes was also calcium dependent. In the presence of 200

μM calcium, 25% of toposome was bound to liposomes and this also occurred with an apparent K_d of 25 μM (Fig. 2.3). The close correlation between the calcium concentration dependence of secondary structure and the binding of toposome to the liposomal membrane suggests that both events are related. The dramatic increase in alpha helical content that accompanies calcium binding facilitates interactions between toposome and, most likely, the phosphoserine head group. The liposome binding and aggregation assays were performed using liposomes in which phosphatidyl serine was the major phospholipid (see Methods). This phosphatidyl serine head group is expected to have no net charge at physiological pH suggesting that toposome binding results from recognition of the head group rather than less specific, electrostatic interactions. In a separate study, preliminary solid-state nuclear magnetic resonance results using liposomes composed of phosphatidyl serine (PS) have shown that the phase transition from liquid-crystal to gel state was unaffected by toposome binding. This data suggests that toposome is peripherally associated with the phosphatidyl serine bilayer. Collectively, these results suggest that toposome–membrane interaction is mediated by a calcium-dependent recognition of the phosphatidyl serine head group. In addition, a recent study by Perera *et al.* (2004) has demonstrated the peripheral association of toposome with the yolk granule membrane: (i) toposome can be dissociated from isolated yolk granules with EGTA resulting in the loss of calcium-dependent yolk granule aggregation. Readdition of purified toposome to the EGTA-treated granules reconstituted calcium-dependent aggregation; (ii) when isolated yolk granules were treated with trypsin, they no longer aggregated in the presence of calcium. Incubation of the trypsin-treated granules with purified toposome again restored calcium-dependent

aggregation; (iii) preincubation of purified toposome with antitoposome antibody resulted in the inability of added protein to reconstitute calcium-dependent aggregation in EGTA-treated yolk granules; and (iv) when purified yolk granules were preincubated with antitoposome antibody followed by assay for calcium-dependent aggregation, no aggregation occurred (Perera and Robinson, unpublished data, 2003). Collectively, these results attest to both a role for toposome in driving calcium-dependent yolk granule aggregation and also affirms the peripheral association of this protein with the yolk granule membrane. Interestingly, our analysis of the lipid content of the egg yolk granule membrane revealed a phosphatidyl serine content of 18.3% (Pelley, Davis and Robinson, unpublished data, 2002) suggesting that toposome–phosphatidyl serine interaction is of physiological importance. We suggest that this recognition of the phosphatidyl serine head group is achieved by a calcium-induced change to the secondary structure of toposome.

We explored the relationship between toposome structure and the mediation of membrane–membrane interaction by examining the effects of calcium on both protein tertiary structure and membrane–membrane interaction. As the calcium concentration was increased, a dramatic change in the tertiary structure of toposome occurred. This effect was characterized by a 60% decrease in tryptophan fluorescence which occurred with an apparent dissociation constant of 240 μM (Fig. 2.4). This quenching of fluorescence suggests that as the calcium concentration is increased, tryptophan residues are exposed to a more polar (aqueous) environment. The effect of calcium on toposome-driven liposome aggregation was also examined. We found that, in the absence of

toposome, liposome aggregation did not occur at calcium concentrations below 1.25 mM (data not shown), while in the presence of toposome, liposome aggregation occurred at greatly reduced concentrations of calcium (Fig. 2.4). When plotted together, the calcium-dependent tertiary structural change appeared to correlate with the calcium dependence of toposome-driven, liposome aggregation, suggesting that a change in the tertiary structure of toposome is required to mediate membrane–membrane interactions.

The results presented here clearly define a two-step model of calcium binding to toposome. Low concentrations of calcium induce a change in secondary structure that facilitates toposome-membrane binding. Even after the calcium concentration exceeds that required to cause a change in secondary structure, calcium continues to bind to toposome. Higher concentrations of calcium then induce a change in tertiary structure. This change in tertiary structure appears to correlate with the ability of toposome to drive membrane–membrane interactions.

This model predicts a role for toposome in mediating biologically relevant membrane–membrane interactions. For some time, it has been noted that injury resulting in plasma membrane disruption is a common cellular event that requires resealing to maintain cell viability (McNeil, 1993). When the sea urchin egg plasma membrane is damaged, the influx of seawater is accompanied by a rapid fusion reaction between yolk granules and the damaged membrane (McNeil *et al.*, 2000). This reaction restores the structural integrity of the membrane. Toposome may help drive this fusion by mediating the juxtaposition of the interacting membranes. The influx of 10 mM calcium during

plasma membrane disruption is more than sufficient to cause a change in the tertiary structure of the yolk granule, membrane-bound toposome, which could then mediate interaction between the yolk granule and plasma membranes (Fig. 2.6). This model supports the data of Matranga and colleagues (Noll *et al.*, 1985; Matranga *et al.*, 1986; Cervello and Matranga, 1989; Cervello *et al.*, 1992) who showed that toposome could mediate adhesion between cells in the sea urchin embryo. Toposome, localized to the cell surface would be exposed to sufficiently high concentrations of calcium to facilitate the required tertiary structural change which accompanies toposome-mediated, membrane–membrane interaction.

Figure 2.6. Putative role of toposome in the patch hypothesis of membrane repair (McNeil, 2000). (A) A normal egg or embryonic cell. The toposome is peripherally associated with the yolk granule membrane (Perera *et al.*, 2004). (B) The plasma membrane of the egg or embryonic cell undergoes damage, resulting in an influx or extracellular calcium. (C) This influx of calcium is more than sufficient to cause a change in the tertiary structure of toposome, which could then mediate membrane-membrane interaction between the yolk granule and plasma membranes, resulting in repair.

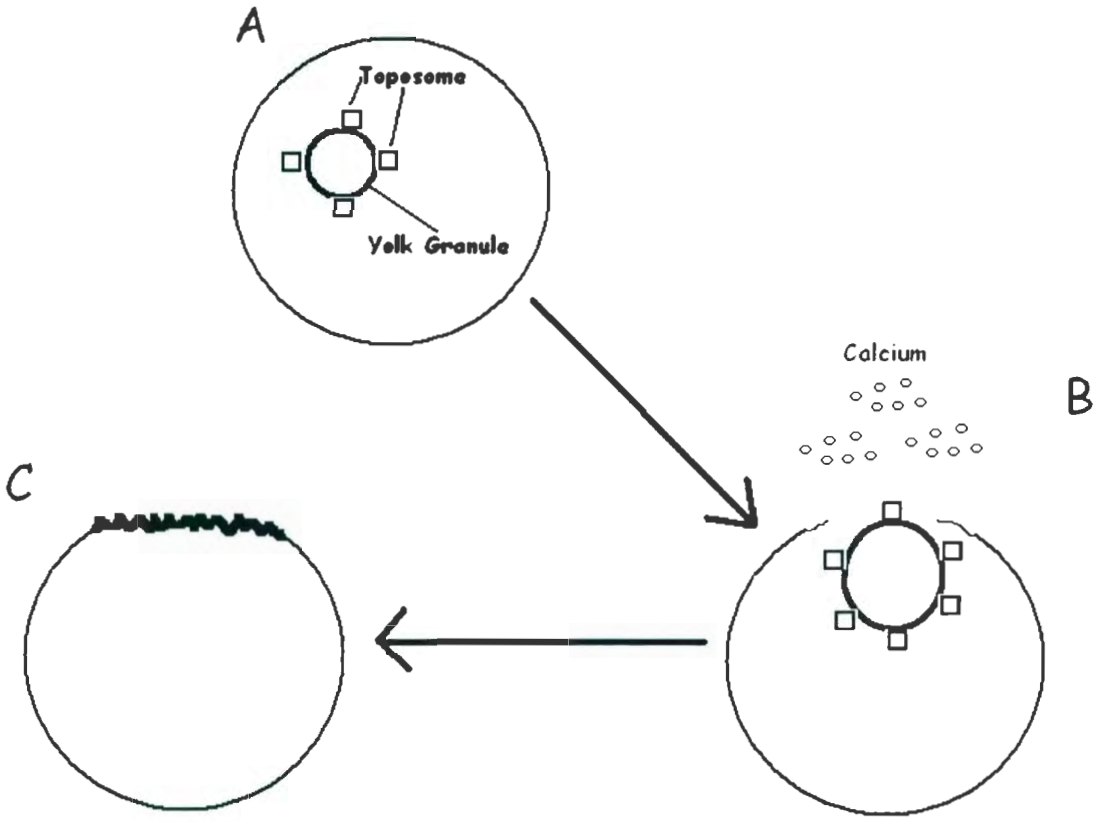
A
Teposome
Yolk Granule
Calcium
B
C

[1]

Chapter 3:

Interaction of toposome from sea-urchin yolk granules with dimyristoyl phosphatidylserine model membranes: a ^{2}H-NMR study

[1] The chapter has been previously published; Hayley, M., Emberley, J., Davis, P.J., Morrow, M.R. and Robinson, J.J. 2006. Biophys. J. 91: 4555-4564.

3.1 Introduction

Evenly distributed throughout the cytoplasm, yolk granules occupy approximately one-third of the cytoplasmic volume and are present in the eggs, embryos and early larvae of the sea urchin. Yolk proteins, ranging in size from 35 – 300 kDa, account for 10 -15 % of the total egg protein (Ichio *et al.*, 1978; Ozaki, 1980; Harrington and Easton, 1982; Kari and Rottmann, 1985). Toposome represents approximately 50% of the total yolk protein and is the major protein component of this organelle (Kari and Rottmann, 1980). First discovered by Malkin and coworkers (1965), toposome was initially isolated from the sea urchin embryo in studies aimed at identifying molecules responsible for cell-cell adhesion (Noll *et al.*, 1985; Matranga *et al.*, 1986).

In the sea urchin *Strongylocentrotus purpuratus*, toposome appears to be a hexameric glycoprotein consisting of six identical subunits each of 160 kDa. The hexamer is characterized by intrachain disulfide bonds and is stabilized with calcium. In the absence of this cation, the hexamer dissociates into trimer, dimer and monomer forms (Noll *et al.*, 1985). The functional unit(s) remains to be determined. In addition to the yolk granule, toposome is also localized to the embryonic cell surface and has been identified as a molecule mediating cell-cell adhesion in the developing embryo (Noll *et al.*, 1985; Matranga *et al.*, 1986). Interestingly, as development proceeds, the 160 kDa polypeptide is proteolytically processed into smaller molecular mass species. This processing is dependent upon a thiol class protease associated with the yolk granule and commences within 6 hr following fertilization. The functional significance of this processing remains to be determined.

We have previously characterized toposome-driven membrane-membrane interactions using both liposomes and purified yolk granules (Perera *et al.*, 2004). This earlier work has recently been extended by the analysis of calcium-toposome interaction. This cation was found to induce two calcium-concentration dependent structural transitions in toposome: a secondary structural change occurred with an apparent k_d (calcium) of 25 μM and this was followed by a tertiary structural change with an apparent k_d (calcium) of 240 μM (Hayley *et al.*, 2006). Interestingly, the first structural change was required to facilitate toposome binding to bilayers while the second structural change correlated with toposome-driven, membrane-membrane interaction. These results provide a structural basis for the previously described toposome-mediated, cell-cell adhesion in the sea urchin embryo.

Quantitatively, the yolk granule organelle represents a significant intracellular store of both membrane and protein, and as such, has been the subject of extensive research. However, while the constituent elements of this organelle have been identified and characterized, its function remains uncertain. Classically, this organelle has been viewed as a reservoir of nutrients for the developing embryo. However, recent work suggests that the yolk granules remain intact throughout the course of embryonic development and are only metabolized in 7-day old larvae (Scott *et al.*, 1990). In addition, when larvae are starved, their yolk granule content remains unchanged. Data from several laboratories suggest a more dynamic role for the yolk granule in the developing embryo. A number of reports have described the localization to the yolk granule of proteins destined for subsequent export to the extracellular environment

(Mayne and Robinson, 1998, 2002). In addition, the large amount of membrane associated with the yolk granule may serve as a reservoir for patching lesions in the plasma membrane of sea urchin eggs and embryos (McNeil, 1993; Terasaki *et al.*, 1997; McNeil *et al.*, 2000). The association of toposome with the yolk granule may equip this organelle with the capacity to engage in processes requiring dynamic membrane-membrane interactions.

The primary objective of the current study was to investigate whether the interaction of toposome with the bilayer is more characteristic of a peripheral protein, with protein-lipid interactions primarily at the bilayer surface, or of an integral protein extending partly into or spanning the lipid bilayer. Toposome-bilayer interactions were examined in the presence of calcium concentrations known to induce either the secondary structural change in toposome or both the secondary and tertiary structural changes. ^{2}H-NMR was used to monitor the effect of toposome on lipid acyl-chain orientational order and bilayer motions in gel and liquid-crystalline DMPS-d_{54} model membranes. DMPS-d_{54} acyl-chain orientational order was examined using chain deuteron quadrupole splitting and first spectral moments. Information regarding the perturbation of bilayer motion by toposome was inferred from the effects of the protein on characteristic decay times for chain deuteron quadrupole echoes and Carr-Purcell-Meiboom-Gill echo trains.

3.2 Materials and Methods

3.2.1 Purification of toposome

Toposome was purified from the sea urchin *Strongylocentrotus purpuratus* purchased from SeaCology (Vancouver, Canada). Eggs were harvested and washed consecutively in Millipore-filtered sea water (MFSW) and calcium, magnesium - free sea water (CMFSW). Preparation of the yolk granule protein extracts was based on a procedure described previously (Perera *et al.*, 2004) but with some modifications. Washed eggs were suspended in 0.5 M KCl (pH 7.0) in a hand-held Dounce homogenizer at 0°C. The homogenate was then fractionated by centrifugation at 400 X g for 4 min at 4°C. The supernant then underwent fractionation by centrifugation at 2400 X g for 10 min at 4°C. The final pellet was resuspended in 0.5 M KCl (pH 7.0) in the presence of 1 mM EDTA, fractionated by centrifugation at 50 000 X g for 1 h at 4°C and the supernatant retained. Aliquots of the supernant were dialyzed against starting buffer (10 mM Tris –HCl, pH 8.0) and were loaded onto a Q-Sepharose Fast Flow column (Amersham Pharmacia, Uppsala, Sweden) that had been previously equilibrated with starting buffer. The column was washed three times to remove any unbound proteins and followed by the elution of bound proteins with a NaCl step gradient (0.1 – 1.0 M), prepared in starting buffer. The eluted proteins were analyzed by sodium dodecyl sulfate polyacrylamide gel electrophoresis (SDS-PAGE) as described by Laemmli (1970), and the gel stained with silver (Amersham Pharmacia, Uppsala, Sweden). The salt fraction containing the purified toposome was stored in small aliquots at – 20°C.

3.2.2 Preparation of multilamellar vesicles

Chain-perdeuterated DMPS-d_{54} was obtained from Avanti Polar Lipids Inc. (Alabaster, AL) and was used without further purification. Multilamellar vesicles used in the ^{2}H-NMR study were prepared using two different protocols. DMPS-d_{54} was hydrated at 45°C for 1 hr in deuterium-depleted buffer (20 mM Tris-HCl, 150 mM NaCl, pH 8.0) containing both toposome and calcium. In one preparation, using a lipid: protein ratio of 80,000:1, DMPS-d_{54} was dissolved in deuterium-depleted buffer (20 mM Tris-HCl, 150 mM NaCl, pH 8.0) and hydrated at 45°C for 1 hr. Toposome and calcium were then added to the preformed multilamellar vesicles. In both protocols, samples were transferred to NMR tubes and each sample contained 5 mg of DMPS-d_{54}. In parallel experiments, the final ratios of lipid: protein in the reconstituted samples were determined following the isolation, by centrifugation, of the liposomal pellets.

3.2.3 Solid-state deuterium-NMR

Wideline deuterium NMR spectra and echo decay measurements were obtained with a locally constructed spectrometer using quadrupole echo pulse sequences (Davis *et al.*, 1976). For all acquisitions, a repetition time of 0.5 s was used. Free induction decays used to obtain spectra of samples of DMPS-d_{54} were obtained in a 9.4 T superconducting solenoid using the quadrupole echo sequence with $\pi/2$ pulses of 5.0-5.5 μs separated by 35 μs. Typically 20,000 transients were averaged for each spectrum. Signals were obtained using oversampling (Prosser *et al.*, 1991) and digitized with effective dwell times of 4 μs for liquid crystal DMPS-d_{54} spectra and 2 μs for gel DMPS-d_{54} spectra. Spectrometer frequency and pulse lengths were adjusted before acquisition to minimize

signal in the imaginary channel. No line broadening was used. Spectra that would correspond to samples with bilayer normals aligned perpendicular to the applied magnetic field were obtained by transforming the multilamellar vesicle spectra using a fast Fourier-transform "de-Pake-ing" algorithm (McCabe and Wassall, 1995).

Quadrupole echo amplitudes for determination of quadrupole echo decay times were recorded by averaging 2000-4000 transients. Decays were plotted as $\ln(A(2\tau))$ versus 2τ and average echo decay times, T_{2e}, were obtained from the inverse slope of the initial decay.

Bloom and Sternin (1987) pioneered use of the quadrupole Carr-Purcell-Meiboom-Gill (q-CPMG) pulse sequence $\left[(\pi/2)_x - \tau - ((\pi/2)_y - 2\tau)_n\right]$ for identification of contributions to quadrupole echo decay from motions with correlation times that are too long to contribute to motional narrowing of spectra. This sequence results in the formation of echoes at multiples of 2τ. Decay of the echo train is less sensitive to motions that modulate the quadrupole interaction with correlation times much longer than τ. By observing the decay of q-CPMG echo decay trains for progressively larger values of τ, it is possible to reintroduce contributions to echo train decay from progressively slower motions and probe the distribution of such motions. In this work, q-CPMG echo trains were recorded for $\tau = 40\,\mu s$, $\tau = 50\,\mu s$, $\tau = 100\,\mu s$, $\tau = 150\,\mu s$, $\tau = 200\,\mu s$, $\tau = 300\,\mu s$, $\tau = 400\,\mu s$, and $\tau = 500\,\mu s$. For $\tau \leq 100\,\mu s$, 40 echoes were recorded in each train. For larger values of τ, the maximum number of echoes recorded

in an echo train was determined by the condition $2n_{max}\tau \leq 8\,\text{ms}$. Echo amplitudes were measured from averages of 4000 acquisitions of each echo train.

As described below, q-CPMG results were fitted to a model for the distribution of motions in a sample by simultaneously minimizing squares of differences between modelled and observed echo amplitudes (χ^2) for all echo train decays in a given experiment. This fitting was carried out using multiple data set fitting capability of Origin 6.1 (Originlab Corporation, Northhampton, Ma.). The fit was applied simultaneously to the 8 echo train decay datasets for a given sample. Except for the value of τ specific to each echo train decay, all parameters in the fit were designated as shared by all data sets. The resulting fits reflect the adjustment of 9 variables in order to fit, simultaneously, 8 non-exponential decay curves.

3.3 Results and Discussion

Toposome was purified using the standard protocol described in Materials and Methods. Analysis by reduced SDS-PAGE revealed that the protein was homogenous. We have previously characterized both the effects of calcium on toposome structure and toposome-driven, membrane-membrane adhesion (Perera *et al.*, 2004; Hayley *et al*). The calcium concentration used in the NMR study reported here as well as the lipid: protein ratios in the toposome-reconstituted liposomes were chosen based on our previous studies noted above. Therefore, the conditions chosen for this study are those which allow for both reconstitution of toposome with the liposomal bilayer and the demonstration of the known biological activity of toposome.

Fig. 3.1 shows ^{2}H NMR spectra at selected temperatures for (A) DMPS-d_{54}, (B) DMPS-d_{54} plus calcium (100 μM) and (C) DMPS-d_{54} plus calcium (100 μM) and toposome (lipid: protein ratio=80,000:1). The sample from which the spectra in Fig 3.1.C were obtained was prepared by adding toposome to preformed multilamellar vesicles. We have previously shown that toposome binds to phosphatidyl serine liposomes in a calcium-dependent manner with an apparent k_d (calcium) of 25 μM (Hayley *et al.*, 2006). At temperatures above 31°C, all the spectra in Fig. 3.1 are characteristic of lipid in the liquid crystalline phase. The spectra are superpositions of Pake doublets that are indicative of axially symmetric CD bond reorientations that modulate the quadrupole interaction with correlation times that are short relative to the characteristic timescale $\left(\sim 10^{-5}\ \mathrm{s}\right)$ of the ^{2}H-NMR measurement (Davis, 1983). The distribution of quadrupole splittings reflects the dependence of CD bond orientational order on position along the perdeuterated acyl chains (Davis, 1983). Below 32 °C, the broader and more continuous spectra are characteristic of the gel phase. This reflects lipid reorientational dynamics that are slower and reorientation that is less axially symmetric on the timescale of the measurement. In all samples studied, the transition from liquid crystal to gel phase proceeded sharply and none of the observed spectra displayed superpositions of liquid crystal and gel phase features that would be indicative of two-phase coexistence.

Comparison of the three series of spectra in Fig. 3.1 suggests that addition of calcium and then toposome at a lipid to protein molar ratio of 80,000:1 has little apparent

Figure 3.1. ^{2}H NMR spectra at selected temperatures for (A) DMPS-d_{54}, (B) DMPS-d_{54} plus calcium (100 μM Ca^{2+}) and (C) DMPS-d_{54} plus Ca^{2+} (100 μM) and toposome (lipid: protein ratio of 80,000: 1). For each series of spectra, a single sample was analyzed.

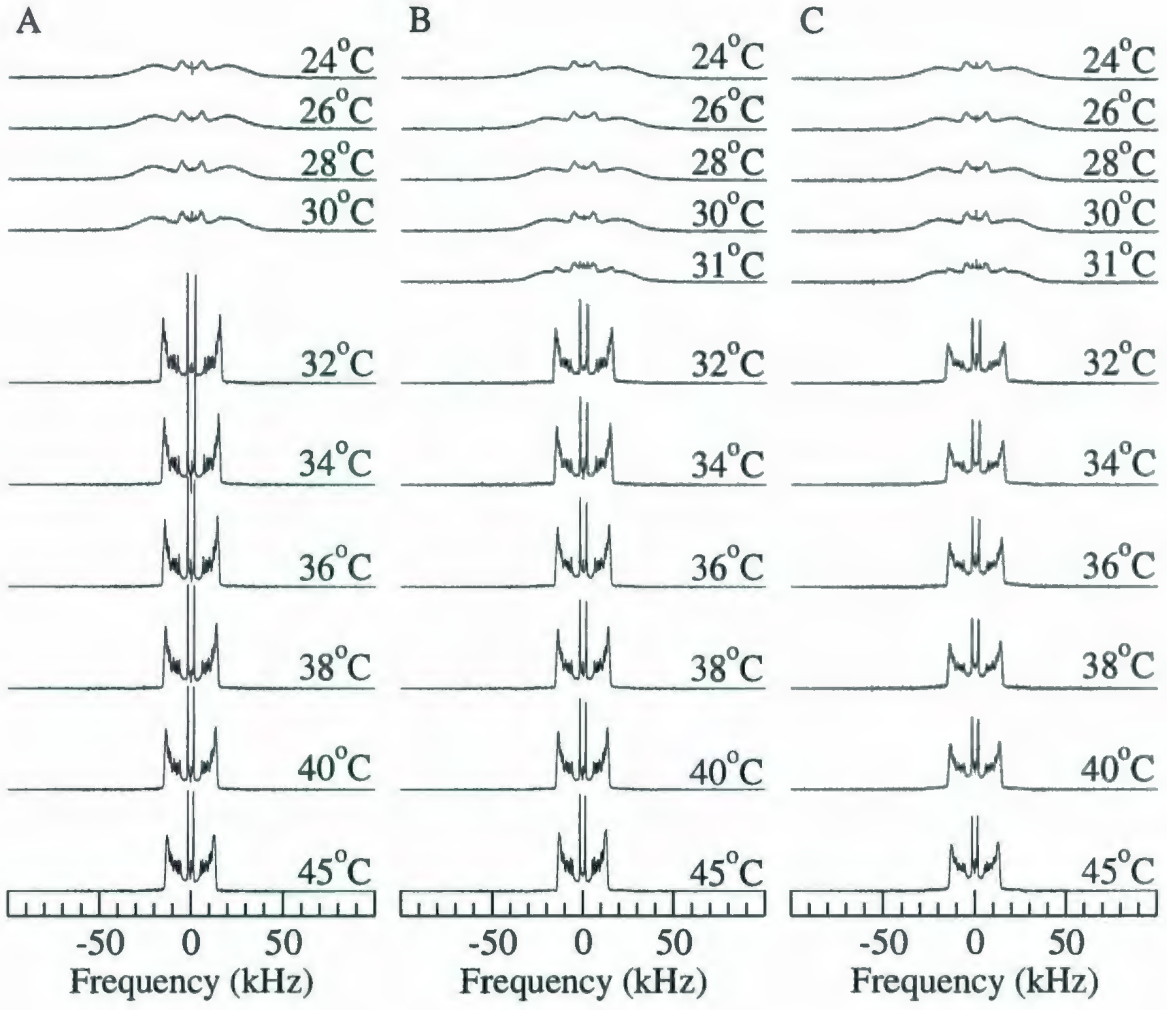
A
B
C
24°C
26°C
28°C
30°C
31°C
32°C
34°C
36°C
38°C
40°C
45°C
-50
0
50
Frequency (kHz)

effect on either the bilayer phase transition or lipid acyl chain orientational order in the liquid crystalline phase. The insensitivity of chain deuteron quadrupole splitting to toposome is illustrated in Fig. 3.2, which compares the right halves of de-Paked spectra, at 40°C for DMPS-d_{54} alone (A) and in the presence of toposome (lipid to protein molar ratio of 80,000:1) and calcium (100 μM) (B). The spectra shown were obtained by transforming the corresponding unoriented-sample spectra from Fig. 3.1 to obtain spectra that would be expected from samples with bilayers uniformly oriented perpendicular to the magnetic field. The vertical lines between the spectra are centered on the peaks of the upper spectrum to aid in comparison of quadrupole splittings of resolvable doublets. This comparison indicates that at a lipid to protein molar ratio of 80,000:1, toposome, in the presence of sufficient calcium to allow its association with the bilayer, does not significantly alter DMPS-d_{54} deuteron quadrupole splittings. This result indicates that toposome does not significantly alter the amplitudes of fast fatty acyl chain motions and suggests a peripheral association of toposome with the bilayer.

A series of DMPS-d_{54}/protein mixtures were also prepared by hydrating the lipid in buffer containing the protein plus calcium. These preparations most likely contain protein and calcium homogenously distributed throughout the multilamellar membrane surfaces. Figure 3.3 shows NMR spectra at selected temperatures for DMPS-d_{54} plus toposome at three lipid to protein molar ratios (80,000:1, 30,000:1, and 15,000:1) in the presence of either 100 - or 500 μM calcium. The spectra for liposomes (lipid: protein, 80,000:1) prepared in this way are effectively identical to those obtained from corresponding samples prepared by addition of toposome to preformed multilamellar

Figure 3.2. Depaked spectra (right halves) at 40°C for (A) DMPS-d_{54} and (B) DMPS-d_{54} in the presence of Ca^{2+} (100 μM) and toposome at a lipid to protein ratio of 80,000:1. Spectra are obtained by transforming unoriented-sample spectra to obtain spectra that would be expected from bilayers oriented with the bilayer normal perpendicular to the applied field.

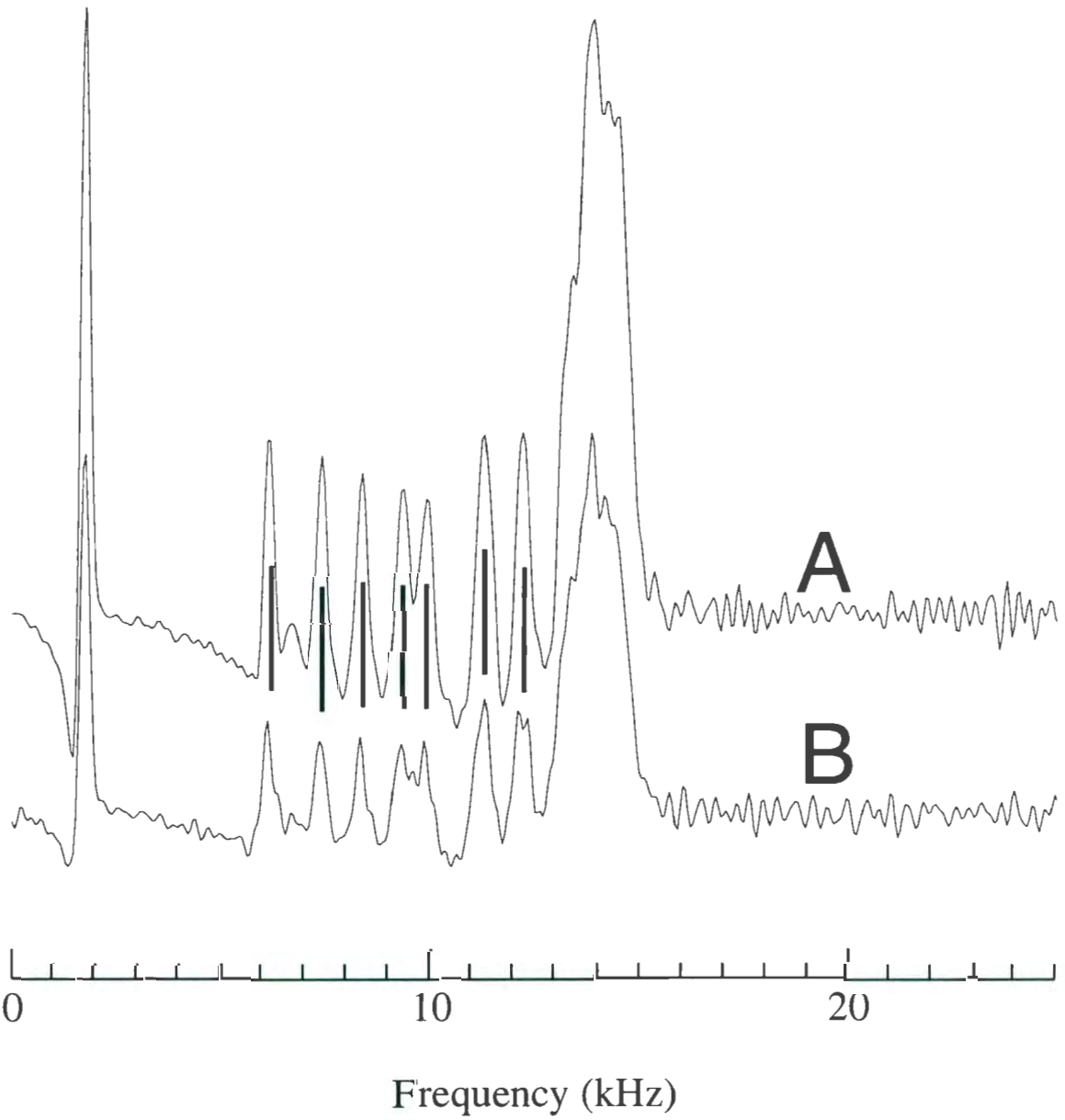
A
B
0
10
20
Frequency (kHz)

Figure 3.3. ^{2}H NMR spectra at selected temperatures for DMPS-d_{54} plus toposome and calcium. Spectra A, C and E, lipid: protein was 80,000:1, 30,000:1 and 15,000:1, respectively and 100 μM Ca^{2+}. Spectra B, D and F, lipid: protein was 80,000:1, 30,000:1 and 15,000:1, respectively and 500 μM Ca^{2+}. For each series of spectra, a single sample was analyzed.

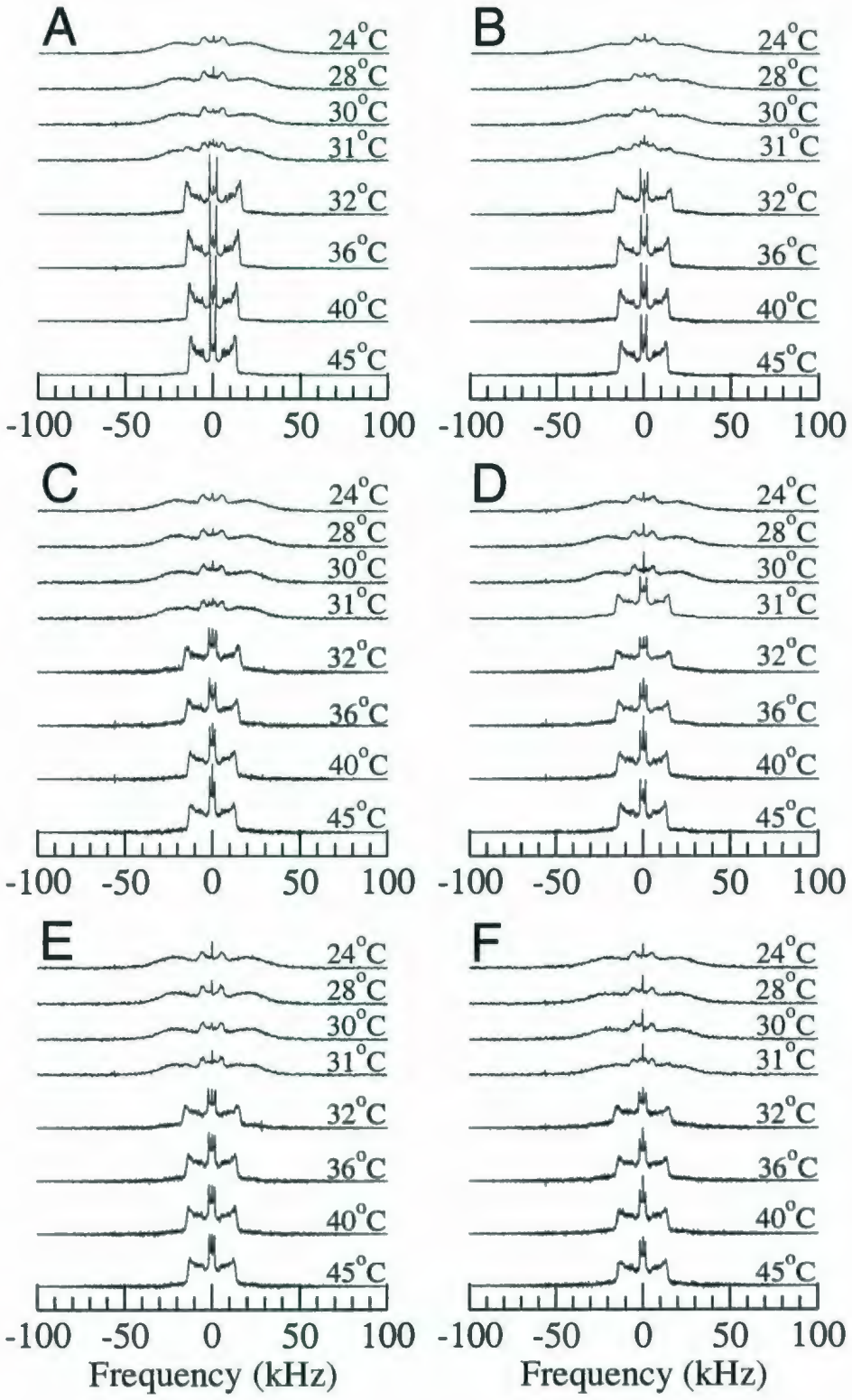
A
B
C
D
E
F
24°C
28°C
30°C
31°C
32°C
36°C
40°C
45°C
-100 -50 0 50 100
Frequency (kHz)

vesicles (compare Fig. 3.1.C and Fig. 3.3.A). For a given temperature, deuteron splittings in the liquid crystalline spectra decrease only slightly with increasing protein concentration. This observation indicates that increased protein concentration has little effect on lipid chain packing within the bilayer. The liquid crystal to gel transition remains sharp at all protein concentrations. Increasing protein concentration does affect the signal to noise ratio and the resolution of superimposed doublets in the liquid crystalline spectra. This reflects changes in the echo decay rate with protein concentration, as described below.

For a symmetric spectrum $s(\omega)$, the first spectral moment, defined as

$$M_1 = \frac{\int_0^\infty \omega s(\omega) d\omega}{\int_0^\infty s(\omega) d\omega}, \qquad (1)$$

is proportional to the intensity-weighted average, over all deuterons, of the quadrupole splitting. Values of M_1 thus reflect the average orientational order of chain-perdeuterated lipid bilayers. Figure 3.4 shows the temperature dependence of M_1 for the spectra of DMPS-d_{54}, DMPS-d_{54} in the presence of 100 μM calcium, DMPS-d_{54} in the presence of 100 μM calcium and toposome at three lipid to protein molar ratios (80,000:1 (Δ and ∇), 30,000:1 ($\square$), and 15,000:1 ($\times$)) and DMPS-d_{54} in the presence of 500 μM calcium and toposome at three lipid to protein molar ratios (80,000:1 ($\triangleright$), 30,000:1 ($\Diamond$), and 15,000:1 (+)). In the liquid crystalline phase, toposome in the presence of calcium reduces average chain orientational order slightly. This reduction in chain order, while small, does appear to depend on the lipid/protein molar ratio but there does not appear to

Figure 3.4. Temperature dependence of first spectral moments (M_1) for the spectra in Figures 1 and 3. DMPS-d_{54} (●); DMPS-d_{54} plus 100 μM Ca^{2+} (■); two preparations of DMPS-d_{54} plus toposome (lipid:protein = 80,000:1) in 100 μM Ca^{2+} (Δ and ∇); DMPS-d_{54} plus toposome (lipid:protein = 80,000:1) in 500 μM Ca^{2+} (▷); DMPS-d_{54} plus toposome (lipid:protein = 30,000:1) in 100 μM Ca^{2+} (□); DMPS-d_{54} plus toposome (lipid:protein = 30,000:1) in 500 μM Ca^{2+} (◊); DMPS-d_{54} plus toposome (lipid:protein = 15,000:1) in 100 μM Ca^{2+} (×); DMPS-d_{54} plus toposome (lipid:protein = 15,000:1) in 500 μM Ca^{2+} (+).

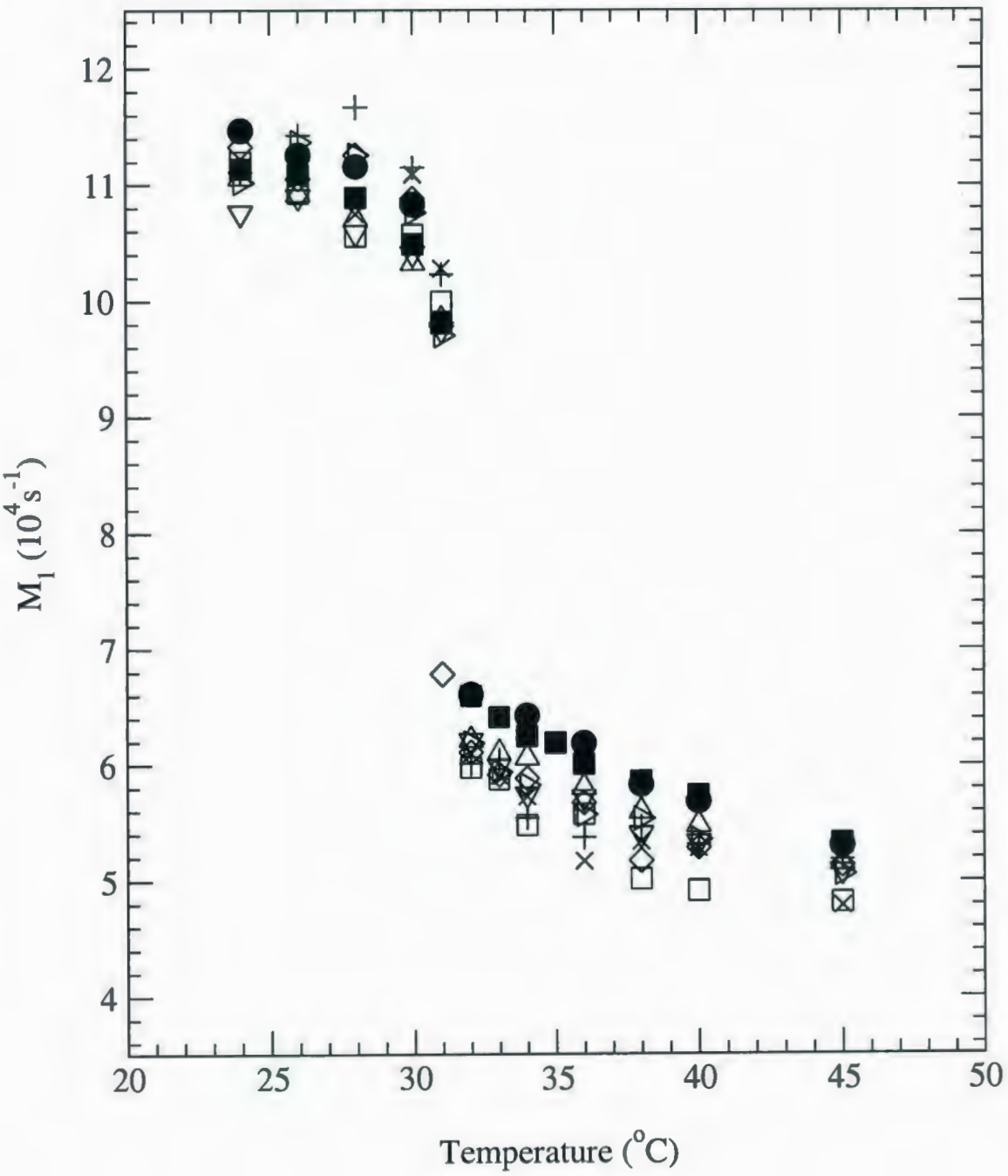
12
11
10
9
8
7
6
5
4
20
25
30
35
40
45
50
M_1 ($10^4 s^{-1}$)
Temperature (^oC)

be any significant difference between the effects of toposome in the presence of calcium at 100 μM or 500 μM indicating that the tertiary structural change induced by the higher concentration of calcium does not result in any additional modulation of toposome-membrane interactions. Any dependence of M_1 on toposome concentration in the gel phase is smaller than the scatter in that data. Despite scatter in the M_1 data in both phases, it is clear that toposome in the presence of calcium has little effect on the DMPS-d_{54} liquid crystal to gel phase transition. This result confirms the absence of any significant effect of toposome on the amplitudes of rapid motions of the fatty acyl chains and again points to a peripheral association of toposome.

Protein-membrane interactions, which have little effect on chain order, may still perturb bilayer motions that are sensitive to reorientation on the 10^{-5}-10^{-4} s timescale. Quadrupole echo decay measurements can be utilized to detect these perturbations. The quadropole echo pulse sequence consists of two $\pi/2$ pulses differing in phase by 90° and separated by an interval τ (Davis *et al.*, 1976). Motions that change the quadrupole interaction while an echo is being formed contribute to echo decay. For motions that have short correlation times (τ_C), relative to the inverse spectral width, the contribution to the echo decay rate is proportional to τ_C (Abragam, 1961). For slower motions, the contribution to the echo decay rate is proportional to τ_C^{-1} (Pauls *et al.*, 1985). Slow diffusive or collective motions and faster local motions can both contribute to echo decay in the liquid crystalline phase (Bloom and Sternin, 1987; Bloom and Evans, 1991; Stohrer *et al.*, 1991). In this phase, motions that contribute to echo decay include slower motions such as collective modes of the bilayer surface and molecular reorientation

resulting from diffusion of molecules around curved bilayer surfaces as well as faster, more localized motions including molecular reorientation and conformational fluctuations (Meier, 1986; Bloom and Sternin, 1987; Stohrer *et al* 1991; Bloom *et al.*, 1991). At the liquid crystal to gel transition, the correlation times for slow motions, such as lateral diffusion and collective motions (membrane undulations), increase and their contributions to echo decay are consequently reduced. In contrast, motions that are fast in the liquid crystalline phase, such as reorientation about the bilayer normal, can slow at the transition and contribute more effectively to echo decay. The result is a sharp drop in the echo decay time at the liquid crystal to gel transition. As the temperature is lowered further in the gel phase, the more localized motions begin to freeze out, thus becoming less effective contributors to echo decay, and T_{2e} increases.

Figure 3.5 shows echo decay times at selected temperatures for DMPS-d_{54} (●), DMPS-d_{54} in the presence of 100 μM calcium (■) and DMPS-d_{54} in the presence of 100 μM calcium plus toposome at three lipid/protein molar ratios (80,000:1 (Δ and ∇), 30,000:1 (□), and 15,000:1 (×)). DMPS-d_{54} in the presence of 500 μM calcium at three lipid/protein molar ratios (80,000:1 (▷), 30,000:1 (◊), and 15,000:1 (+)) was also studied. In the liquid crystalline phase (> 32°C), addition of toposome at a lipid/protein molar ratio of 80,000:1 increases the quadrupole echo decay rate significantly as reflected by the reduced values for T_{2e}. Decreasing the lipid/protein molar ratio to 30,000:1 increases the quadrupole echo decay rate even further as shown by a more dramatic fall in the T_{2e} values. No further change in T_{2e} values was observed when the lipid/protein

Figure 3.5. Temperature dependence of average quadrupole echo decay time (T_{2e}) extracted from Figures 1 and 3. DMPS-d_{54} (●); DMPS-d_{54} plus 100 μM Ca^{2+} (■); two preparations of DMPS-d_{54} plus toposome (lipid:protein = 80,000:1) in 100 μM Ca^{2+} (Δ and ∇); DMPS-d_{54} plus toposome (lipid:protein = 80,000:1) in 500 μM Ca^{2+} (▷); DMPS-d_{54} plus toposome (lipid:protein = 30,000:1) in 100 μM Ca^{2+} (□); DMPS-d_{54} plus toposome (lipid:protein = 30,000:1) in 500 μM Ca^{2+} (◊); DMPS-d_{54} plus toposome (lipid:protein = 15,000:1) in 100 μM Ca^{2+} (×); DMPS-d_{54} plus toposome (lipid:protein = 15,000:1) in 500 μM Ca^{2+} (+).

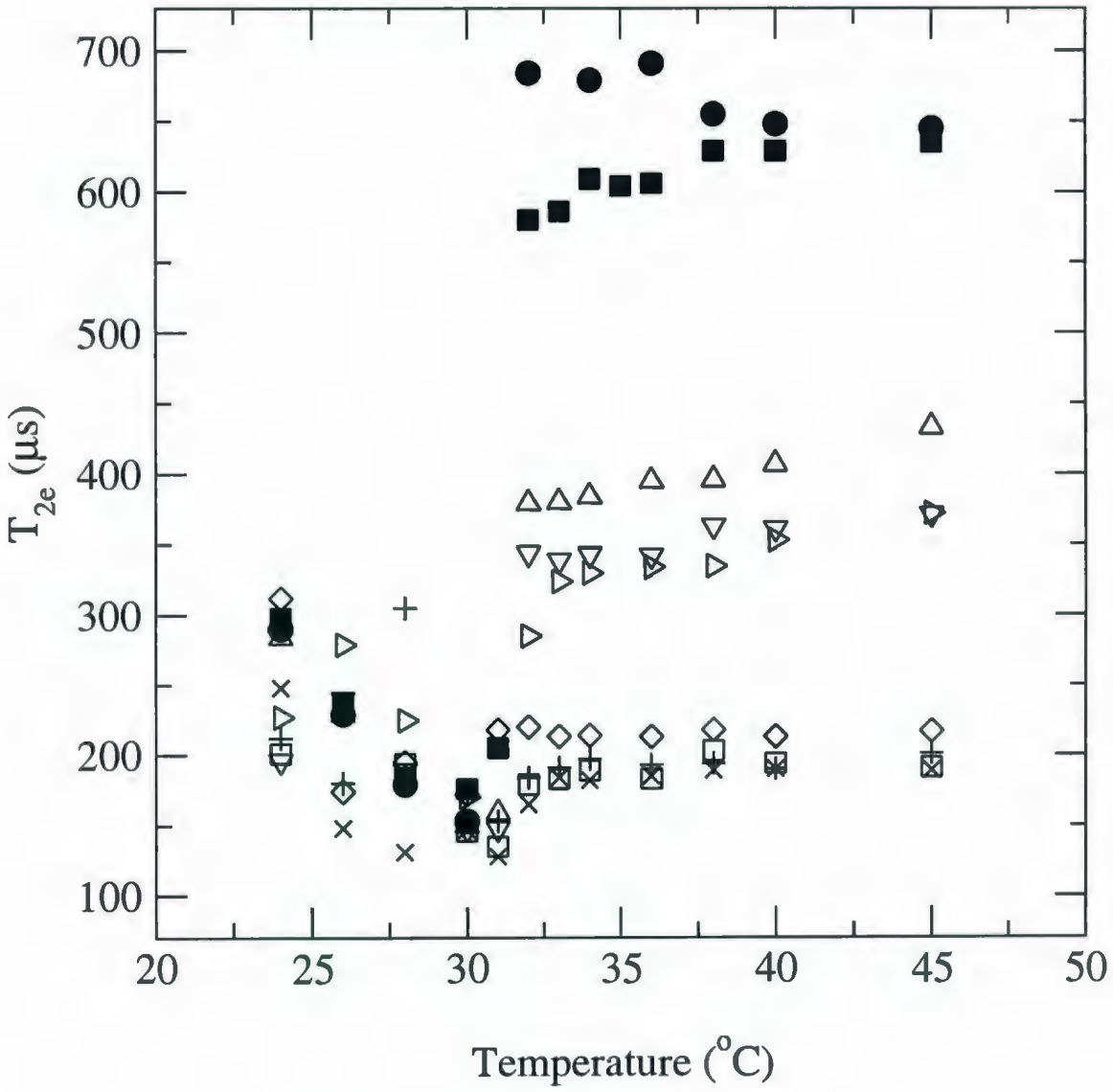
700
600
500
400
300
200
100
T_{2e} (μs)
20
25
30
35
40
45
50
Temperature (°C)

molar ratio was decreased below 30,000:1. Interestingly, the magnitude of the T_{2e} changes was similar in the presence of either 100 – or 500 μM calcium.

The effect of toposome on quadrupole echo decay rate in the liquid crystal phase is much more pronounced than its effect on average chain orientational order over the same temperature range. Chain orientational order reflects averaging of the quadrupole interaction on timescales that are short relative to the characteristic time (~ 10^{-5} s) for the NMR observation. Therefore, it is likely that the observed effect of toposome on quadrupole echo decay in the liquid-crystalline phase reflects perturbation of diffusive or collective motions (membrane undulations) with longer correlation times rather than the faster local motions that influence orientational order parameters for each segment. This suggests that toposome may modulate the rate or path of diffusion of phospholipid molecules, which in turn may alter the dynamics of membrane undulations.

In principle, a systematic protein-induced reduction in vesicle radius might account for the observed reduction in liquid crystal phase quadrupole echo decay time with increasing toposome concentration. However, the observation that the change in echo decay time due to toposome at a lipid: protein ratio of 80,000:1 is not sensitive to whether toposome is added to preformed multilamellar vesicles or vesicles are formed by hydration of lipid in buffer containing protein is interesting (see Fig. 3.5, Δ and ∇). This observation does not explicitly preclude a systematic decrease in average vesicle radius with increasing protein concentration. Nevertheless, such an explanation would imply that the addition of protein to preformed multilamellar vesicles promotes substantial

reorganization of multilamellar material into vesicles of the same average size as those resulting when vesicles are formed by hydration in buffer containing protein and that such reorganization does not substantially perturb lipid chain order. An explanation involving more local perturbations of bilayer surface curvature and the spectrum of bilayer surface undulations seems more likely.

Below the liquid crystal to gel phase transition, quadrupole echo decay times increase slightly with decreasing temperature. However, this effect was independent of the lipid/protein molar ratio. Motions that are slow in the liquid-crystalline phase are generally even slower at low temperature and are not expected to contribute significantly to quadrupole echo decay as the bilayer becomes more ordered. Rotations about the bilayer normal, or about individual bonds, that are fast in the liquid-crystalline phase can slow, on cooling, into the regime where their contributions to the echo decay rate are inversely proportional to their correlation times. Quadrupole echo decay times in the gel phase are thus generally expected to increase with decreasing temperature.

Integral membrane proteins have a tendency to reduce the rate at which echo decay time increases with decreasing temperature in the gel phase. This may reflect a protein-induced interference with ordering and a consequent reduction in temperature-dependent slowing of motions that contribute to quadrupole echo decay in the gel phase (Simatos *et al.*, 1990; Dico *et al.*, 1997). The apparent absence of a significant perturbation of quadrupole echo decay rate by toposome in the gel phase suggests that its interaction with the bilayer primarily perturbs motions, such as bilayer undulation and

collective motion, that contribute significantly to echo decay in the liquid crystalline phase but not in the gel phase. Taken along with the relatively weak perturbation of chain orientational order, the echo decay observations suggest that toposome is not integral to the membrane but interacts primarily at the bilayer surface.

Additional information regarding the nature of the perturbation by toposome can be obtained from multiple pulse experiments. Adiabatic motions are ones that contribute to the quadrupole echo decay but have correlation times that are too long for them to contribute to the motional narrowing of the spectra. Bloom and Sternin (1987) demonstrated that the quadrupole Carr-Purcell-Meiboom-Gill (q-CPMG) pulse sequence could be used to assess the relative contribution to quadrupole echo decay from slow adiabatic motions for a given sample.

For deuterons whose quadrupole interaction is modulated by a given superposition of motions, the train of echoes formed by the q-CPMG sequence at times $2n\tau$ decays with a rate that is the sum of contributions from each of the motions. The extent to which a given motion i modulates the quadrupole Hamiltonian can be characterized by the second moment of that modulation, ΔM_{2i}. If the correlation time for that motion is τ_{Ci}, then the contribution to the decay rate of the q-CPMG echo train is

$$R_i = \Delta M_{2i}\tau_{Ci}\left[1-\frac{\tau_{Ci}}{\tau}\tanh\left(\frac{\tau}{\tau_{Ci}}\right)\right] \qquad (2)$$

where 2τ is the separation of echoes in the q-CPMG echo train (Blicharski, 1986; Bloom and Sternin, 1987; Bloom *et al.*, 1991) . The effect of the factor in square brackets is to

substantially reduce the contribution to q-CPMG echo train decay from motions with $\tau_{Ci} >> \tau$. Varying the pulse spacing from short to long progressively reintroduces the effect of motions with longer correlation times and thus probe the distribution of slower bilayer motions in a sample.

Figure 3.6 shows q-CPMG echo train decays at 38°C for DMPS-d_{54} alone and in the presence of 100 μM calcium and toposome at a lipid/protein molar ratio of 80,000:1. Echo trains were collected for $40\,\mu s \le \tau \le 500\mu s$. The echo train decays are plotted as $\ln(A(2n\tau)/A(2\tau_{min}))$ versus $2n\tau$ where $A(2n\tau)$ is the amplitude of a particular echo and $A(2\tau_{min})$ is the amplitude of the first echo for the experiment using the shortest τ ($40\,\mu s$ for this work). The strongly non-exponential echo train decays, particularly for larger values of τ, are typical of multilamellar vesicle samples and are similar to previous observations on chain-perdeuterated lipid samples (Bloom and Sternin, 1987; Fiech *et al.*, 1998). The results shown in Fig. 3.6, for both samples, are characterized by rapid initial decays of increasing fractions of the signal with increasing τ coupled with similar limiting rates of echo train decay at large $2n\tau$ for all values of τ. The limiting rates at large $2n\tau$ reflect fast, presumably local, motions that modulate the quadrupole interaction of all deuterons in a given sample. The vertical spread of the limiting decay curves suggests that deuteron quadrupole interactions are also modulated by slower motions whose contributions to echo train decay are sensitive to τ and that different populations of deuterons are affected by slow motions with different correlation times. The presence of toposome results in a faster initial decay of the echo train signal for all

Figure 3.6. Quadrupole Carr-Purcell_Meiboom-Gill (q-CPMG) echo train decays for (A) DMPS-d_{54} and (B) DMPS-d_{54} plus toposome (lipid:protein = 80,000:1) in 100 μM Ca^{2+}. Decays are plotted as $\ln[A(2n\tau)/A(2\tau_{min})]$ versus $2n\tau$ where $A(2n\tau)$ is the amplitude of the n^{th} echo in the train collected with echoes separated by 2τ and $A(\tau_{min})$ is the amplitude of the first echo obtained with the shortest value of τ. Echo trains were recorded for $\tau = 40\ \mu s$ (○); $\tau = 50\ \mu s$ (□); $\tau = 100\ \mu s$ (Δ); $\tau = 150\ \mu s$ (◊); $\tau = 200\ \mu s$ (●); $\tau = 300\ \mu s$ (■); $\tau = 400\ \mu s$ (▲); and $\tau = 500\ \mu s$ (♦). Quadrupole Carr-Purcell-Meiboom-Gill analysis was performed on single samples of either DMPS-d_{54} or DMPS-d_{54} plus toposome (80,000:1 and 100 μM Ca^{2+}).

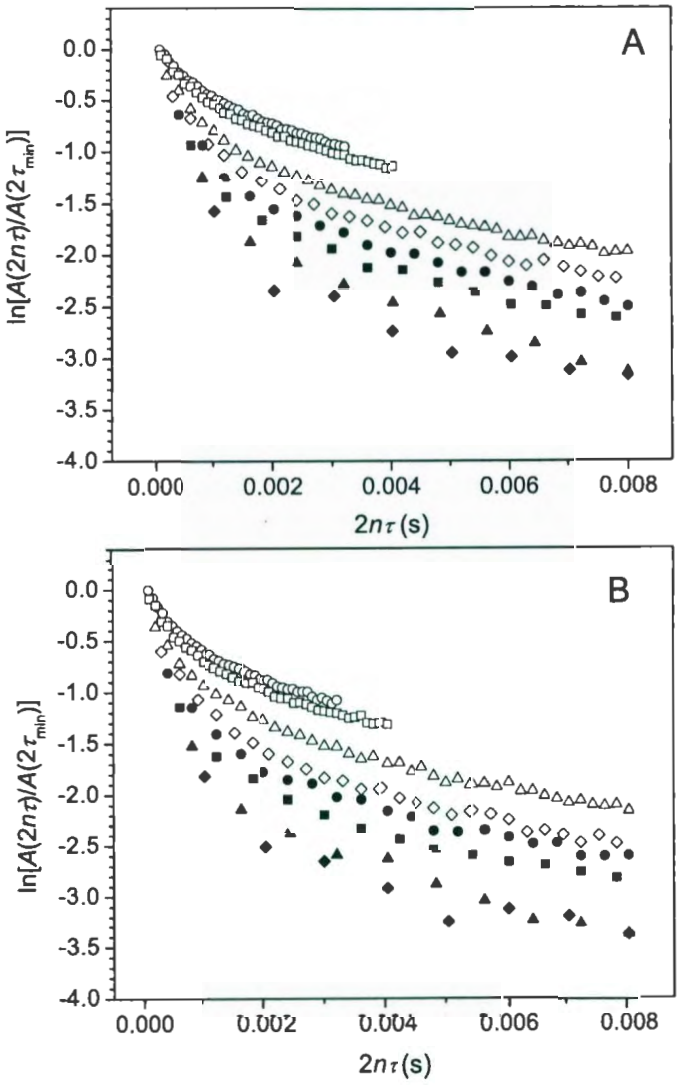
A
B
0.0
-0.5
-1.0
-1.5
-2.0
-2.5
-3.0
-3.5
-4.0
0.000
0.002
0.004
0.006
0.008
$2n\tau$ (s)
$\ln[A(2n\tau)/A(2\tau_{min})]$

values of τ but does not significantly alter the vertical separation of limiting decays for a given pair of τ values.

The τ-dependence of the echo train decays can be understood as follows. For short τ, only a small fraction of the deuterons are affected by slow motions that are nevertheless fast enough to contribute to echo train decay for that value of τ. The small portion of the signal from this fraction decays rapidly. The remaining deuterons are affected by slow motions with longer correlation times that do not contribute to echo train decay for this value of τ and the slow decay of signal from these populations is due to the fast common motion. As τ is increased, the fraction of the sample with slow motions that can contribute significantly to echo train decay increases. For each value of τ, the signal from this fraction of the sample decays rapidly leaving the signal from the rest of the sample to decay at the rate characteristic of fast common motions.

The q-CPMG echoes in multilamellar samples of chain perdeuterated lipids are sums of signals from populations of deuterons in which the quadrupole interaction is modulated to different extents by different superpositions of slow and fast motions. While the contributions from slow motions covering a wide and effectively continuous range of correlation times precludes precise characterization of the relevant slow motions, the non-exponential character and τ-dependence of the decays can be reproduced using models that approximate the actual spectrum of slow motions by a small number of discrete slow motions. Observing how the parameters of such a model must change in order to reproduce observed differences between q-CPMG observations on two samples

can provide some indication as to the extent to which the changes reflect either a change in the effective spectrum of slow motion correlation times or a change in the amplitudes of such motions.

The simplest model that can reproduce the τ -dependence of the non-exponential decays observed in multilamellar vesicle samples is one in which the quadrupole interaction of each deuteron is modulated by a superposition of one fast and one slow motion (Fiech *et al.*, 1998). The fast motion is assumed to be common to the entire sample and results in a contribution to the echo train decay rate of $1/T_2'$. A particular slow motion, denoted *i*, is assumed to be specific to particular population of magnitude A_i. For an echo train decay collected with a particular value of τ, the amplitude of the n^{th} echo can be then be written as (Fiech *et al.*, 1998)

$$A(2n\tau) = \sum_i^N A_i \exp\left(-2n\tau\left\{\Delta M_{2i}\tau_{Ci}\left[1-\frac{\tau_{Ci}}{\tau}\tanh\left(\frac{\tau}{\tau_{Ci}}\right)\right]+\frac{1}{T_2'}\right\}\right) \qquad (3)$$

where τ_{Ci} is the correlation time of motion i and ΔM_{2i} is the second moment of the portion of the quadrupole interaction modulated by motion *i*. The sum over populations in Eq. 3 thus approximates what is likely a more continuous distribution of slow motions within a given sample.

The echo train decays of Fig. 3.6 were fit to a model based on Eq. 3. The amplitude of the free induction decay following the initial pulse is generally not observable in wideline ^{2}H-NMR experiments because of the finite time required for preamplifier recovery following that pulse. In order to fit the initial decay of the q-CPMG echo train, though, it is necessary to estimate the amplitude of the initial free-

induction decay. Fortunately, extrapolating the slow decay of the shortest τ echo train back to $2n\tau = 0$ provides a good estimate of the initial amplitude for all of the echo train decays. The initial point obtained in this way was added to each of the decay data sets for a given sample before fitting.

It was found that the distribution of slow motions in a given sample could be adequately approximated by assuming 4 discrete populations with correlation times ranging from close to the characteristic time of the quadrupole echo experiment $\left(\sim 10^{-5}\ \mathrm{s}\right)$ to roughly 4 orders of magnitude longer. The precise way in which the continuous range of correlation times is binned into discrete values affects the magnitude of the population associated with each bin. As long as comparisons are based on fits using the same correlation time bins, relative changes in the population magnitude associated with each bin can still give some indication of the extent to which changes in q-CPMG decay behaviour reflect changes in the distribution of slow motions. The discrete correlation times used here were $\tau_{C1} = 2\times10^{-5}\ \mathrm{s}$, a value slightly shorter than the smallest τ used in collection of the echo train decays; $\tau_{C2} = 3\times10^{-4}\ \mathrm{s}$, a value of the order of the longest τ used; $\tau_{C3} = 6\times10^{-3}\ \mathrm{s}$, a value of about an order of magnitude larger than of the longest τ used; and, $\tau_{C4} = 1\times10^{-1}\ \mathrm{s}$, a value much longer than the longest τ used.

Simultaneous fits to eight sets of $\ln[A(2n\tau)/A(2\tau_{\min})]$ versus $2n\tau$ data corresponding to different values of τ for a given sample were thus carried out by using Eq 3 to calculate $A(2n\tau)$ as a sum of 4 exponentials. The 4 correlation times, τ_{Ci} were

fixed as described above. The nine remaining parameters were then varied to simultaneously minimize the discrepancy between the modeled decays and the eight decays observed for each sample. These nine fitting parameters comprise a population magnitude (A_i) for each of the 4 populations, a second moment (ΔM_{2i}) measuring the modulation of the interaction for each of the 4 populations, and a single decay rate $(1/T_2')$ due to fast motions and assumed to be common to all 4 populations. In the calculation of χ^2 during the fitting procedure, each data point was weighted equally.

The results of the fitting procedure are shown in Fig. 3.7. The decays corresponding to the parameters obtained in the fit are shown as solid lines superimposed on the observed decays. The values of A_i and ΔM_{2i} corresponding to each of the selected correlation times are shown as bar graphs in the figure. Error bars shown are the standard errors in the fitted value of each parameter. Both fits gave similar values for the contributions to the echo decay rate from common fast motions. These were $(1/T_2') = 76 \pm 3\,s^{-1}$ and $(1/T_2') = 73 \pm 4\,s^{-1}$ for DMPS-d_{54} and DMPS-d_{54} plus toposome, respectively. As noted above, partitioning of the sample between populations corresponding to different slow motions is expected to depend on how the range of slow motion correlation times is sampled by the fixed times selected. In this case, the values of τ_{Ci}, selected to give roughly uniform intervals in the values of $\ln(\tau_{Ci})$, gave rise to a monotonic decrease in population from the shortest to the longest correlation time for fits to both data sets. Toposome does not appear to change the population magnitudes for the slowest motions but does appear to induce a small shift from the second shortest correlation time to the shortest correlation time. This effect persists when the fit is

Figure 3.7. Results of simultaneously fitting q-CPMG decays for (A) DMPS-d_{54} and (B) DMPS-d_{54} plus toposome (lipid:protein = 80,000:1) in 100 μM Ca^{2+}. Symbols denote observed echo amplitudes for $\tau = 40\,\mu s$ (○); $\tau = 50\,\mu s$ (□); $\tau = 100\,\mu s$ (Δ); $\tau = 150\,\mu s$ (◊); $\tau = 200\,\mu s$ (●); $\tau = 300\,\mu s$ (■); $\tau = 400\,\mu s$ (▲); and $\tau = 500\,\mu s$ (♦). Solid lines are result of modeling sample as 4 populations with different slow motions and a common fast motion. Parameters for the fits were obtained by minimizing χ^2 based on all datapoints and requiring that all parameters except τ be common to all decays for a given sample. Slow motion correlation times for the 4 populations were fixed at $\tau_{C1} = 2\times10^{-5}$ s, $\tau_{C2} = 3\times10^{-4}$ s, $\tau_{C3} = 6\times10^{-3}$ s, and $\tau_{C4} = 1\times10^{-1}$ s. (C) comparison of the population magnitudes A_i obtained from the fit to DMPS-d_{54} echo train decays (open bar) and the fit to echo decays for DMPS-d_{54} plus toposome (shaded bars). (D) Comparison of the second moments, ΔM_{2i}, of the quadrupole interaction modulation associated with the slow motion in each population obtained from the fit to DMPS-d_{54} echo train decays (open bar) and the fit to echo decays for DMPS-d_{54} plus toposome (shaded bars). The contributions to the echo decay rate from common fast motions were $(1/T'_{2e}) = 76.3\,s^{-1}$ and $(1/T'_{2e}) = 72.9\,s^{-1}$ for DMPS-d_{54} and DMPS-d_{54} plus toposome respectively.

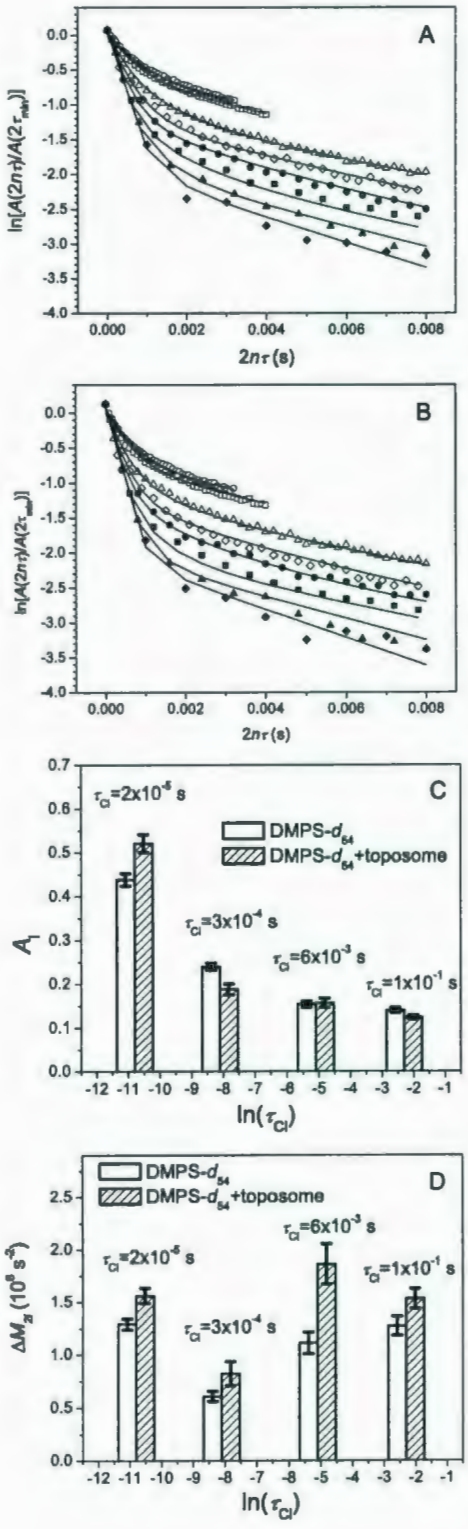
A
B
C
D
$2n\tau$ (s)
$\ln[A(2n\tau)/A(2\tau_{min})]$
τ_{Cl}=2x10^{-5} s
τ_{Cl}=3x10^{-4} s
τ_{Cl}=6x10^{-3} s
τ_{Cl}=1x10^{-1} s
DMPS-d_{54}
DMPS-d_{54}+toposome
A_1
$\ln(\tau_{Cl})$
ΔM_z (10^6 s^{-2})

redone with a slightly different set of fixed correlation times and might thus be of interest.

A more significant difference between the samples, though, is seen in the values of ΔM_{2i} obtained from the fits. Toposome appears to induce an increase in ΔM_{2i} for all populations. This likely accounts for the observed effect of toposome on quadrupole echo decay time in the liquid crystalline phase. An increase in ΔM_{2i} for a given motion likely indicates a larger amplitude of reorientation. Possible interpretations include larger amplitude orientational fluctuations within the bilayer or larger amplitude undulations of the bilayer surface. Distortion of the surface due to local interaction with protein interacting at the surface might also increase ΔM_{2i} as long as diffusion of lipids through the region of local distortion is not constrained. In the present case, any suggested interpretation must also be consistent with the lack of a significant observed perturbation of lipid acyl chain order or bilayer phase behaviour by toposome.

The data presented here define the nature of the association of toposome with the bilayer. The effects of toposome on bilayer lipid motion suggest that this protein interacts peripherally with the membrane. This interaction occurs in the presence of 100 μM calcium and is not further modulated by increased concentrations of this cation. These results correlate well with those from a previous study in which we examined the effect of calcium on toposome structure (Hayley *et al.*, 2006). At concentrations of calcium below 100 μM, apparent k_d = 25 μM, toposome underwent a change in secondary structure which facilitated binding to the bilayer. At higher concentrations of calcium, apparent k_d = 240 μM, toposome underwent a change in tertiary structure which

enabled this protein to drive membrane-membrane adhesive interactions. The NMR study reported here clearly demonstrates that the calcium-induced, tertiary structural change in toposome does not modulate protein-membrane interaction and thus more likely facilitates interaction between toposome molecules on opposing cell membranes, a reaction occurring at the cell surface. Collectively, these studies provide a mechanistic basis for the known cell-cell adhesive activity of toposome in the sea urchin embryo.

The patch hypothesis has been advanced as a model to explain the ability of sea urchin eggs to repair lesions in their plasma membrane (McNeil, 1993; Terasaki *et al.*, 1997; McNeil *et al.*, 2000). This model builds on the observation that yolk granules fuse into large vesicles when exposed to millimolar amounts of calcium. The large vesicles may then fuse with and reseal the plasma membrane. We have previously provided evidence that toposome associates peripherally with the outer surface of the yolk granule membrane (Perera *et al.*, 2004): (i) Toposome can be dissociated from isolated yolk granules with EGTA resulting in the loss of calcium-dependent yolk granule aggregation. Readdition of purified toposome to the EGTA-treated granules reconstituted calcium-dependent aggregation; (ii) Preincubation of purified toposome with anti-toposome antibody resulted in the inability of added protein to reconstitute calcium-dependent aggregation in EGTA-treated yolk granules; (iii) When purified yolk granules were preincubated with anti-toposome antibody followed by assay for calcium-dependent aggregation, no aggregation occurred. These data, along with results described here, suggest the intriguing possibility that toposome may be an important player on the pathway leading to plasma membrane repair. A lesion in the egg plasma membrane

would result in an influx of sea water containing 10 mM calcium. This calcium would drive the tertiary structural change in toposome associated with the yolk granule membrane. Toposome-Toposome interaction would then serve to juxtapose yolk granule membranes, which would subsequently fuse in a process driven by SNARE proteins (Steinhardt *et al.*, 1994).

[1]

Chapter 4:

Biochemical analysis of the interaction of calcium with toposome, a major protein component of the sea urchin egg and embryo.

[1] The chapter has been previously published; Hayley, M., Sun, M., Merschrod S, E.F., Davis P.J and Robinson, J.J. J. Cell. Biochem. In press.

4.1 Introduction

The yolk granules of sea urchin eggs and embryos occupy approximately one-third of the cytoplasmic volume. The major protein component of the granule is toposome, comprising 50% of the total yolk protein (Kari and Rottmann, 1980). Toposome, isolated from the sea urchin *Tripneustus gratilla* or *Paracentrotus lividus* appears to be a glycoprotein composed of six identical polypeptides of 160-170 kDa in size, depending on the species (Noll *et* al., 1985). Interestingly, as development proceeds the 160 kDa polypeptide is proteolytically processed, post-fertilization into smaller molecular mass species, apparently as the result of a cathepsin B-like activity, sensitive to thiol-protease inhibitors (Yokota and Kato, 1988; Scott and Lennarz, 1989; Mallya *et al.*, 1992; Yokota *et al.*, 2003). Although the functional significance of this processing remains to be determined, it has been suggested that it might serve to produce variants in a cell surface protein to direct morphogenic cell movements and generate epigenetic diversity (Noll *et al.*, 1985; Matranga *et al.*, 1986). In addition to the yolk granule, toposome is also localized to the embryonic cell surface (Gratwohl *et al.*, 1991) and has been identified as a molecule mediating cell-cell adhesion in the developing embryo (Noll *et* al., 1981; Noll *et* al., 1985; Matranga *et al.*, 1986; Cervello *et al.*, 1992).

In a previous study using both purified yolk granules and liposomes, we have characterized toposome-driven, membrane-membrane interactions (Perera *et al.*, 2004). This work has recently been extended with the analysis of calcium-toposome interaction (Hayley *et al.*, 2006a). This cation was found to induce two calcium-concentration dependent structural transitions in toposome: a secondary structural change occurred with

an apparent k_d (calcium) of 25 μM and this was followed by a tertiary structural change with an apparent k_d (calcium) of 240 μM. Interestingly, the first structural change was required to facilitate toposome binding to bilayers while the second structural change correlated with toposome-driven, membrane-membrane interaction. These results provide a structural basis for the previously described toposome-mediated, cell-cell adhesion in the sea urchin embryo (Noll *et al.*, 1985; Matranga *et al.*, 1986; Cervello *et al.*, 1992). In another study, we have defined the nature of the association of toposome with the bilayer using ^{2}H-NMR (Hayley *et al.*, 2006b). The results of this study suggest that toposome interacts peripherally with the membrane and this interaction occurs in the presence of 100 μM calcium and is not further modulated by increased concentrations of this cation. These results correlate well with those from the previous study examining calcium-toposome interaction. Furthermore, the NMR study clearly demonstrated that the calcium-induced, tertiary structural change in toposome did not further modulate protein-membrane interactions. Collectively, these studies provide a mechanistic basis for the known cell-cell adhesive activity of toposome in the sea urchin embryo.

In the study reported here, we have utilized atomic force microscopy, thermal denaturation and protease digestion analyses to further characterize calcium-toposome interactions. In addition, we have probed the specificity of the calcium-binding sites on toposome. Collectively, our results provide further evidence for the calcium-induced structural changes in toposome and suggest that under physiological conditions, the function(s) of toposome is regulated by calcium.

4.2 Materials and Methods

4.2.1 Preparation of yolk granule protein extracts and fractionation by ion exchange chromatography

Strongylocentrotus purpuratus were purchased from SeaCology, Vancouver, Canada. Eggs were harvested and washed consecutively in Millipore-filtered sea water (MFSW) and calcium, magnesium-free sea water (CMFSW). Preparation of the yolk granule protein extract followed the procedure described previously with some modifications (Perera *et al.*, 2004). Washed eggs were suspended in 0.5 M KCl (pH 7.0) and homogenized in a hand-held Dounce homogenizer at 0°C. The homogenate was then fractionated by centrifugation at 400 X g for 4 min at 4°C. The supernatant was harvested and fractionated by centrifugation at 2400 X g for 10 min at 4°C. The final pellet was resuspended in 0.5 M KCl (pH 7.0) containing 1 mM EDTA, fractionated by centrifugation at 50, 000 X g for 1 h at 4°C and the supernatant retained. Aliquots of the supernatant were dialyzed against starting buffer (10 mM Tris –HCl, pH 8.0) and were loaded onto a Q-Sepharose Fast Flow column (Amersham Pharmacia, Uppsala, Sweden) that had been previously equilibrated with starting buffer. The column was washed with three column volumes of buffer to remove any unbound proteins followed by the elution of bound proteins with a NaCl step gradient (0.1 – 1.0 M), prepared in starting buffer. The eluted proteins were analyzed by sodium dodecyl sulfate polyacrylamide gel electrophoresis (SDS-PAGE) (Hayley *et al.*, 2006a) as described by Laemmli (1970), and the gel stained with silver (Amersham Pharmacia, Uppsala, Sweden).

4.2.2 Lipid stamping

Multilamellar vesicles used in the lipid-stamping study were prepared as follows. Dimyristoyl phosphatidyl serine was dissolved in a 2:1 chloroform: methanol solution and vortexed for 4 min. The chloroform: methanol was evaporated under N_2 and vacuum dried for 24 h. Dimyristoyl phosphatidyl serine (0.1mg/mL) was then hydrated at 45°C for 1 h in dH_2O. Aliquots, 10 µL, were then transferred onto a micropatterned, polydimethylsiloxane-stamp and allowed to dry for 5 min. The stamp was pressed directly on a glass slide and then removed upon transfer of lipids to the silicon (Hovis and Boxer, 2001). Toposome, followed by specific concentrations of Ca^{2+}, was directly added to the lipid stamp. Imaging was performed on an MFP-3D (Asylum Research Inc) in contact mode using gold-coated, silicon cantilevers (Micromasch). Images are presented with minimal post-processing with a simple planefit used to correct for curvature.

4.2.3 Circular dichroism spectroscopy measurements

Circular dichroism spectra in the far-ultraviolet region (190-230 nm) were recorded using a Jasco - 810 spectrapolarimeter. Samples were dissolved and dialysed against 20mM Tris – HCl, pH 8.0 (unless otherwise stated) and the ellipticity at 222 nm of the protein / reagents mixture was checked to ensure that it did not exceed 1.0. A water-jacketed cell (light path = 5mm) was used and spectra were collected between 190 and 300 nm. Baselines were established using the appropriate buffers and twelve spectra were collected for each temperature and averaged. The temperature range (5 – 75°C) was controlled by a CTC-345 circulating water bath. The heating rate used in all experiments

was 30 °C per hour. Heating rates of 15 and 60°C per hour were also used to confirm that the samples had reached thermal equilibrium (data not shown). The scanning speed of the instrument was set at 100 nm / min with normal sensitivity.

4.2.4 Toposome digestion with chymotrypsin

In a total volume of 100 μL, aliquots of toposome (5 μg), in 20 mM Tris-HCl (pH 8.0), were incubated with chymotrypsin (0.5 μg) at room temperature for 30 min. The serine protease inhibitor PMSF (1 mM) was added to stop the digestion. In digestions where calcium and/or liposomes were present, toposome was preincubated for 30 min at room temperature in the presence of calcium and/or liposomes before the addition of chymotrypsin. In digestions containing both toposome and liposomes in the presence of 500 μM calcium, toposome and liposomes were initially incubated with 100 μM calcium for 30 min. After the 30 min incubation, the calcium concentration was increased to 500 μM and the incubation continued for an additional 30 min. Following incubation with chymotrypsin, the liposome pellets (1 mg) were harvested by centrifugation and fractionated in an 8% (w/v) SDS-PAGE gel which was stained with Coomassie Brilliant Blue R-250 (Laemmli, 1970).

4.2.5 Endogenous tryptophan fluorescence measurements

Tryptophan fluorescence was measured at room temperature in a Shimadzu Model RF-540 spectrofluorimeter. The excitation wavelength was 287 nm and emission spectra were measured between 300 and 400 nm. In all cases, samples were dissolved in

20 mM Tris-HCl, pH 8.0 followed by the addition of the specified ion to the final concentration indicated.

4.2.6 Displacement assay

Displacement assays were performed as described previously (Robinson, 1989). Aliquots (5μg each) of toposome were dot blotted onto a nitrocellulose membrane. The membrane was then equilibrated for 120 min at room temperature with calcium binding buffer (60mM KCl, 10mM imidazole-HCl, pH 6.8). Two pieces of the nitrocellulose membrane, one containing toposome and the second with no bound toposome as a control for background binding of ^{45}Ca, were incubated at room temperature for 15 min in calcium binding buffer containing ^{45}Ca (2 mCi/L). Directly after the 15 min incubation, the membranes were washed at room temperature for 5 min in 1mM Tris-HCl (pH 7.5) or in the same buffer containing 30 μM concentrations of various salts. The membranes were then air dried and counted in 10 mL of Scinti Verse E (Fisher Scientific) in a Beckmann model LS9000 liquid scintillation counter. Background binding was corrected for by subtracting the counts of the blank membranes from those of the membranes containing bound protein.

4.3 Results and Discussion

In a previous study, we demonstrated that low concentrations of calcium (k_d = 25 μM) induce a change in toposome secondary structure that facilitates toposome binding to bilayer lipids. In addition, we showed that higher concentrations of calcium (k_d = 240 μM) induced a change in tertiary structure which correlated with the ability of toposome

to drive membrane-membrane interactions. In the study reported here, we have further investigated toposome-Ca^{2+} interaction. Atomic force microscopy (AFM) was utilized to confirm our previous finding implicating the Ca^{2+}-induced, secondary structural change as the facilitator of toposome binding to bilayer lipids. Phosphatidyl serine bilayers were stamped onto glass slides and probed with toposome. In the absence of added Ca^{2+}, toposome binding to the bilayer was minimal (Fig 4.1A). However, when toposome was preincubated with sufficient Ca^{2+} to induce the secondary structural change, protein binding to the bilayer occurred as evidenced by the increased number of small dots on the membrane background (Fig 4.1B). The white streaks indicate that the protein remained mobile while bound to the membrane. Further increasing the Ca^{2+} concentration, to induce the tertiary structural change, did not result in any significant increased binding of toposome to the bilayer, as seen in Fig 4.1C (a digital zoom at 1/10 resolution). In control experiments, minimal binding of toposome occurred in the presence of 100- or 500 μM Mg^{2+} (Fig 4.1D, also a digital zoom at 1/10 resolution). This latter result clearly attests to the specificity of Ca^{2+} in modulating toposome-bilayer interaction.

Thermal denaturation experiments were performed, in the presence or absence of various concentrations of calcium, to determine if this cation modulated the stability of toposome. We chose concentrations of calcium that would induce the secondary structural change alone or both the secondary and tertiary changes. A temperature–dependent change in far–UV ellipticity was apparent in all thermal denaturation experiments (data not shown). In all the above experiments, the ellipticity at 222 nm decreased markedly with increasing temperature. At a temperature of 5°C, toposome was assumed to be fully folded. Denaturation of toposome in the presence and absence of

Figure 4.1. Atomic force microscopic analysis of toposome binding to phosphatidyl serine bilayers in the presence of various concentrations of calcium. Representative images are presented. (A) Toposome binding to phosphatidyl serine bilayers in the absence of exogenously added calcium. (B) Toposome binding to phosphatidyl serine bilayers in the presence of 100 μM calcium. (C) Toposome binding to phosphatidyl serine bilayers in the presence of 500 μM calcium. (D) Toposome binding to phosphatidyl serine bilayers in the presence of 100 μM magnesium.

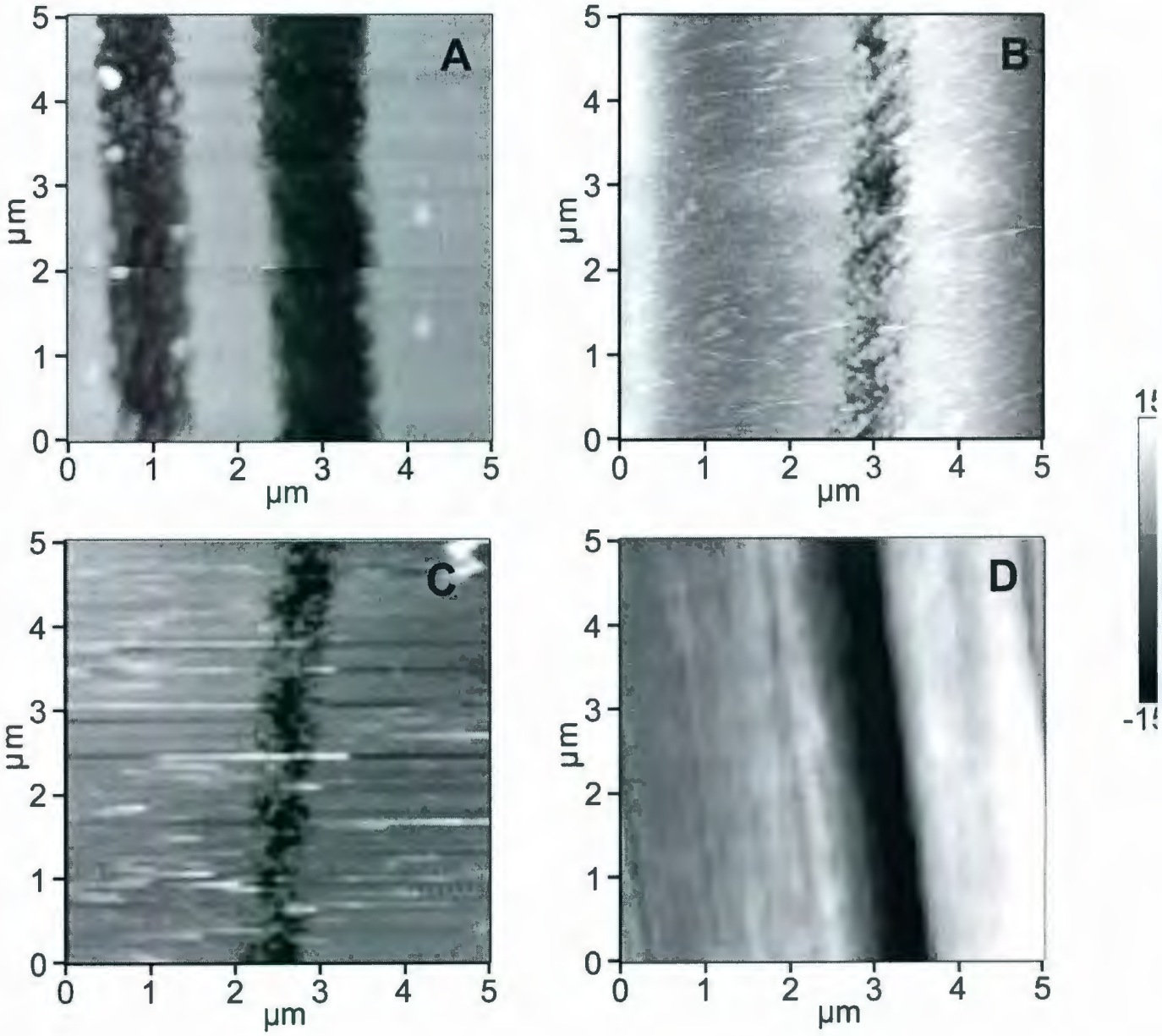
A
B
C
D
μm
0
1
2
3
4
5

calcium was monitored using the ellipticity values at 222 nm. The temperature dependent unfolding profile of toposome in the presence of 6 M urea was also measured. Figure 4.2 summarizes the thermal unfolding of toposome in the presence and absence of calcium, as well as in the presence of urea. The unfolding profile of toposome in the presence of 100 - and 500 μM calcium provides further evidence for calcium-dependent structural changes in toposome. At a calcium concentration (100 μM) sufficient to induce a change in secondary structure, the protein has an increased resistance to thermal denaturation compared to toposome in the absence of calcium: at 50^0C, toposome was 12.6% unfolded in the presence of 100μM Ca^{2+} compared to 36.8% in the absence of added Ca^{2+}. Interestingly, at a calcium concentration (500 μM) that induces a change in tertiary structure, the thermal stability of toposome is increased in comparison with that seen in the absence of calcium but is less stable when compared with toposome in the presence of 100 μM calcium, 26.4% vs 12.6% unfolded at 50^0C. As was expected, the thermal unfolding profile of toposome was greatly affected by the presence of 6 M urea, rendering the protein structurally unstable at much lower temperatures, 57.5% unfolded at 50^0C. The above results agree with our previous data suggesting that toposome undergoes two distinct structural changes as a result of increasing concentrations of calcium. Interestingly, these changes in structure result in quantitatively significant differences in the thermal stability of toposome.

In the study reported here, we used limited proteolysis in the presence and absence of Ca^{2+} to examine the structure of toposome, both in the membrane-free and membrane-bound forms. Figure 4.3 depicts the chymotryptic digestion patterns of free

Figure 4.2. Determination of the thermal unfolding profile of toposome under various conditions. Ellipticity at 222 nm was used to determine the percentage folding of the protein as a function of temperature. Reaction mixtures containing toposome and the indicated concentrations of calcium or urea were incubated at room temperature for 30 min prior to collection of the thermal unfolding data. 0 μM Ca^{2+} (Δ); 100 μM Ca^{2+} (□); 500 μM Ca^{2+} (●); 6 M urea (■).

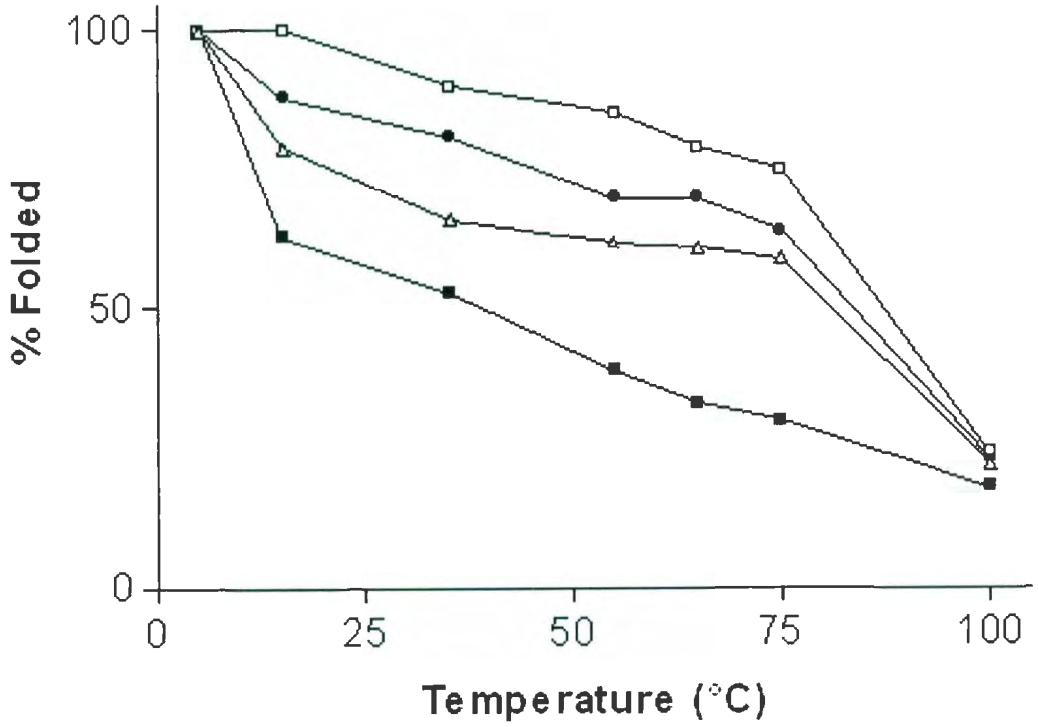
100
50
0
% Folded
0
25
50
75
100
Temperature (°C)

Figure 4.3. SDS-PAGE analysis of the chymotryptic digestion products of toposome in the presence or absence of calcium and /or liposomes. Undigested toposome (lane 1). Digestion pattern for toposome in the absence of added calcium and liposomes (lane 2). Digestion pattern for toposome in the presence of 100μM calcium (lane 3) or 500μM calcium (lane 4). Digestion pattern for toposome in the presence of phosphatidyl serine liposomes and 100μM calcium (lane 5) or 500μM calcium (lane 6). Equal amounts of toposome were loaded in each lane and the peptides visualized by silver staining.

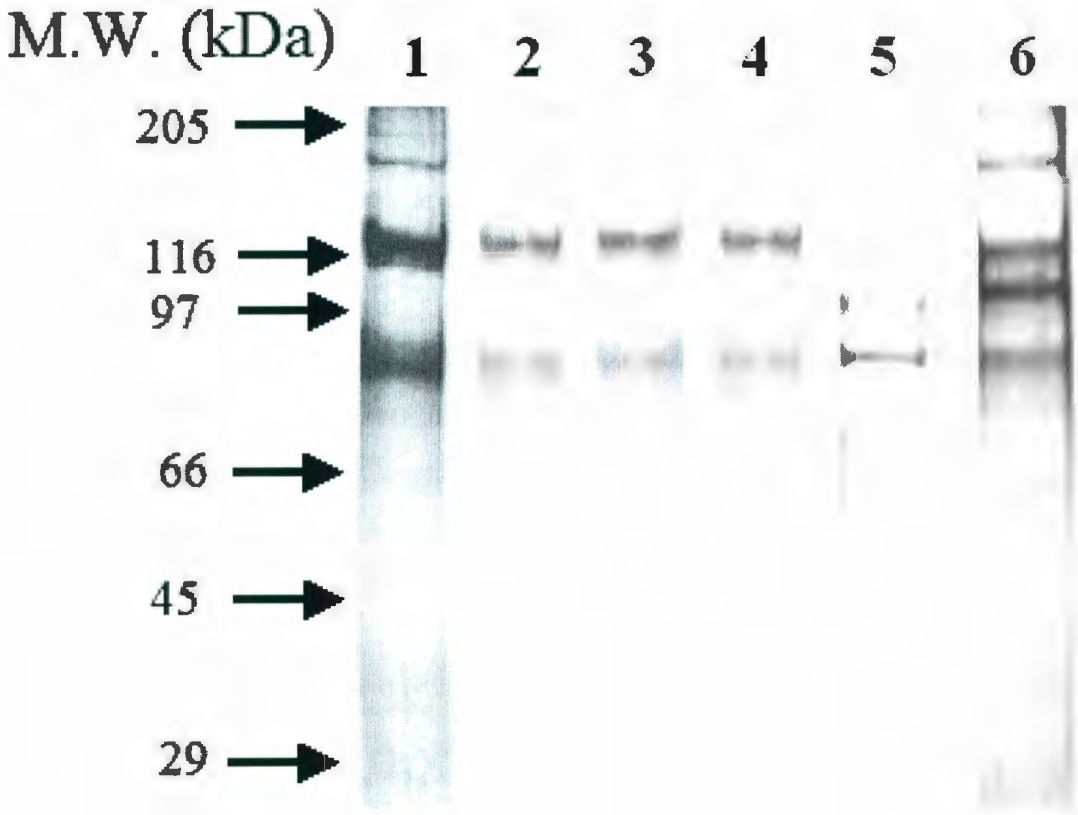
M.W. (kDa)
1
2
3
4
5
6
205
116
97
66
45
29

and membrane-bound toposome. In the presence of chymotrypsin, the 160-, 120- and 90 kDa polypeptides of toposome are all susceptible to cleavage, with complete digestion of the 160 kDa species occurring (lane 2). At a concentration of calcium (100 μM) sufficient to induce a change in the secondary structure of toposome, there was no difference in the chymotryptic digestion pattern compared to toposome in the absence of calcium (lane 2 vs. lane 3). Similarly, there was no change in the digestion pattern at a concentration of calcium (500 μM) that induced both the secondary and tertiary structural changes in the protein (lane 4). It was of interest to investigate the chymotryptic digestion pattern of toposome bound to liposomes composed of phosphatidyl serine at different concentrations of calcium. In previous experiments, we have shown that a calcium concentration of 100 μM, which is sufficient to induce the secondary structural change in toposome, facilitates quantitative binding of toposome to the bilayer (Hayley *et al.*, 2006a). Membrane-bound toposome ($[Ca^{2+}]$ = 100 μM) showed a significant difference in the chymotryptic digestion pattern when compared to the unbound form of the protein at the same calcium concentration (lane 5 vs. lane 3). This result most likely accrues from steric hindrance resulting from the binding of toposome to the bilayer. Following toposome binding to the bilayer, the calcium concentration was increased to 500 μM and the chymotryptic digestion profile determined. In this case the digestion pattern of membrane-bound toposome was unique (lane 6). The 160 kDa species appeared refractory to digestion while the 120- and 90 kDa polypeptides were partially digested. This result confirms that Ca^{2+} can induce the tertiary structural change in toposome bound to the bilayer.

To further explore calcium-toposome interactions, we designed experiments to characterize the cation binding sites of toposome. We analyzed the effects of other cations on toposome structure. Endogenous tryptophan fluorescence emission spectra were measured by excitation at 287 nm and monitoring the emitted light between 300 to 400 nm. The maximum emission wavelength (λ_{MAX}) for toposome was 333 nm. The steady state fluorescence emission spectrum of toposome was compared in the presence of various metal ions (Ca^{2+}, Mn^{2+}, Ba^{2+}, Cd^{2+}, Mn^{2+} and Fe^{3+}). As shown in Figure 4.4, all metal ions were capable of binding to toposome. As was the case for all metal ions tested, an increase in the cation concentration resulted in an emission spectrum that was altered. Although the λ_{MAX} for toposome remained unchanged at 333 nm, each metal ion tested had a quenching effect on the amplitude of the fluorescence emitted by toposome. Each metal ion quenched the fluorescence to a different extent; $Fe^{3+} > Cd^{2+} > Ca^{2+} > Mn^{2+} > Mg^{2+} > Ba^{2+}$.

A calcium displacement assay was used to determine if the metal ions examined in the fluorescence study were binding at the calcium binding sites on toposome. The displacement assay involved the binding of ^{45}Ca to toposome, dot blotted onto a nitrocellulose membrane, followed by quantification of displacement of the bound ^{45}Ca with a competing ion (Fig 4.5). Magnesium, Ba^{2+} and Fe^{3+} were largely unable to displace Ca^{2+}. In contrast, both Cd^{2+} and Mn^{2+} effectively displaced Ca^{2+}. These results show that metal ions possessing an ionic radius similar to that of calcium, Cd^{2+} and Mn^{2+}, can occupy the Ca^{2+}-binding sites on toposome while metal ions having an ionic radius

Figure 4.4. Tryptophan fluorescence emission spectra of toposome in the presence of increasing concentrations of various metal ions. Aliquots of toposome were preincubated with the indicated concentrations of various metal ions for 30 min at room temperature prior to spectrophotometric analysis. Ba^{2+} (●); Ca^{2+} (■); Cd^{2+} (○); Fe^{3+} (+); Mg^{2+} (x); Mn^{2+} (□).

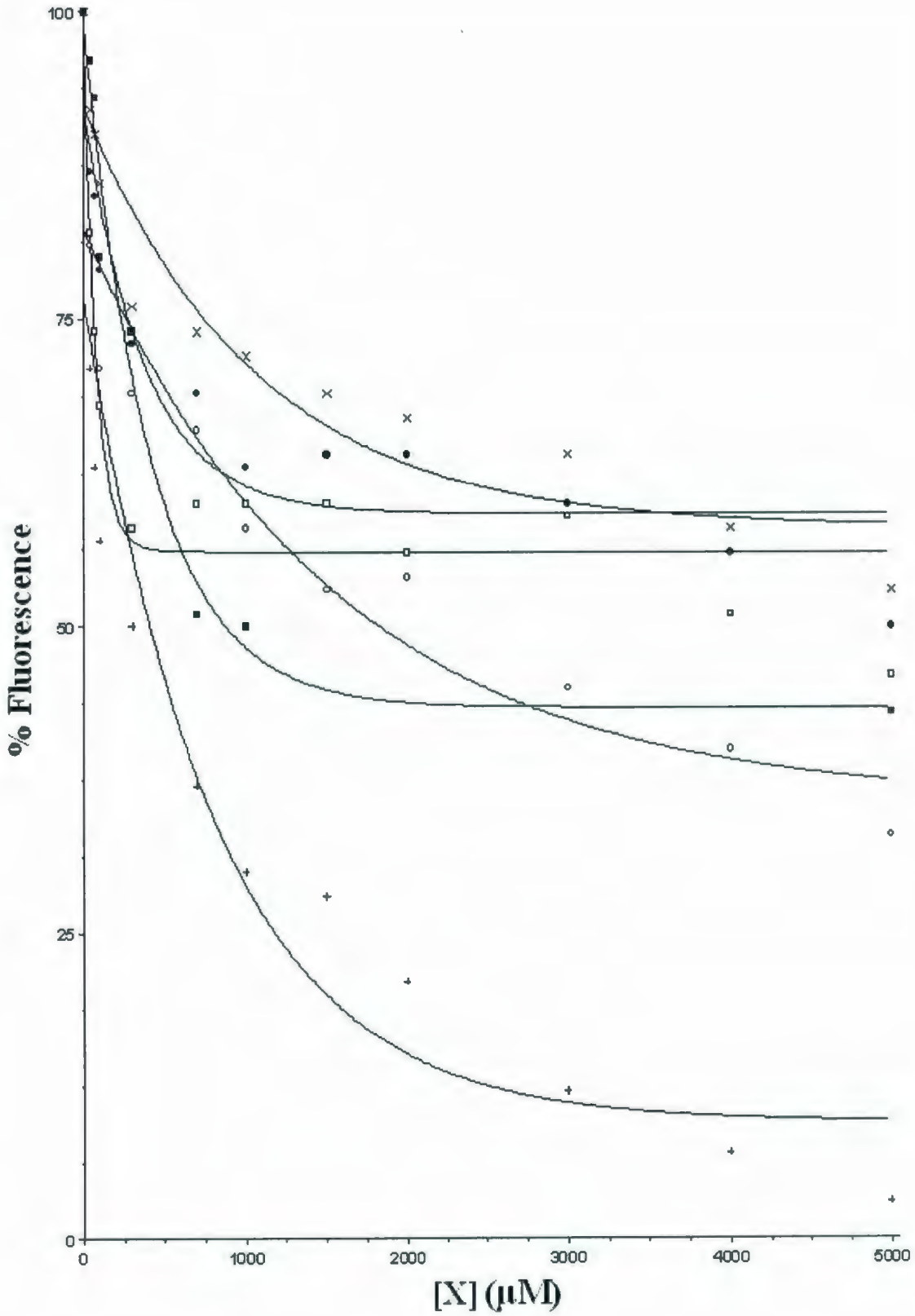
100
75
50
25
0
% Fluorescence
0
1000
2000
3000
4000
5000
[X] (µM)

Figure 4.5. Displacement of toposome-bound calcium by selective metal ions. Aliquots (5 μg each) of toposome were dot blotted onto nitrocellulose membrane and probed with ^{45}Ca as described in Materials and Methods.

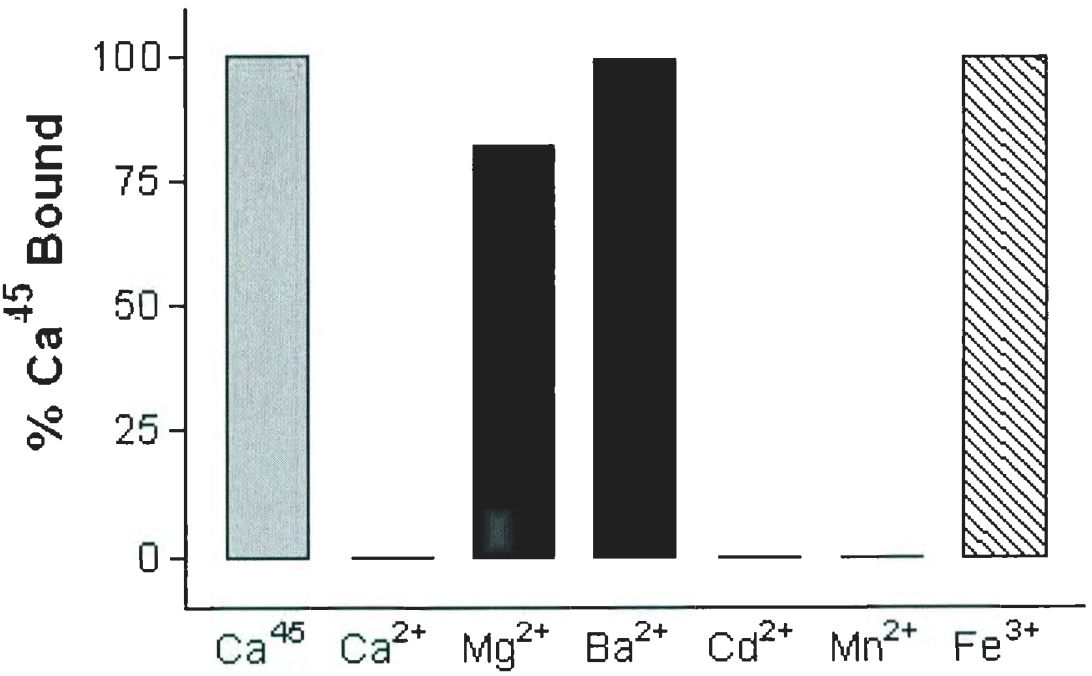
% Ca^{45} Bound
100
75
50
25
0
Ca^{45}
Ca^{2+}
Mg^{2+}
Ba^{2+}
Cd^{2+}
Mn^{2+}
Fe^{3+}

much smaller or larger than that of calcium cannot occupy these sites, Mg^{2+}, Ba^{2+} and Fe^{3+}. These results clearly indicate that the calcium-binding sites on toposome can selectively accommodate other divalent cations. However, these metal ions, Cd^{2+} and Mn^{2+}, are present in trace amounts in seawater, and therefore, are unable to interfere with the calcium-dependent functions of toposome. It is of interest to note that although magnesium is present in seawater at a concentration of 50 mM, it is excluded from the calcium-binding sites on toposome.

Recent research suggests that toposome is a transferrin-like iron binding protein and suggests that toposome transports free iron in the coelomic fluid to the testis and ovary, supporting gametogenesis (Brooks and Wessel, 2002). As observed in the endogenous tryptophan fluorescence experiment (Fig. 4.4), toposome is capable of binding iron. Functional transferrins bind iron as Fe^{3+} with an extremely high affinity and are capable of transporting concentrations of iron at or below the nano-molar range (Baker *et al.*, 2003). However, our fluorescence data indicate that toposome has an apparent dissociation constant (Fe^{3+}) of 275 μM and appears to be insensitive to low concentrations of iron. Based on the apparent dissociation constant and the trace amounts of iron present in seawater, we suggest that toposome, although transferrin-like in sequence, is unlikely to function as an iron transporter in the developing sea urchin egg and embryo.

In conclusion, the results reported here further confirm and expand upon our knowledge of toposome structure and function. Thermal denaturation and chymotryptic

digestion studies both provide further evidence for the two distinctive, Ca^{2+}-dependent structures of toposome. Atomic force microscopy confirmed our previous finding that the Ca^{2+}-dependent secondary structural change is necessary to facilitate toposome binding to the bilayer. In a previous study we showed that the Ca^{2+}-dependent tertiary structural change was required for toposome-driven, membrane-membrane interaction (Hayley *et al.*, 2006a). These data are significant in the context of the ability of sea urchin eggs and embryos to repair lesions in their plasma membranes. The patch hypothesis describes a two step model in which yolk granules fuse in response to millimolar concentrations of Ca^{2+} and the resulting large vesicles then fuse with the damaged plasma membrane (Terasaki *et al.*, 1997; McNeil *et al.*, 2000). Our previous data, supported by the results reported here suggest the intriguing possibility that toposome may be an important player on the pathway leading to plasma membrane repair. A lesion in the egg plasma membrane would result in an influx of sea water containing 10 mM Ca^{2+}. This Ca^{2+} would drive the tertiary structural change in toposome which in turn would drive membrane-membrane interaction. There are two possible models for defining a role for toposome in this process. The tertiary structural change may generate protein-protein interaction sites allowing toposome molecules on apposing membranes to interact. Alternatively, the tertiary structural change may expose a second membrane binding site on toposome. This latter model precluded the necessity for toposome to be present on both interacting surfaces.

Chapter 5:

Localization of toposome in the sea urchin egg and embryo

5.1 Introduction

Research has described several storage compartments in the sea urchin egg whose components are destined to be exported to the apical and / or basal laminas during embryonic development. The well characterized cortical granules lie along the periphery of the egg, and secrete their contents onto the apical surface of the egg immediately following fertilization (Hylander and Summers, 1982; McClay and Fink, 1982; Anstrom *et al.*, 1988). Hyalin, a major component of the hyaline layer, is housed in the cortical granules, along with other hyaline components such as ovoperoxidase and mucopolysaccharides (Schuel *et al.*, 1974; Hylander and Summers, 1982; Alliegro and Schuel, 1988). As well, some cytoplasmic storage granules contain proteins which are transported bidirectionally, to the apical and basal laminas, while others are exported unidirectionally, to either the apical or basal lamina (Wessel *et al.*, 1984; Alliegro and McClay, 1988; Fuhrman *et al.*, 1992; Matranga *et* al., 1992; Matese *et al.*, 1997; Mayne and Robinson, 1998; Tesoro *et al*, 1998; Kato *et al.*, 2004).

As discussed earlier, toposome represents approximately 8% of the total egg protein and is a major protein component of the yolk granule (Kari and Rottmann, 1980). Toposome appears to be a hexameric glycoprotein consisting of six identical subunits each of 160 kDa (Noll *et al.*, 1985). The ultrastructural localization of toposome has been investigated in a number of laboratories with conflicting results (Scott and Lennarz, 1989; Gratwohl *et al.*, 1991).

Scott and Lennarz (1989) showed that in all stages of development of the sea urchin Strongylocentrotus *purpuratus*, toposome was localized exclusively in the yolk granules. This subcellular localization was identical to that shown by Armant *et al.* (1986), using gold conjugated to concanavalin A in Arbacia *punctulata* eggs, and to that shown by Shyu *et al.*(1986) using the immunogold technique with an antibody directed toward the 160 kDa polypeptide in Strongylocentrotus *purpuratus* eggs. Even as late as 96 hr in development, toposome was found exclusively in the yolk granules and no evidence could be obtained for its presence in other organelles or at the cell surface (Scott and Lennarz, 1989).

On the contrary, immunofluorescent labeling of sectioned blastulae with a toposome specific monoclonal antibody stained all cell surfaces, apical, lateral and basal (Noll *et al.*, 1985). In addition, Gratwohl *et al.* (1991) demonstrated that in the unfertilized egg, toposome is present in the yolk granules, in the lamellar compartment of the cortical granules, and on the entire cell surface. Development from unfertilized egg to blastula affected the pattern of toposome labeling. Toposome localized to the lamellar compartment of the cortical granules is exocytosed at fertilization to become part of a double layer enveloping the hatched blastula on the outside of the hyaline layer (Gratwohl *et al.*, 1991).

In the current study, we utilized immunoelectron microscopy to identify the storage compartment(s) for toposome within the egg and its localization in various stage

embryos to help resolve the conflicting data concerning the localization of this protein throughout development.

5.2 Materials and Methods

5.2.1 Growth of Embryos

Strongylocentrotus *purpuratus* were purchased from Seacology, Vancouver, British Columbia, and gametes were obtained by intra-coelomic injection of 0.5 M KCl. Eggs were washed three times in ice-cold Millipore-filtered seawater (MFSW; 0.45 μm filter size) and fertilized with a 100-fold numerical excess of sperm. Embryos were cultured with constant aeration, at 12 °C, in cylindrical chambers containing paddles rotating at 40 rpm. Samples were harvested at the times indicated after fertilization.

5.2.2 Fixation and Embedding of Eggs and Embryos for Electron Microscopy

Eggs and various stage embryos were fixed as previously described by Spiegel *et al.* (1989). Fixation was carried out by adding aliquots of eggs and various stage embryos to an equal volume of the stock fixative containing 4% (v/v) glutaraldehyde and 1% (w/v) paraformaldehyde in 75% MFSW buffered with 0.15 M sodium cacodylate, pH 7.6, without osmium postfixation. Eggs and embryos were rinsed in 85% MFSW containing 0.1 M sodium cacodylate, pH 7.6, three times for 30 min at room temperature. Samples were then rinsed three times for 30 min in 0.1 M sodium cacodylate, pH 7.6, followed by three 30 min rinses with distilled water. Samples were then dehydrated in an ethanol series and embedded in Spurrs resin overnight at room temperature in an evacuated container. The blocks were cured overnight at 70 °C.

Thin sections (150 nm) of eggs and embryos were prepared and placed on nickel grids. Grids were incubated on drops of a solution containing 1% (w/v) BSA, 0.01 M phosphate buffered saline (PBS), consisting of 0.01 M phosphate in 0.15 M NaCl, pH 7.4, and 0.5% (v/v) Tween-20 three times for 15 min at room temperature. Grids were then transferred to a drop of anti toposome antibody (1:100 dilution in 0.01 M PBS, pH 7.4, containing 1% (w/v) BSA and 0.5% (v/v) Tween-20) for two hours at room temperature. After antibody incubation, the grids were rinsed five times for 5 min on drops of 0.01 M PBS, pH 7.4, containing 0.5% (v / v) Tween-20, then incubated on drops of 0.01 M PBS, pH 7.4, containing 1% (w/v) BSA and 0.5% (v/v) Tween-20 three times for 5 min. Grids were incubated on drops of protein A-gold (Sigma Co.; 10 nM colloidal gold) diluted 1:50 in a solution of 0.01 M PBS, pH 7.4, containing 1% (w/v) BSA and 0.5% (v/v) Tween-20 for 60 min at room temperature. Following several rinses in a solution containing 0.01 M PBS, pH 7.4, and then distilled water, the grids were allowed to air dry.

Sections were stained on a drop of 2% (w / v) uranyl acetate in 50% ethanol for 20 min at room temperature, then rinsed with 50% ethanol, followed by 25% ethanol and finally distilled water, and stained on a drop of Reynold's lead citrate for 10 min at room temperature. Sections were rinsed with distilled water, allowed to air dry and viewed in a Zeiss EM 109 transmission electron microscope at 80 kV.

5.2.3. Preparation of polyclonal anti toposome antibody

Polyclonal anti toposome antibody was prepared by Dr. J Robinson using methodology that has been previously described (Robinson, 1990).

5.3 Results

We employed high resolution, immunogold labeling analysis to localize toposome in eggs and various stage embryos. Polyclonal antiserum prepared against purified toposome, was used for the immunolocalization study. The specificity of the antiserum was tested by western blot analysis of egg proteins. A single species at 180 kDa was detected (Fig. 5.1). The antiserum preparation and western blot analysis was performed by Dr. John Robinson. We then utilized this antiserum for the immunogold analysis. In the unfertilized egg, labeling was evident in the matrix of the yolk granule (Fig. 5.2, Panel A). The membrane bounding the matrix was also labeled (Panel A). Labeling was also found in the lamellar compartment of the cortical granules and over the entire plasma membrane (Panel B). The mitochondria and lipid vacuoles were unlabeled (Panel C). In control experiments, using preimmune serum, no labeling was detected in the yolk granules, the cortical granules or on the plasma membrane (Panels D and E). These results confirm the previous findings of Gratwohl *et al.* (1991), who also showed that that toposome in the unfertilized egg is present in the yolk and cortical granules, and, on the entire cell surface.

One hour post fertilization (1 HPF, 2 cell stage), toposome was detected in the apically located hyaline layer (Fig. 5.3, Panel A). As well, the yolk granules (Panels B and C) and plasma membrane (Panel D) retained label. Toposome label was again apparent on the surface of the yolk granule (Panels B and C). At 9 hours post fertilization (9 HPF, cleavage stage), toposome was detected in the apically located hyaline layer, the yolk granules and on the cell

Figure 5.1: Western blot analysis of sea urchin eggs using the anti-toposome antiserum. An aliquot (15 μg) of egg was fractionated in a 3-12% (w/v) polyacrylamide gradient gel and transferred to a nitrocellulose membrane. Lane 1 is egg protein fractionated on the polyacrylamide gradient gel. Lane 2 is the nitrocellulose membrane that was probed with the anti-toposome antiserum at a dilution of 1:200 (v/v).

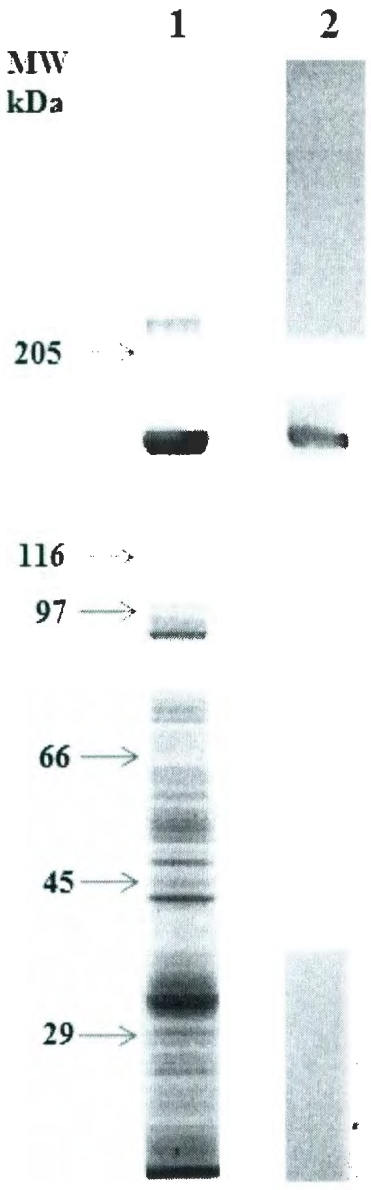
1
2
MW
kDa
205
116
97
66
45
29

Figure 5.2. Immunogold labeling of sea urchin eggs. Panels A-C represent sections of unfertilized eggs probed with the anti toposome antibody (1:100 (v / v) dilution in 0.01 M PBS, pH 7.4, containing 1% (w / v) BSA and 0.5% (v / v) Tween-20). Panels D and E were used as a control and were probed with pre-immune serum at a dilution of 1:100 (v / v). CG, cortical granule; YG, yolk granule; LV, lipid vacuole; M, mitochondrion.

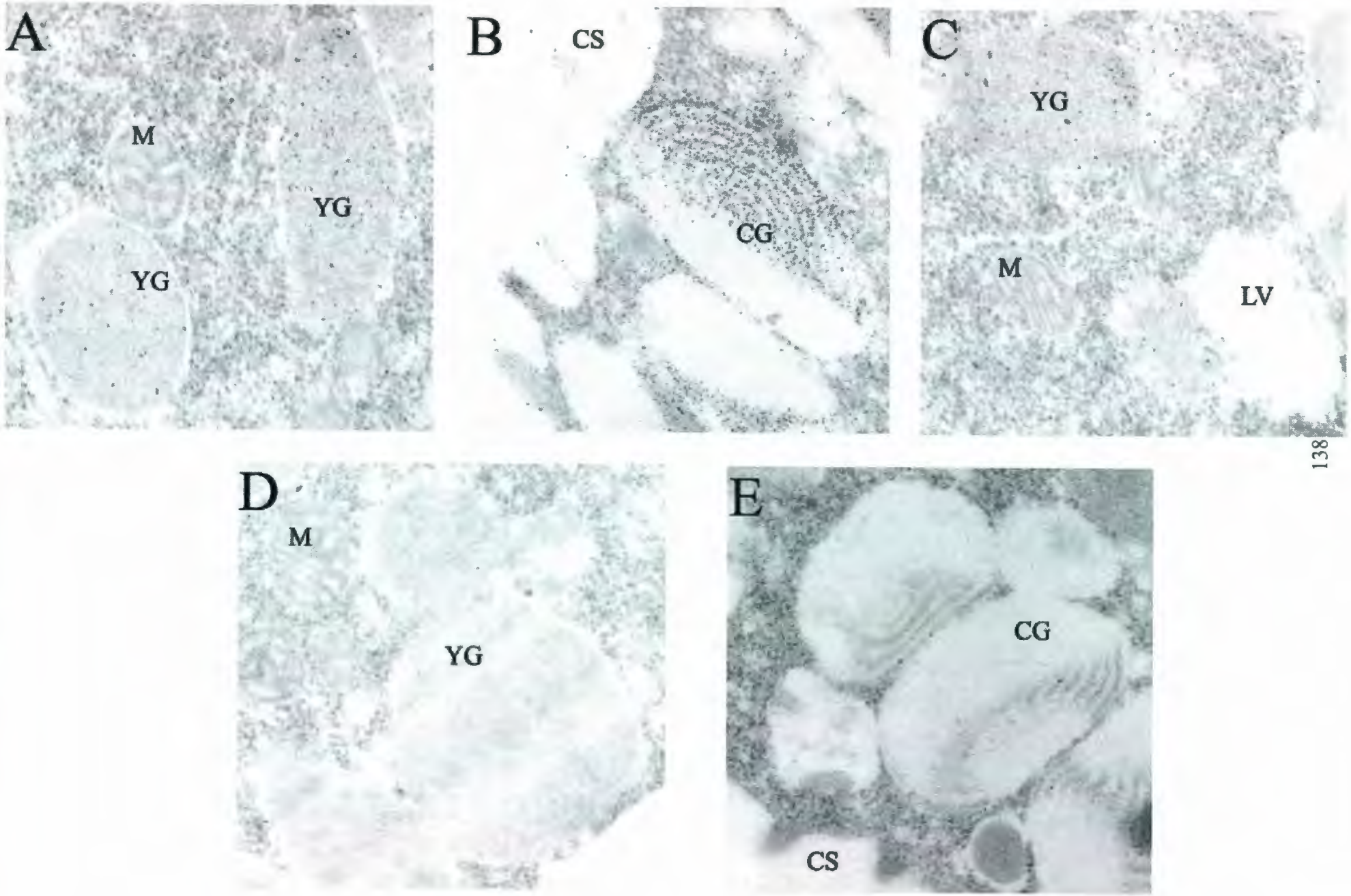
A
M
YG
YG
B
CS
CG
C
YG
M
LV
D
M
YG
E
CG
CS

Figure 5.3. Immunogold labeling of various stage embryos. Panels A-D represent sections of one hour old embryos probed with the anti toposome antibody (1:100 (v / v) dilution in 0.01 M PBS, pH 7.4, containing 1% (w / v) BSA and 0.5% (v / v) Tween-20). Panels E-G represents sections of nine hour old embryos probed with the anti toposome antibody at a dilution of 1:100 (v / v). HL, hyaline layer; CS, cell surface; YG, yolk granule. M, mitochondrion; L, lipid vacuole.

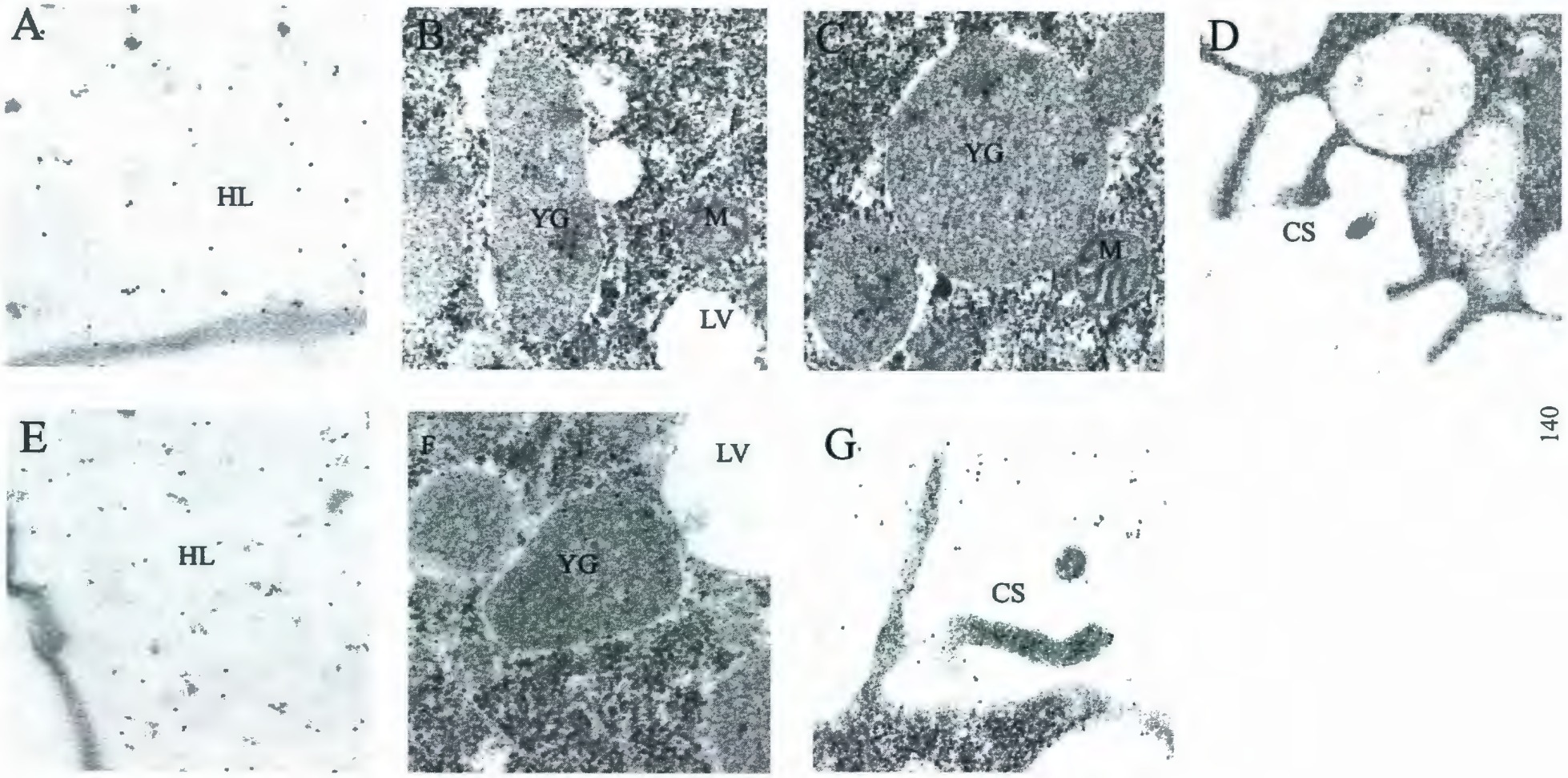
A
HL
B
YG
M
LV
C
YG
M
D
CS
E
HL
F
YG
LV
G
CS

surface (Panels E, F and G). Again, toposome was detected on the surface of the yolk granule (Panel F).

In blastula stage embryos (24 HPF), toposome was again present in the hyaline layer as well as in the yolk granules (Fig. 5.4, Panels A and B). As seen in all stages of development thus far, toposome remained detectable on the surface of the yolk granule (Panel B). Panel C contains a cortical granule from an egg that was not fertilized and retained its label exclusively in the lamellar compartment, providing a positive internal control. In gastrula stage embryos (45 HPF), toposome was present in both ECMs, the hyaline layer (Panel D) and basal lamina (Panel E), while the yolk granules still retained their label (Panel F). Labeling of toposome in the pluteus stage (69 HPF) was similar to the labeling of toposome seen in the gastrula stage. The hyaline layer (Panel G) and basal lamina (Panel H), as well as the yolk granules (Panel H), were labeled. Quantitation of immunogold labeling clearly identifies the cortical and yolk granules as storage compartments for toposome (Table 5.1). Throughout development, toposome label in the yolk granule remained constant, while label was absent from both the mitochondria and lipid vacuoles (Table 5.1). In addition, toposome label also remained constant in both the hyaline layer and basal lamina between blastula and pluteus stage embryos (Table 5.1).

Figure 5.4. Immunogold labeling of various stage embryos. Panels A-C represent sections of blastula stage embryos (24 HPF) probed with the anti toposome antibody (1:100 (v / v) dilution in 0.01 M PBS, pH 7.4, containing 1% (w / v) BSA and 0.5% (v / v) Tween-20). Panels D-F represents sections of gastrula stage embryos (45 HPF) probed with the anti toposome antibody at a dilution of 1:100 (v / v). Panels G and H represents sections of pluteus stage embryos (69 HPF) probed with the anti toposome antibody at a dilution of 1:100 (v / v). CG, cortical granule; BL, basal lamina; HL, hyaline layer; YG, yolk granule; LV, lipid vacuole.

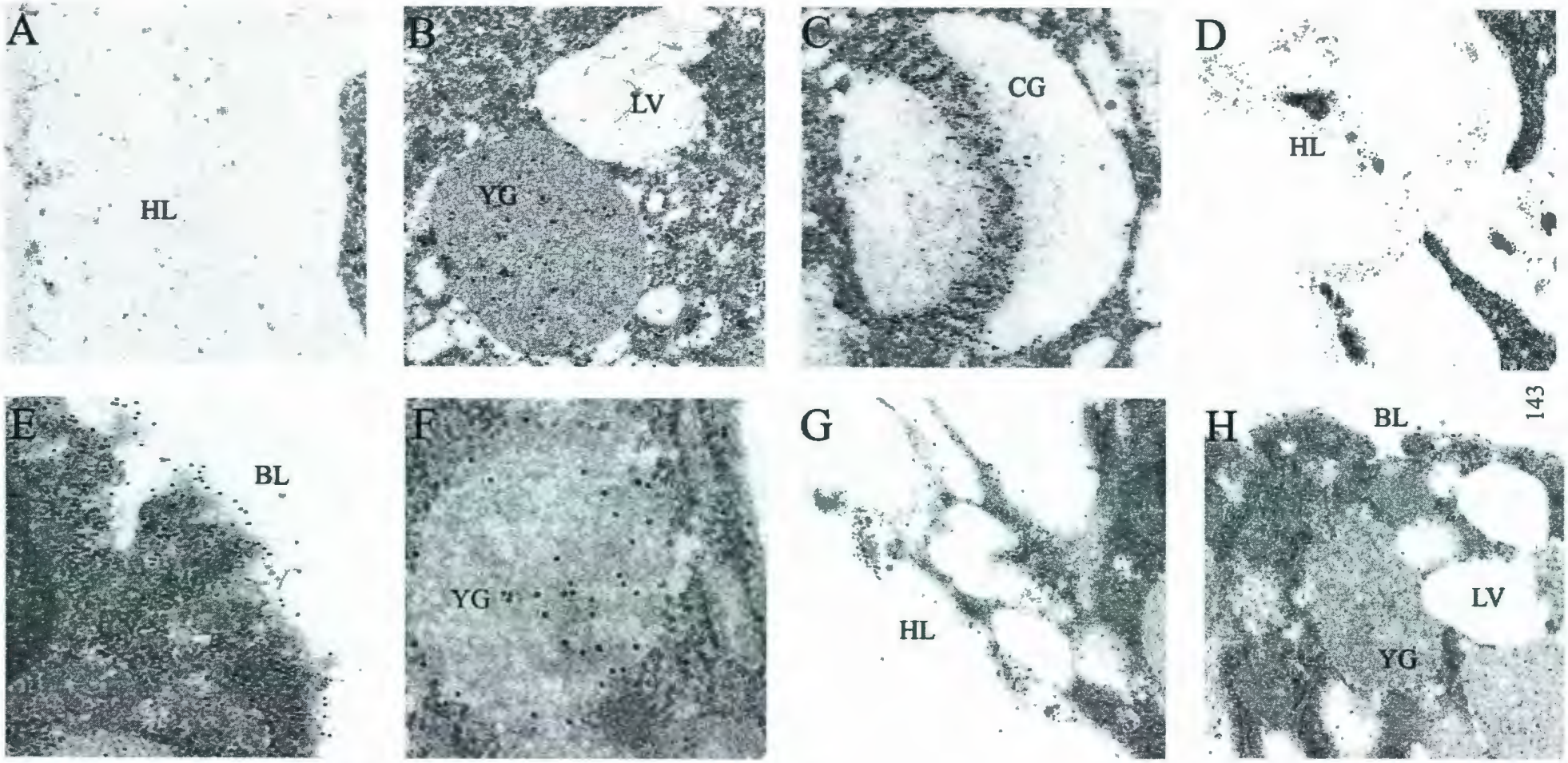
A
HL
B
LV
YG
C
CG
D
HL
E
BL
F
YG
G
HL
H
BL
LV
YG

Table 5.1: Quantitation of Immunogold Labeling

Organelle	Egg	1HPF	9HPF	24HPF	45HPF	69HPF
Cortical Granules	25.6 +/ 6.4 [100%]	----	----	----	----	----
Yolk Granules	3.9 +/- 1.8 [91%]	4.1 +/- 2.0 [80%]	3.0 +/- 1.3 [70%]	3.7 +/- 1.7 [82%]	3.1 +/- 1.6 [76%]	3.3 +/- 1.3 [79%]
Mitochondria	0	0	0	0	0	0
Lipid Vacuoles	0	0	0	0	0	0
Hyaline Layer	----	0.9 +/- 0.2 [48%]	1.9 +/- 0.4 [70%]	0.8 +/- 0.2 [48%]	0.9 +/- 0.3 [48%]	1.8 +/- 0.6 [68%]
Basal Membrane	----	----	----	ND	5.4 +/- 0.3 [85%]	5.9 +/- 0.7 [85%]

Values represent means +/- standard error of the mean (n=50). Quantitation was based on counting the number of Immunogold particles in a 0.50 μm^2 area. Values are corrected for background binding by subtracting the number of Immunogold particles in the same area of cytoplasm. Values in parentheses represent the percentage of structures labeled above background. HPF = hours post-fertilization; ND = not determined. 1HPF, 2 cell stage; 9HPF, cleavage stage; 24HPF, hatched blastula; 45HPF, gastrula stage; 69HPF, pluteus stage.

5.4 Discussion

This study examines the subcellular distribution of toposome in the sea urchin egg and various stage embryos. In the unfertilized egg, toposome was found on the entire surface of the plasma membrane as well as stored in two different compartments, the yolk and cortical granules. Interestingly, toposome was also found to be localized on the surface of the yolk granule. This confirms previously provided evidence that toposome associates peripherally with the outer surface of the yolk granule membrane (Perera *et al.*, 2004; Hayley *et al.*, 2006b): (i) Toposome was dissociated from isolated yolk granules with EGTA resulting in the loss of calcium-dependent yolk granule aggregation. Readdition of purified toposome to the EGTA-treated granules reconstituted calcium-dependent aggregation; (ii) Preincubation of purified toposome with anti-toposome antibody resulted in the inability of added protein to reconstitute calcium-dependent aggregation in EGTA-treated yolk granules; (iii) When purified yolk granules were preincubated with anti-toposome antibody followed by assay for calcium-dependent aggregation, no aggregation occurred; (iv) The effects of toposome on bilayer lipid motion suggest that this protein interacts peripherally with the membrane. The localization of toposome to the plasma membrane, as well as being stored in both the yolk and cortical granules confirms the results of Gratwohl *et al.* (1991).

Previous attempts at localizing toposome by immunogold-labeling detected its presence in yolk granules, but failed to detect it in both cortical granules and on the cell surface (Shyu *et al.*, 1986; Scott and Lennarz, 1989). Gratwohl *et al.* (1991) suggests that

in both these cases, the negative results may be due to a combination of low immunoreactivity and poor preservation of membranes. On the other hand, there is a wide variety of evidence suggesting a cell surface localization for toposome; (i) Blocking of contact sites on the cell surface with genus-specific anti-toposome antibodies resulted in live embryos dissociating into single cells. The dissociation of live embryos could be reversed by neutralizing the blocking antibodies with toposome (Noll *et al.*, 1981). (ii) Embryos treated with butanol dissociated into single cells. Readdition of purified toposome reconstituted reaggregation and development of the butanol-extracted cells (Matranga *et al.*, 1986). (iii) Loss of reaggregation by the removal of toposome from dissociated cells by treatment with trypsin (Matranga *et al.*, 1986), (iv) fluorescent labeling of all cell surfaces of blastula cells with toposome-specific monoclonal antibodies (Noll *et al.*, 1985), and finally (v) immunogold-labeling (Gratwohl *et* al., 1991).

In the sea urchin, yolk granules comprise nearly one-third the volume of the unfertilized egg and were historically viewed as a storage compartment for nutrients required by the developing embryo. Recently, the yolk granule has been identified as a storage compartment for proteins destined for export from the developing embryo, challenging the above view of the yolk granule as a benign organelle (Mayne and Robinson, 1998, 2002). Scott *et al.* (1990) showed that Strongylocentrotus *purpuratus* embryos at the feeding larvae stage did not consume yolk granule proteins under starvation conditions, challenging the notion that yolk granules contained nutrients that

could be used by the embryo. In fact, the opposite was true. They showed that it was the fed larvae that utilized the yolk granule proteins, suggesting that this organelle may contain components necessary for development. The hypothesis that the yolk granule contains nutrients that are utilized during development has also been refuted based on the evidence that the total composition of the yolk granule does not change throughout embryonic development (Armant *et al.*, 1986; Yakota and Kato, 1988; Mallya *et al.*, 1992).

The yolk granule is an abundant organelle in the cytoplasm of insects, annelids, amphibians and echinoderm embryos and several reports suggest that it is a dynamic entity. For instance, Liao and Wang (1994) identified yolk granules of the bull frog (*Rana catesbeiana*) oocyte as the storage compartment for ribonuclease. The majority (94%) of activity was localized in yolk granules with the remaining 6% found in the cytoplasm (Wang *et al.*, 1995). These findings have been presented as evidence that yolk granules serves as a compartment that regulates the cytoplasmic access of some intracellular enzymes. In early embryos of the insect, *Blattella germanica*, a cysteine protease was found labeled in only a sub-population of yolk granules. As development proceeded, the protease was found to be distributed to all yolk granules. Interestingly, label spread throughout the yolk granule population coincident with the "budding-off" of small vesicles from labeled yolk granules and their fusion to unlabeled granules (Giorgi *et al.*, 1997). Collectively, these results suggest that yolk granule membranes can engage in both budding and fusion reactions. In *Xenopus laevis*, Outenreath *et al.* (1988) identified a cell surface lectin that was stored in the yolk granules prior to export. Mayne

and Robinson (1998, 2002) have shown that both the 41 kDa collagenase/gelatinase and HLC-32, protein components of the extra-embryonic matrix, were found to be localized in the yolk granules of unfertilized eggs. However, as development proceeded, these proteins were detected on the embryonic cell surface. These results collectively establish the yolk granule as a dynamic storage compartment.

The yolk granule is currently viewed as a dynamic organelle, rather than a benign storage compartment for nutrients required by the developing embryo. In the sea urchin, in addition to playing a role in protein export, the yolk granule also appears to be required for membrane repair. During plasma membrane disruption, an influx of seawater results in a high local concentration of calcium which triggers fusion between individual yolk granules. Once tethered together, the yolk granules then fuse with the plasma membrane in a rapid, organized manner that patches the damaged area (McNeil, 1993; McNeil *et al.*, 2000). This reaction restores the structural integrity of the membrane. Toposome, associated on the surface of the yolk granule is responsible for the tethering of these organelles, suggesting that the dynamic properties of the yolk granule membrane are facilitated by this protein. In addition, toposome may be a component of the molecular machinery responsible for driving the fusion between the yolk granule and plasma membrane. Toposome may help drive this fusion by mediating the juxtaposition of the interacting membranes.

Chapter 6: Discussion

5.1 Overview

In the developing sea urchin embryo, membrane-membrane interaction is an important process for both cell-cell contacts and the repair of lesions in the plasma membrane. Toposome, a protein found in the sea urchin egg and embryo, has been implicated in both of these processes (Noll *et* al., 1981; Noll *et* al., 1985; Matranga *et al.*, 1986; Cervello *et al.*, 1992; Perera *et al.*, 2004). The focus of the current study was to examine calcium-toposome interaction and define how calcium modulates the interaction between toposome and the membrane bilayer. In addition, we were interested in probing the specificity of the calcium-binding sites on toposome and identifying the storage compartment(s) for toposome within the egg and its localization in various stage embryos to help resolve the conflicting data concerning the localization of this protein throughout development.

The data presented here defines both the calcium-toposome interaction as well as the nature of the association of toposome with the bilayer. Calcium was found to induce two calcium-concentration dependent structural transitions in toposome: a secondary structural change occurred with an apparent k_d (calcium) of 25 μM and this was followed by a tertiary structural change with an apparent k_d (calcium) of 240 μM. Interestingly, the first structural change was required to facilitate toposome binding to bilayers while the second structural change enabled this protein to drive membrane-membrane adhesive interactions. Further analysis on the calcium-toposome interaction using both thermal denaturation and chymotryptic digestion studies provided further evidence for the two distinctive, calcium-dependent structures of toposome. The NMR study, which examined

the effects of toposome on the lipid bilayer suggests that this protein interacts peripherally with the membrane and that the interaction occurs in the presence of 100 μM calcium and is not further modulated by increased concentrations of this cation. Atomic force microscopy confirmed this finding, showing that the calcium-dependent secondary structural change is necessary to facilitate toposome binding to the bilayer and that further increasing the calcium concentration, to induce the tertiary structural change, did not result in any significant increased binding of toposome to the bilayer. The data presented here also illustrates that toposome can bind metal ions other than calcium. However, at physiological concentrations, it was shown that the metal ion binding sites on toposome are calcium-specific. Together, these results provide a structural basis for role of toposome in mediating biologically relevant membrane–membrane interactions and suggest that under physiological conditions, the function(s) of toposome is regulated by calcium. In addition, we were able identify the storage compartments for toposome within the egg and its subcellular localization in various stage embryos. In the unfertilized egg, toposome was found associated with the plasma membrane and was found to be stored in two different compartments, the yolk and cortical granules, confirming the findings of Gratwohl *et al.* (1991).

Toposome is known to be involved in the process of cell-cell adhesion in the developing sea urchin embryo (Noll *et al.* 1985, Matranga *et al.* 1986, Cervello and Matranga 1989, Cervello *et al.* 1992). It has been suggested that toposome is responsible for position-specific cellular adhesion as they are released to newly formed cells. In fact, cells lacking toposome fail to aggregate, even in the presence of calcium. This suggests

that both toposome and calcium must cooperate in a manner promoting cell-cell interactions. Collectively, the study reported in this thesis provides a mechanistic basis for the cell-cell adhesive activity of toposome in the sea urchin embryo. There are two possible models for defining a role for toposome in this process. Toposome, localized to the cell surface, would be exposed to sufficiently high concentrations of calcium to facilitate the required tertiary structural change which could generate protein-protein interaction sites allowing toposome molecules on apposing cell membranes to interact (Fig. 6.1, Panel A) Alternatively, the tertiary structural change may expose a second membrane binding site on toposome (Panel B).

It has been known for some time that injury resulting in plasma membrane disruption is a common cellular event that requires resealing to maintain cell viability (McNeil 1993). When the sea urchin egg plasma membrane is damaged, there is a rapid fusion reaction between yolk granules and the damaged membrane driven by an influx of seawater (McNeil *et al.* 2000). This fusion reaction reestablishes the structural integrity of the membrane. The influx of 10 mM calcium during plasma membrane disruption is more than sufficient to cause a change in the tertiary structure of yolk granule-associated toposome resulting in yolk granule aggregation (Fig. 2.6). Subsequently, the aggregated yolk granules fuse with the plasma membrane. Toposome may help drive this fusion by mediating the juxtaposition of the interacting membranes. Again, the same two models are possible for defining a role for toposome in the repair of damaged plasma membranes. The tertiary structural change in toposome may either generate protein-protein interaction sites allowing toposome molecules on apposing cell membranes to

Figure 6.1: Working Model for the known cell-cell adhesive activity of toposome in the sea urchin embryo. Toposome, localized to the cell surface would be exposed to sufficiently high concentrations of calcium to facilitate the required tertiary structural change which could either (A) generate protein-protein interaction sites allowing toposome molecules on apposing cell membranes to interact, or (B) expose a second membrane binding site on toposome.

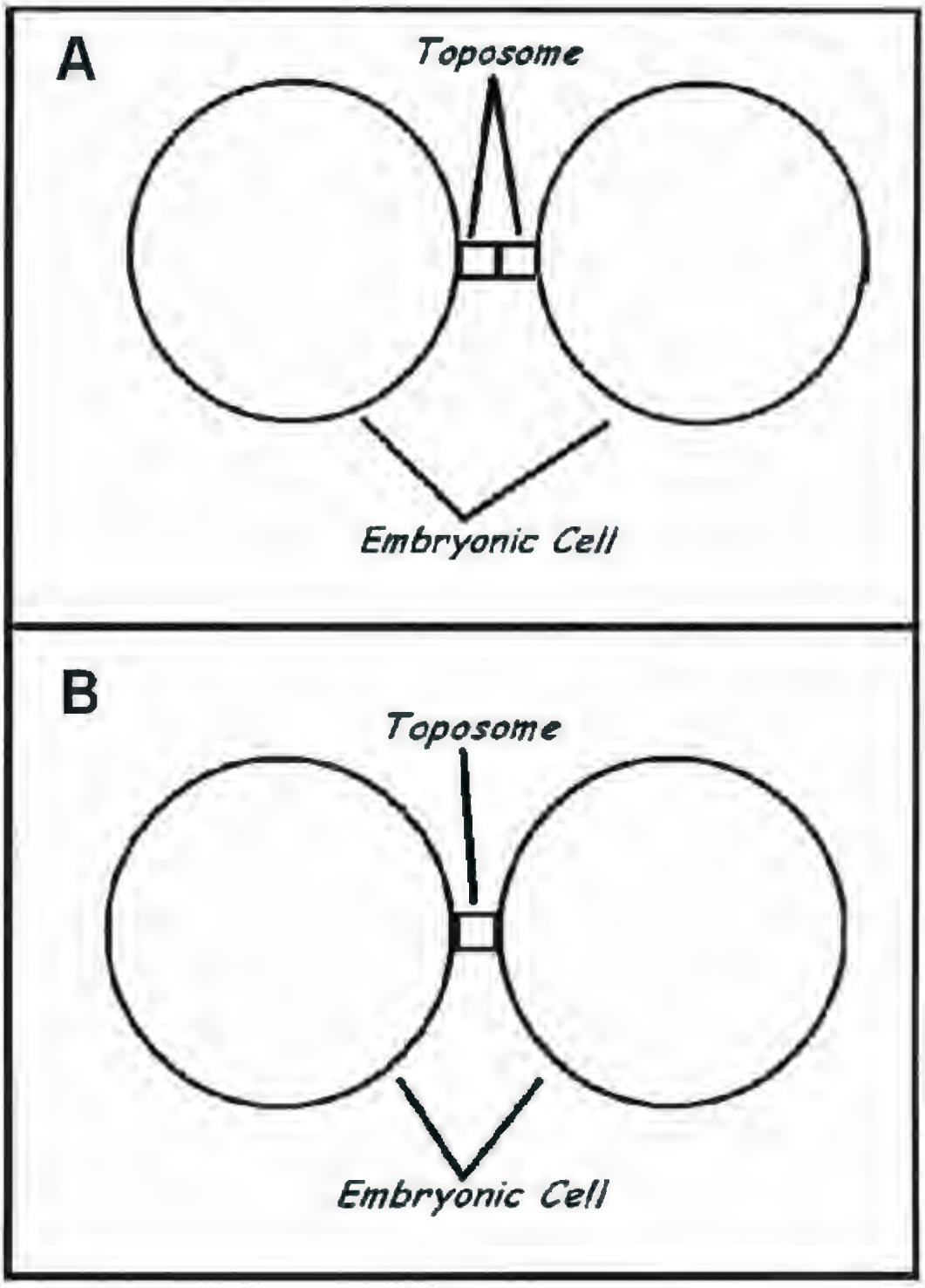
A
Toposome
Embryonic Cell
B
Toposome
Embryonic Cell

interact or expose a second membrane binding site on toposome. This latter model precludes the necessity for toposome to be present on both interacting surfaces and seems more likely since both immunolocalization studies carried out by our group and Gratwohl *et al.* (1991) observed that the localization of toposome occurs only on the exterior surface, and not on the interior surface, of the plasma membrane.

The current study provides a mechanistic basis for the role of toposome in mediating membrane-membrane interactions. This study has also been important in clarifying and confirming previously published data concerning toposome. First, Chapter 4 provides evidence that toposome, although transferrin-like in sequence, is unlikely to function as an iron transporter in the developing sea urchin egg and embryo based on its apparent dissociation constant (Fe^{3+}) and the trace amounts of iron present in seawater. Secondly, Chapter 5 confirms the results of a toposome localization study carried out by Gratwohl *et al.* (1991). Like Gratwohl *et* al. (1991), we have found that in the unfertilized egg, toposome is localized on the surface of the plasma membrane and is stored in two different compartments, the yolk and cortical granules. However, this study has made no attempt to understand the functional significance of the proteolytic processing of toposome, nor did it make an attempt to identify the functional domain(s) of this protein. In future, it would be of great interest to attempt to isolate the 120- and 90 kDa proteolytic products of toposome. Once isolated, the interaction between each proteolytic product and calcium could be examined using circular dichroism and fluorescence spectroscopy to observe any calcium-dependent structural changes. Membrane binding studies could also be carried out to determine if calcium can modulate

the interaction between the proteolytic products of toposome (the 120- and 90 kDa) and the membrane bilayer. Both of the above experiments would help to identify the functional unit(s) of toposome and would provide insight concerning the significance of toposome processing during development.

5.2 References

Abragam, A. 1961. The Principles of Nuclear Magnetism. Oxford University Press, London.

Andrade, M.A., Chacon, P., Merelo, J.J. and Moran, F. 1993. Evaluation of secondary structure of proteins from UV circular dichroism spectra using an unsupervised learning neural network. Prot. Eng. **6**: 383-390.

Anstrom, J.A., Chin, J.E., Leaf, D.S., Parks, A.L. and Raff, R.A. 1988. Immunocytochemical evidence suggesting heterogeneity in the population of sea urchin egg cortical granules. Dev. Biol. **125**: 1-7.

Alliegro, M.C. and McClay, D.R. 1988. Storage and mobilization of extracellular matrix proteins during sea urchin development. Dev. Biol. **125**: 208-216.

Alliegro, M.C. and Schuel, H. 1988. Immunocytochemical localization of the 35-kDa sea urchin egg trypsin-like protease and its effects upon the egg surface. Dev. Biol. **125**: 168-180.

Armant, D.R., Carson, D.D., Decker, G.L., Welply, J.K. and Lennarz, W.J. 1986. Characterization of yolk platlets isolated from developing embryos of *Arbacia punctulata*. Dev. Biol. **113**: 342-355.

Baker, H.M, Anderson, B.F. and Baker, E.N. 2003. Dealing with iron: common structural principles in proteins that transport iron and heme. Proc. Natl. Acad. Sci. U S A. **100**: 3579-3583.

Baker, E.N. and Lindley, P.F. 1992. New perspectives on the structure and function of transferrins. J. Inorganic Biochem. **47**: 147-160.

Bergink, E.W. and Wallace, R.A. 1974. Precursor-product relationship between amphibian vitellogenin and the yolk proteins, lipovitellin and phosvitin. J. Biol. Chem. **249**: 2897-2903.

Blicharski, J. S. 1986. Nuclear-spin relaxation in the presence of Mansfield-Ware-4 multipulse sequence. Can. J. Phys. **64**: 733-735.

Bloom, M., and E. Evans. 1991. Observation of surface undulations on the mesoscopic length scale by NMR. In Biologically Inspired Physics. L. Peliti, editor. Plenum Press, New York. 137-147.

Bloom, M., E. Evans, and O. G. Mouritsen. 1991. Physical properties of the fluid lipid-bilayer component of cell membranes: a perspective. Quarterly Reviews of Biophysics. **24**: 293-397.

Bloom, M., and E. Sternin. 1987. Transverse nuclear spin relaxation in phospholipids bilayer membranes. Biochemistry. **26**: 2101-2105.

Boldt, D.H. 1999. New perspectives on iron: An introduction. Am. J. Med. Sci. **318**: 207–212.

Brooks, J.M. and Wessel, G.M. 2002. The major yolk protein in the sea urchin is a transferrin-like, iron binding protein. *Dev. Biol.* **245**: 1-12.

Brooks, J.M. and Wessel, G.M. 2003. Selective transport and packaging of the major yolk protein in the sea urchin. Dev. Biol. **261**: 353-370.

Brooks, J.M. and Wessel, G.M. 2004. The major yolk protein of sea urchins is endocytosed by a dynamin-dependent mechanism. Biology of Reproduction **71**: 705-713.

Cameron, R.A. and Davidson, E.H. 1991. Cell type specification during sea urchin development. TIG. **7**: 212-218.

Cecchettini, A., Falleni, A., Gremigini, V., Locci, M.T., Massetti, M., Bradley, J.T. and Giorgi, F. 2001. Yolk utilization in stick insects entails the release of vitelline polypeptides into the perivitelline fluid. Eur. J. Cell. Biol. **80**: 458-465.

Cervello, M., Arizza, V., Lattuca, G., Parrinello, N. and Matranga, V. 1994. Detection of vitellogenin in a subpopulation of sea urchin coelomocytes. Eur. J. Cell. Biol. **64**: 314-319.

Cervello, M., Di Ferro, D., D'Amelio, L., Zito, F. and Matranga, V. 1992. Calcium-dependent self-aggregation of toposome, a sea urchin embryo cell adhesion molecule. Biol Cell. **74**: 231-234.

Cervello, M. and Matranga, V. 1989. Evidence of a precursor-product relationship between vitellogenin and toposome, a glycoprotein complex mediating cell adhesion. Cell. Differ. Dev. **26**: 67-76.

Chothia, C. and Jones, E.Y. 1997. The molecular structure of cell adhesion molecules. Annu. Rev. Biochem. **66**: 823–862.

Cox, K.H., Angerer, L.M., Lee, J.J., Davidson, E.H. and Angerer, R.D. 1986. Cell lineage specific programs of expression of multiple actin genes during sea urchin embryogenesis. J. Mol. Biol. **188**: 159-172.

Davis, J. H. 1983. The description of membrane lipid conformation, order and dynamics by ^{2}H-NMR. *Biochim. Biophys. Acta.* **737**: 117-171.

Davis, J. H., K. R. Jeffrey, M. Bloom, M. I., Valic, and T. P. Higgs. 1976. Quadrupole echo deuteron magnetic resonance spectroscopy in ordered hydrocarbon chains. Chem. Phys. Lett. **42**: 390-394.

Dico, A. S., J. Hancock, M. R. Morrow, J. Stewart, S. Harris, and K. M. W. Keough. 1997. Pulmonary surfactant protein SP-B interacts similarly with dipalmitoylphosphatidylglycerol and dipalmitoylphosphatidylcholine in phosphatidylcholine/phosphatidylglycerol mixture. Biochemistry. **36**: 4172-4177.

Edelman, G.M and Crossin, K.L. 1991. Cell adhesion molecules: implications for a molecular histology. Annu. Rev. Biochem. **60**:155–190.

Fausto, A.M., Gambellini, G., Mazzini, M., Cecchettina, A., Masetti, M. and Giorgi, F. (2001a). Yolk granules are differentially acidified during embryo development in the stick insect *Carausius morosus.* Cell. Tissue. Res. **305**: 43-443.

Fausto, A.M., Gambellini, G., Mazzini, M., Cecchettina, A., Masetti, M, Locci, M.T. and Giorgi, F. (2001b). Serosa membrane plays a key role in transferring vitellin polypeptides to the perivitelline fluid in insect embryos. Dev. Growth Differ. **43**: 725-733.

Fiech, D. C., B. B. Bonev, and M. R. Morrow. 1998. Effect of pressure on dimyristoylphosphatidylcholine headgroup dynamics. Phys. Rev. E. **57**: 3334-3343.

Flytzanis, C.N., McMahon, A.P., Hough-Evans, P.J., Katula, B.R., Britten, K.S. and Davidson, E.H. 1985. Persistence and integration of closed DNA in post-embryonic sea urchins. Dev. Biol. **108**: 431-442.

Fuhrman, M.H., Suhan, J.P. and Ettensohn, C.A. 1992. Developmental expression of echinonectin, an endogenous lectin of the sea urchin embryo. Dev. Growth Differ. **34**: 137-150.

Fuji, A. 1969. Studies on the biology of the sea urchin. Superficial and histological gonadal changes in the gametogenic process of two sea urchins, *Strongylocentrotus nudus* and *Strongylocentrotus intermedius*. Bull. Fac. Fish. Hokkaido. Univ. **11**: 1-14.

Geary, E.D. 1978. Oogenesis in the Pacific sand dollar *Dendraster excentricus* (Eschscholtz). MS Thesis, University of Alberta.

Gratwohl, E.K.M., Kellenberger, E., Lorand, L. and Noll, H. 1991. Storage, ultrastructural targeting and function of toposomes and hyaline in sea urchin embryogenesis. Mech. Dev. **33**: 127-138.

Giorgi, F., Yin, L., Cecchettini, A. and Nordin, J. H. 1997. The vitellin-processing protease of *Blattella germanica* is derived from a pro-protease of maternal origin. Tissue Cell. **29**: 293-303.

Giudice, G. 1962. Restitution of whole larvae from disaggregated cells of sea urchin embryos. Dev. Biol. **5**: 402-411.

Hall, H.G. and Vacquier, V.D. 1982. The apical lamina of the sea urchin embryo: Major glycoproteins associated with the hyaline layer. *Dev. Biol.* **89**: 168–178.

Harrington, F.E. and Easton, D.P. 1982. A putative precursor to the major yolk protein of the sea urchin. Dev. Biol. **94**: 505-508.

Harrington, F.E. and Ozaki, H. 1986. The major yolk glycoprotein precursor in echinoids is secreted by coelomocytes into the coelomic plasma. Cell Differ. **19**: 51-57.

Hayley, M., Emberley, J., Davis, P.J., Morrow, M.R. and Robinson, J.J. 2006b. Interaction of toposome from sea-urchin yolk granules with dimyristoyl phosphatidylserine model membranes: a ^{2}H-NMR study. Biophys. J. **91**: 4555-4564.

Hayley, M., A. Perera, and J. J. Robinson. 2006a. Biochemical analysis of a Ca^{2+}-dependent membrane-membrane interaction mediated by the sea urchin yolk granule protein, toposome. Develop. Growth Differ. **48**: 401-409.

Heilbrunn, L.V. 1930a. The action of various salts on the first stage of the surface precipitation reaction in Arbacia egg protoplasm. Protoplasm **11**: 558-573.

Heilbrunn, L.V. 1930b. The surface precipitation reaction of living cells. Proc. Am. Philos. Soc. **LXIX**: 295-301.

Herbst, C. 1900. Uber das Auseinandergehen Van Furchungs- und Gewebezellen in Kalkfreim Medium. *Wilhelm Roux' Arch. EntwMech. Org.* **9**: 424-463.

Hovis, J.S. and Boxer, S.G. 2001. Patterning and composition arrays of supported lipid bilayers by microcontact printing. Lang. **91**: 3400-3405.

Hylander, B.L. and Summers, R.G. 1982. An ultrastructural immunocytochemical localization of hyalin in the sea urchin egg. Dev. Biol. **93**: 368-380.

Ichio, I., Deguchi, K., Kawashima, S., Endo, S. and Ueta, N. 1978. Water-soluble lipoproteins from yolk granules in sea urchin eggs. Isolation and general properties. J. Biochem. (Tokyo). **84**: 737-749.

Kari, B.E. and Rottmann, W.L. 1980. Analysis of the yolk glycoproteins of the sea urchin embryo. J. Cell Biol. **87**: 144a.

Kari, B.E. and Rottmann, W.L. 1985. Analysis if changes in a yolk glycoprotein complex in the developing sea urchin embryo. Dev. Biol. **108**: 18-25.

Kato, K.H., Abe, T., Nakashima, S., Matranga, V., Zito, F. and Yokota, Y. 2004. Nectosome: a novel cytoplasmic vesicle containing nectin in the egg of the sea urchin *Temnopleurus hardwickii*. Dev. Growth and Differ. **46**: 239-247.

Kimble, J. and Sharrock, W.J. 1983. Tissue specific synthesis of yolk proteins in *Caenorhabditis elegans*. Dev. Biol. **96**: 189-196.

Laemmli, U.K. 1970. Cleavage of structural proteins during assembly of the head bacteriophage T4. Nature (London). **272**: 680-685.

Lee, G.F., Fanning, E.W., Small, M.P. and Hille, M.B. 1989. Developmentally regulated proteolytic processing of a yolk glycoprotein complex in the embryos of the sea urchin *Strongylocentrotus purpuratus*. Cell. Differ. Dev. **26**: 5-18.

Liao, Y.D. and Wang, J.J. 1994. Yolk granules are the major component for bullfrog (*Rana catesbeiana*) oocyte-specific ribonuclease. Eur. J. Biochem. **222**: 215-220.

Lynn, D.A., Angerer, L.M., Bruskin, A.M., Klein, W.H. and Angerer, R.C. 1983. Localization of a family of mRNAs in a single cell type and its precursors in sea urchin embryos. Proc. Nat. Acad. Sci. **80**: 2656-2660.

Malkin L. I., Mangan, J. and Gross, P.R. 1965. A crystalline protein of high molecular weight from cytoplasmic granules in sea urchin eggs and embryos. Dev Biol. **12**:520-42.

Mallya, S.K., Partin, J.S., Valdizan, M.C. and Lennarz, W.J. 1992. Proteolysis of the major yolk glycoprotein is regulated by acidification of the yolk platelets in sea urchin embryos. J. Cell. Biol. **117**: 1211-1220.

Matese, J.C., Black, S. and McClay, D.R. 1997. Regulated exocytosis and sequential construction of the extracellular matrix surrounding the sea urchin zygote. Dev. Biol. **186**: 16-26.

Matranga, V., Di Ferro, D., Zito, F., Cervello, M. and Nakano, E. 1992. A new extracellular matrix protein of the sea urchin embryo with properties of a substrate adhesion molecule. Roux's Arch. Dev. Biol. **201**: 173-178.

Matranga V, Kuwasaki B, Noll H. 1986. Functional characterization of toposomes from the sea urchin blastula embryos by a morphogenetic cell aggregation assay. The EMBO Journal. 5: 3125-3132.

Matranga, V., Zito, F. and Cervello, M. 1987. A monoclonal antibody recognizes a subclass of toposomes specifying for mesodermal structures. Eur. J. Cell Biol. **44**: 45.

Mayne, J. and Robinson, J.J. 1998. The sea urchin egg yolk granule is a storage compartment for HLC-32, an extracellular matrix protein. Biochem. Cell. Biol. **76**: 83-88.

Mayne, J. and Robinson, J.J. 2002. Localization and functional role of a 41 kDa collagenase/ gelatinase activity expressed in the sea urchin embryo. Dev. Growth. Differ. **44**: 345-356.

McCabe, M. A., and S. R. Wassall. 1995. Fast-Fourier-transform dePaking. ***J. Magn. Reson. B.*** **106**: 80-82.

McClay, D.R. and Fink, R. 1982. Sea urchin hyalin; Appearance and function in development. Dev. Biol. **92**: 285-293.

McGregor, D.A. and Laughton, B. 1977. Amino acid composition, degradation and utilization of locust vitellogenin during embryogenesis. Wilhelm Roux's Archives. **181**: 113-122

McNeil, P.L. 1993. Cellular and molecular adaptations to injurious mechanical force. Trends Cell Biol. **3**: 302-307.

McNeil, P.L. and Kirchhausen, T. 2005. An emergency response team for membrane repair. Mol. Cell Biol. **6**: 499-505.

McNeil, P.L., Vogel, S.S., Miyake, K. and Terasaki, M. 2000. Patching plasma membrane disruptions with cytoplasmic membrane. J. Cell. Sci. **113**: 1891-1902.

Medina, M., Leon, P. and Vallejo, C.G. 1988. Drosphila cathepsin B-like protease: a suggested role in yolk degradation. Dev. Growth Differ. **31**: 241-247.

Meier, P., E. Ohmes, and G. Kothe. 1986. Multipulse dynamic nuclear magnetic resonance of phospholipids membranes. J. Chem. Phys. **85**: 3598-3614.

Nappi, A.J. and Vass, E. 2002. Interactions of iron with reactive intermediates of oxygen and nitrogen. Dev Neurosci. **24**: 134-42.

Noll, H., Alcedo, J., Daube, M., Frei, E., Schiltz, E., Hunt J., Humphries, T., Matranga, V., Hochstrasser, M., Aebersold, R., Lee, H. and Noll, M. 2007. The toposome, essential for sea urchin cell adhesion and development, is a modified iron-less calcium-binding transferring. Dev. Biol. **310**: 54-70.

Noll, H., Matranga, V., Cascino, D. and Vittorelli, L. 1979. Reconstitution of membranes and embryonic development in dissociated blastula cells of the sea urchin by reinsertion of aggregation-promoting membrane proteins extracted with butanol. Proc. Natl. Acad. Sci. U S A. **76**: 288-292.

Noll, H., Matranga, V., Palma, P., Cutrono, F. and Vittorelli, M.L. 1981. Species-specific dissociation of live sea urchin embryos by Fab against membrane components of *Paracentrotus lividus* and *Arbacia lixula*. Develop. Biol. **87**: 229-241.

Noll , H., Matranga, V., Cervello, M., Humphreys, T., Kuwasaki, B. and Adelson, D. 1985. Characterization of toposomes from sea urchin blastula cells: a cell organelle mediating cell adhesion and expressing positional information. Proc. Natl. Acad. Sci. **82**: 8062-8066.

Okada, Y. and Yokota, Y. 1990. Purification and properties of cathepsin B from sea urchin eggs. Comp. Biochem. Physiol. **96B**: 381-386.

Outreath, R.L., Roberson, M.M. and Barondes, S.H. 1988. Endogenous lectin secretion into the extracellular matrix of early embryos of *Xenopus laevis*. Dev. Biol. **125**: 187-194.

Ozaki, H. 1980. Yolk proteins of the sand dollar *Dendraster execentricus*. *Dev*. Growth Differ. **22**: 365-372.

Ozaki, H., Moriya, O. and Harrington, F.E. 1986. A glycoprotein in the accessory cells of the echinoid ovary and its role in vitellogenesis. Roux's Arch. Dev. Biol. **195**: 74-79.

Pauls, K. P., A. L. MacKay, O. Söderman, M. Bloom, A. K. Tangea, and R. S. Hodges. 1985. Dynamic properties of the backbone of an integral membrane peptide measured by ^{2}H-NMR. Eur. Biophys. J. **12**: 1-11.

Pederson, T. 2006. The sea urchin's siren. Dev. Biol. **300**: 9-14.

Perera, A., Davis, P. and Robinson, J.J. 2004. Functional role of a high mol mass protein complex in the sea urchin yolk granule. Develop. Growth Differ. **46**: 201-211.

Prosser, R. S., J. H. Davis, F. W.Dahlquist, and M. A. Lindorfer. 1991. ^{2}H nuclear magnetic resonance of the gramicidin A backbone in a phospholipids bilayer. Biochemistry. **30**:4687-4696.

Reimer, C.L. and Crawford, B.J. 1995. Identification and partial characterization of yolk and cortical granule proteins in eggs and embryos of the starfish, *Pisaster ochracens*. Dev. Biol. **167**: 439-457.

Robinson, J.J. 1989. Selective metal ion binding at the calcium-binding sites of the sea urchin extraembryonic coat protein hyalin. Biochem. Cell. Biol. **67**: 808-812.

Robinson, J.J. 1990. Polypeptide composition and organization of the sea urchin extraembryonic matrix, the hyaline layer. Biochem. Cell Biol. **68**: 1083-1089.

Scaturro, G., Zito, F. and Matranga, V. 1998. The oligomeric integrity of toposome is essential for its morphogenetic function. Cell Biol. Int. **22**: 321-326.

Schuel, H., Kelly, J.W., Berger, E.R. and Wilson, W.L. 1974. Sulfated acid mucopolysaccharides in the cortical granules of eggs. Effects of quaternary ammonium salts on fertilization. Exp. Cell Res. **88**: 24-30.

Schuel, H., Wilson, W.L., Wilson, J.R. and Bressler, R.S. 1975. Heterogeneous distribution of lysosomal hydrolases in yolk platelets isolated from unfertilized sea urchin eggs by zonal centrifugation. Dev. Biol. **46**: 404-412.

Scott, L.B., Leahy, P.S., Decker, G.L. and Lennarz, W.J. 1990. Loss of yolk platelets and yolk glycoproteins during larval development of the sea urchin embryo. Dev. Biol. **137**: 368-377.

Scott, L.B. and Lennarz, W.J. 1989. Structure of a major yolk glycoprotein and its processing pathway by limited proteolysis are conserved in echinoids. Dev. Biol. **132**: 91-102.

Sea Urchin Genome Sequencing Consortium. 2006. The genome of the sea urchin *Strongylocentrotus purpuratus*. Science. **314**: 941-952.

Shyu, A.B., Blumenthal, T. and Raff, R.A. 1987. A single gene encoding vitellogenin in the sea urchin Strongylocentrotus purpuratus: sequence at the 5' end. Nucleic Acids Res. **15**: 10405-10417.

Shyu, A.B., Raff, R.A. and Blumental, T. 1986. Expression of the vitellogenin gene in female and male sea urchins. Proc. Natl. Acad. Sci. USA. **83**: 3865-3869.

Simatos, G. A., K. B. Forward, M. R. Morrow, and K. M. W. Keough. 1990. Interaction between perdeuterated dimyristoylphosphatidylcholine and low molecular weight pulmonary surfactant protein SP-C. Biochemistry. **29**: 5807-5814.

Snigirevskaya, E.S., Hays, A.R. and Raikhel, A.S. 1997. Secretory and internalization pathways of mosquito yolk protein precursors. Cell Tiss. Res. **290**: 129-142.

Speigel, E., Howard, L. and Speigel, M. 1989. Extracellular matrix of the sea urchin and other marine invertebrates. Journal of Morphology **199**: 71-92.

Steinhardt, R.A., Bi, G. and Alderton, J.M. 1994. Cell membrane resealing by a vesicular mechanism similar to neurotransmitter release. Science. **263**: 390-393.

Stohrer, J., G. Gröbner, D. Reimer, K. Weisz, C. Mayer, and G. Kothe. 1991. Collective lipid motions in bilayer membranes studied by transverse deuteron spin relaxation. J. Chem. Phys. **95**: 672-678.

Takashima, Y. and Takashima, R. 1966. Electron microscope investigations of the modes of yolk and pigment formation in sea urchin oocytes. Okajimas Folia Anat. Jpn. **42**: 249-264.

Takeichi, M. 1977. Functional correlation between cell adhesive properties and some cell surface proteins. J. Cell Biol. **75,** 464-474.

Tamm, L.K., Crane, J. and Kiessling, V. 2003. Membrane fusion: a structural perspective on the interplay of lipids and proteins. Curr. Opin. Struct. Biol. **13**: 453–466.

Tata, J.R. 1976. The expression of the vitellogenin gene. Cell. **9**: 1-4.

Terasaki, M., Miyake, K. and McNeil, P.L. 1997. Large plasma membrane disruptions are rapidly resealed by calcium-dependent vesicle-vesicle fusion events. J. Cell Biol. **139**: 63-74.

Tesoro, V., Zito, Y., Yokota, Y., Nakano, E., Sciarrino, S. and Matranga, V. 1998. A protein of the basal lamina of the sea urchin embryo. Dev. Growth. Diff. **40**: 527-535.

Tsukahara, J. 1971. Electron microscope studies on the behavior of glycogen particles during oogenesis in the sea urchin. Dev. Growth Differ. **13**: 367-368.

Tsukahara, J. and Sugiyama, M. 1969. Ultrastructural changes in the surface of the oocyte during oogenesis of the sea urchin, *Hemicentrotus pulcherrimus*. Embryologia (Nagoya) **10**: 343-355.

Unuma, T., Suziki, T., Kurokawa, T., Yamamoto, T. and Akiyama, T. 1998. A protein identical to the yolk protein is stored in the testes in male red sea urchin, *Reudocentrotus depressus*. Biological Bulletin. **194**: 92-97.

Unuma, T., Okamoto, H., Konishi, K., Ohta, H. and Mori, K. 2001. Cloning of cDNA encoding vitellogenin and its expression in red sea urchin *Pseudocentrotus depressus*. Zool. Sci. **18**: 559-565.

Unuma, T., Yamamoto, T., Akiyama, T., Shiraishi, M. and Ohta, H. 2003. Quantitative changes in yolk protein and other components in the ovary and testis of the sea urchin *Pseudocentrotus depressus*. J. Exp. Biol. **206**: 365-372.

Wahli, W., Dawid, I.B., Pyffel, G.U. and Weber, R. 1981. Vitellogenesis and the vitellogenin gene family. Science. **212**: 298-304.

Wallace, R.A. 1985. Vitellogenins and oocytes growth in non-mammalian vertebrates. Dev. Biol. **110**: 127-177.

Wang, J.J., Tang, P.C., Chao, S.H., Cheng, C.H., Ma, H.J. and Liao, Y.D. 1995. Immunocytochemical localization of ribonuclease in yolk granules of adult *Rana catesbeiana* oocytes. Cell Tissue Res. **280**: 259-265.

Wessel, G.M., Marchase, R.B. and McClay, D.R. 1984. Ontogeny of the basal lamina in the sea urchin embryo. Dev. Biol. **103**: 235-245.

Wilcox, M.E., Brown, N., Piovant, M., Smith, R.J. and White, R.A.H. 1984. The Drosophila position-specific antigens are a family of cell surface glycoprotein complexes. EMBO J. **3**: 2307--2313.

Willey, H.S. and Wallace, R.A. 1981. The structure of vitellogenin. Multiple vitellogenins in Xenopus laevis give rise to multiple forms of the yolk proteins. J. Biol. Chem. **256**: 8626-8634.

Williams, J. (1967). Yolk utilization. The Biochemistry of Animal Development. R. Weber, editor. Academic Press, New York. Vol. **2**: 341-382.

Wilson, E.B. 1924. The cell in development and heredity. New York: Macmillan.

Wojchowski, D.M., Parsons, P., Nordin, J.H. and Kunkel, F.R. 1986. Processing of pro-vitellogenin in insect fat body: A role for high mannose oligosaccharide. Dev. Biol. **116**: 422-430.

Yamashita, O. and Indraasith, L.S. 1988. Metabolic fates of yolk proteins during embryogenesis in Arthropods. Dev. Growth. Differ. **30**: 337-346.

Yakato, Y. and Kato, K.H. (1988). Degradation of yolk proteins in sea urchin eggs and embryos. Cell Differ. **23**: 191-200.

Yakota, Y., Kato., K.H. and Mita, M. 1993. Morphological and biochemical studies on yolk degradation in the sea urchin, *Hemicentrotus pulcherrimus*. Zool. Sci. **10**: 661-670.

Yamada, R., Yamahama, Y. and Sonobe, H. 2005. Release of ecdysteroid-phosphates from egg yolk granules and thier dephosphorylation during early embryonic development in Silkworm, *Bombyx mori*. Zool. Sci. **22**: 187-198.

Yokota Y, Unuma T, Moriyama A, Yamano K. 2003. Cleavage site of a major yolk protein (MYP) determined by cDNA isolation and amino acid sequencing in sea urchin, *Hemicentrotus pulcherrimus*. Comp. Biochem. Physiol. B Biochem. Mol. Biol. 135: 71-81.